Formation and Evolution of Shatsky Rise Oceanic Plateau: Insights from IODP Expedition 324 and Recent Geophysical Cruises

William W. Sager[1,*], Takashi Sano[2], and Jörg Geldmacher[3]

[1]Department of Earth and Atmospheric Sciences, University of Houston, Houston, TX 77204 USA; wwsager@uh.edu

[2]Department of Geology and Paleontology, National Museum of Nature and Science, 4-1-1 Amakubo, Tsukuba 305-0005, Japan; sano@kahaku.go.jp

[3]GEOMAR Helmholtz Center for Ocean Research Kiel, Wischhofstrasse 1-3, 24148 Kiel, Germany; jgeldmacher@geomar.de

*corresponding author

Key words:

Oceanic plateau

Large igneous provinces

Mantle plume

Pacific Ocean

Shatsky Rise

Tamu Massif

Integrated Ocean Drilling Program

Seismic reflection

Seismic refraction

Geochemistry

Geochronology

Isotopic chemistry

Plate tectonics

Table of Contents

Abstract

Recent research from the Shatsky Rise in the western Pacific Ocean provides new insights on the formation and evolution of this oceanic plateau as well as tests of mantle models to explain anomalous large igneous province (LIP) volcanism. Recent Shatsky Rise studies cored the igneous pile (Integrated Ocean Drilling Program Expedition 324), imaged the interior with seismic refraction and multichannel seismic reflection data, and mapped magnetic anomalies adjacent to the plateau to provide new constraints on its tectonic history. Coring data show that Tamu Massif, the largest edifice within Shatsky Rise, is characterized by massive sheet flows, similar to flows caused by voluminous eruptions in continental flood basalts. Core data also indicate that the massive eruptions waned as the plateau evolved and smaller edifices were built. Seismic data show intrabasement reflectors within Tamu Massif that indicate volcanism from its center, indicating that this is an enormous shield volcano with abnormally low flank slopes and thick crust (~30 km). Paleomagnetic data record minimal geomagnetic field variations, consistent with the inference of massive, rapid volcanism. Altogether, the physical picture indicates that Shatsky Rise was built by massive, rapid eruptions that formed enormous volcanoes. Geochronologic data support the previously inferred age progression, with the volcanic massifs formed along the trace of a triple junction starting from Tamu Massif and becoming progressively younger to the northeast. These data weaken support for rapid emplacement because they show that the last eruptions atop Tamu Massif encompassed several million years between the final massive flows as well as a long hiatus of ~15 Myr until late stage eruptions that formed a summit ridge. They may also indicate that the last eruptions on Tamu and Ori massifs occurred while the triple

junction was hundreds of kilometers distant. Furthermore, magnetic anomaly data indicate that the plate boundary reorganization associated with Shatsky Rise formation occurred several million years prior to the first Tamu Massif eruptions, suggesting plate boundary control of Shatsky Rise initiation. Geochemical and isotopic data show that Shatsky Rise rocks are variably enriched, with the majority of lavas being similar to mid-ocean ridge basalts (MORB). However, the data indicate deeper (>30 km) and higher partial degree of melting (15-23%) as compared with normal MORB. Melting models indicate that the magma experienced a mantle temperature anomaly, albeit only a small one (~50°C). Some lava compositions suggest the involvement of recycled subducted slab material. Recent investigations of Shatsky Rise initially envisaged a competition between two end-member models: the thermal plume head and the fertile mantle melting beneath plate extension (aka, plate model). Both hypotheses find support from new data and interpretations, but both do not fit some data. As a result, neither model can be supported without reservation. Noting that most basaltic oceanic plateaus have formed at triple junctions or divergent plate boundaries, we suggest that this dichotomy is artificial. Oceanic plateau volcanism is anomalous and focused at spreading ridges for reasons that are still poorly understood, mainly owing to uncertainties about mantle convection and geochemical reservoirs. Shatsky Rise investigations have vastly improved our understanding of the formation of this oceanic plateau, but highlight that important work remains to understand the underlying nature of this volcanism.

1. Introduction

Oceanic plateaus are mostly submarine LIPs, representing an immense transfer of magma from mantle to crust (Duncan and Richards, 1991; Coffin and Eldholm, 1994; Ernst and Buchan, 2001; Bryan and Ernst, 2008). Some oceanic plateaus, such as the enormous Ontong Java Plateau (OJP), appear to have formed rapidly (a few Myr) (Tarduno et al., 1991; Mahoney et al., 1993; Tejada et al., 1996; 2002), implying immense volcanic eruptions with global impact (Larson, 1991; Coffin and Eldholm, 1994). Others, such as Kerguelen-Broken Ridge or the Caribbean LIP, seemed to have assembled over longer time periods (Coffin et al., 2002; Hoernle et al., 2004). Many of the plateaus scattered across the ocean basins were formed during the Cretaceous period, suggesting these eruptions were part of an episodic magmatic outbreak related to mantle convection (Larson, 1991). These inferences led to wide interest over the past two decades in investigating the origin and evolution of oceanic plateaus. Despite increased research focus on these features, most remain poorly understood because they are immense and in remote locations, making sampling and study difficult and require the inference and testing of models from small data sets.

Shatsky Rise, located ~1500 km east of Japan in the northwest Pacific Ocean, is one of the largest oceanic plateaus with an area of ~5.3 x 10^5 km^2 (Sager et al., 1999; Zhang et al., 2016). It consists of three major edifices, Tamu, Ori, and Shirshov massifs, in southwest-northeast alignment (Fig. 1). A low ridge, Papanin Ridge, extends to the northeast from Shirshov Massif and a cluster of several dozen seamounts, the Ojin Rise Seamounts, are scattered around Shirshov Massif and the area to its east (Fig. 1). Shatsky Rise is unique among large Mesozoic oceanic plateaus because geologic evidence suggests two competing hypotheses for plateau formation: the plume head and fertile mantle models (Sager, 2005) and it also contains

magnetic anomalies to constrain contemporaneous spreading ridge locations. The former model envisages plateau formation resulting from a massive, thermal diapir arising from the deep mantle (Richards et al., 1989; Duncan and Richards, 1991; Coffin and Eldholm, 1994), whereas the latter explains excess volcanism by the melting of particularly fertile (lower melting point) upper mantle material owing to decompression caused by plate extension (Foulger, 2007; Anderson and Natland, 2014). This dichotomy and the interest that it sparked, led to several recent studies of Shatsky Rise, including coring of the igneous pile by Integrated Ocean Drilling Program (IODP) Expedition 324 (Sager et al., 2010; 2011a; 2011b), seismic imaging by the R/V *Marcus G. Langseth* (Korenaga and Sager, 2012; Sager et al., 2013; Zhang et al., 2015), and geophysical data collection by R/V *Yokosuka* (Nakanishi et al., 2015). In this review, we encapsulate results of these recent research projects and explore their ramifications regarding the formation and evolution of Shatsky Rise and by inference, other oceanic LIPs. The various Shatsky Rise studies provide improved understanding of the life cycle of an oceanic plateau, but an unambiguous answer to the plume versus plate debate is not attained. In part this results from the difficulty of inferring the depth of the source region from surface rock characteristics and the lack of consensus about mantle structure, geochemistry, and geodynamics. Instead, the strong evidence that Shatsky Rise volcanism was extraordinary coupled with the clear connection to mid-ocean ridge tectonics implies that the dichotomy may be miscast. The "end-member" models may, in fact, coexist in this setting.

1.1 Source Models: Plume Versus Plate

After the apparent success of the thermal plume model to explain linear seamount chains (Wilson, 1963; Morgan, 1971; 1972), this hypothesis became a popular mechanism to account for other examples of intraplate volcanism. It seemed an elegant mechanism to explain the emergence of excess magma from the mantle distant from plate boundaries. With

their large volumes, oceanic plateaus seem simply explained by a massive thermal plume and consistent with the emergence of a plume head, a large volume of buoyant hot material formed by the detachment of a nascent plume from a thermal boundary layer (Griffiths and Campbell, 1990; Campbell and Griffiths, 1990). This boundary layer is usually assumed to be the core-mantle boundary, where the thermal contrast could cause a large volume of material to detach from the boundary layer and rise through the mantle over a period of millions of years (Richards et al., 1989). If this plume head arrived at the base of continental lithosphere, spread out and underwent adiabatic melting, a continental flood basalt province (CFB) would be formed, and if beneath oceanic lithosphere, an oceanic plateau would be the result (Fig. 2) (Richards et al, 1989; Duncan and Richards, 1991). This hypotheses makes several important predictions: the buoyant plume head should cause significant (~1-3 km) initial uplift, the plume head should emplace a large volume of volcanic material in a short period of time (1-2 Myr), the magma source temperature and degree of melting should be higher than at spreading ridges or small seamounts, the rising plume should carry primitive lower mantle material to the surface, and the voluminous plume head should give way to a narrower, underlying, plume tail reflected by a decrease in eruption volume and spatial distribution with time (Campbell and Griffiths, 1992; Coffin and Eldholm, 1994; Campbell, 2005; 2007).

Because the plume head model predicts massive, rapid magma emplacement, it seemed a good way to explain Earth's two largest oceanic LIPs, Ontong Java and Kerguelen plateaus, but evidence from Ocean Drilling Program (ODP) expeditions provided equivocal support. Although ODP cores recovered thick subaerial basaltic lava flows, Kerguelen Plateau was found to have erupted over a much longer time period (~25 Ma) than expected (Coffin et al., 2002). Moreover, gneiss and granitoid rocks were cored at one site (Site 1137 on Elan Bank),

a surprise implying that Kerguelen Plateau incorporated continental components (Coffin et al., 2002; Frey et al., 2003). In addition, the geochemistry of basalt samples indicates an interaction of the magma with these continental rocks (Neal et al., 2002), compromising their use for investigating the pristine mantle source. In contrast, construction of OJP appears to have occurred rapidly over a period of ~5 Myr centered at ~122 Ma (Neal et al., 1997; Tejada et al., 1996; 2002), emplacing a large volume of tholeiitic basalts with remarkably uniform geochemistry (Tejada et al., 2004) formed at high degrees of partial melting (~30%, Fitton and Godard, 2004; Herzberg, 2004), as would be expected of a plume head. However, OJP was mostly emplaced in a deep submarine environment, so its uplift was far less than predicted for active hotspots and its subsidence afterwards was anomalously small (Neal et al, 1997; Ito and Clift, 1998; Ito and Taira, 2000; Roberge et al., 2005), observations that are inconsistent with a simple, thermal plume model.

At about the same time, the scientific community began to question the wide application of the plume hypothesis, with some going as far as to say that thermal plumes from the deep mantle do not occur (Anderson, 1995; 2001; Foulger 2002; 2005; 2011; Anderson and Natland, 2014). An alternate mechanism was proposed for excess volcanism, with mantle melting caused by decompression of especially fertile mantle in places where plate boundaries or cracks in the lithosphere lower the hydrostatic pressure (Fig. 2) (Foulger and Natland, 2003; Foulger et al., 2005a; Natland and Winterer, 2005; Korenaga, 2005; Foulger, 2007; Anderson and Natland, 2014). Although this model is currently not as specific in regards to surface expression as that of the thermal plume, it yields several implications: volcanism should be constrained by the geometry of the fertile source mantle and lithospheric extension zone and may not be emplaced within a limited radius as implied by a plume, the duration of volcanism

is not controlled by the impact of a plume head, so it may be more time extensive, and volcanic material is entirely from the upper mantle.

Views of mantle plumes have also changed over time. Whereas plumes were initially thought to be narrow, columnar, upwelling jets caused by thermal buoyancy, initiated in the lower mantle or near the core-mantle boundary, modern views of mantle plumes are more complex. Plumes can be driven by compositional contrast relative to the host mantle as well as thermal contrast, a so-called thermochemical plume (Tackley, 1998; Farnetani and Samuel, 2005). This allows a plume to occur without a large thermal contrast and to cause only negligible surface uplift (Dannberg and Sobolev, 2014). Thermochemical plumes may also have more complex shapes than the simple, narrow columnar form or may arise from other depths in the mantle, such as the transition zone (Tackley, 1998; Davaille, 1999; Farnetani and Samuel, 2005; Kumagai et al., 2008). Modeling studies also suggest that chemical heterogeneities from subducting slabs and primitive material can be preserved in thermochemical piles at the base of the mantle and that plumes can carry this heterogeneity back to the surface (Farnetani et al., 2002), producing rocks with varied geochemical signatures that may change over time or resulting in spatially zoned hot spot tracks (Hoernle et al. 2000; 2015; Abouchami et al., 2005). Seismic tomography studies have sought to find and trace narrow plumes from the deep mantle, but have not delivered a clear answer, perhaps because seismic tomography cannot resolve such features (e.g., Nolet et al., 2007; Hwang et al., 2011). Studies by Montelli et al. (2004, 2006) perhaps come closest to the original idea of mantle plumes, suggesting sub-vertical, low-velocity zones beneath a large number of known hotspots, with many of such features observable through a significant portions of the mantle. In contrast, a recent model (French and Romanowicz, 2015) displays broad low velocity zones

beneath many hotspots but unclear connections through the upper mantle. Thus, despite improvements in tomography, the impact of these studies remains unclear.

1.2 Geologic Background: Evolution of Shatsky Rise

Shatsky Rise began to form near the equator, in the middle of the Pacific Ocean, near the time of the Jurassic-Cretaceous boundary (Sager et al., 1988; 1999; Nakanishi et al., 1999; Mahoney et al., 2005). The plateau sits at the confluence of the southwest-northeast trending Japanese magnetic lineations and the northwest-southeast trending Hawaiian magnetic lineations (Fig. 2), implying that it formed at a triple junction (Hilde et al., 1976; Sager et al., 1988). Although there is no preserved record of the third plate boundary, because the formerly adjacent Izanagi and Farallon plates have been subducted (Woods and Davies, 1982), kinematic stability implies that the triple junction probably had a ridge-ridge-ridge geometry (Sager et al., 1988; Nakanishi et al., 1999). Available age evidence and gravity anomalies also indicate that Shatsky Rise formed near the triple junction. A radiometric age of 144.6 ±0.8 Ma for igneous rocks recovered at ODP Site 1213 on the south flank of Tamu Massif (Mahoney et al., 2005) is approximately the same as magnetic chron M19 (Sager, 2005), which transects the north flank of the massif. Thus, the edifice top is approximately the same age as the lithosphere beneath it. Although precise radiometric ages were hitherto not available for the other parts of the plateau, gravity anomalies indicate that the entire plateau is in complete Airy isostatic compensation, implying that it formed near the spreading ridges (Sandwell and MacKenzie, 1989). Because the magnetic lineations become progressively younger to the northeast, a similar age progression for the volcanic edifices is implied (Sager et al., 1999; Nakanishi et al., 1999).

Magnetic lineations imply that the triple junction was migrating northwest relative to the Pacific plate prior to M21, when Shatsky Rise began to form (Fig. 3; Sager et al., 1988). Tamu Massif formed first, near the time of the Jurassic-Cretaceous boundary, and the triple junction simultaneously jumped NE ~800 km to the location of the massif (Sager et al., 1988; 1999). At the same time, the spreading direction changed ~24° on the Pacific-Izanagi ridge (Japanese magnetic lineations) and one or more microplates were created (Sager et al., 1988; 1999; Nakanishi et al, 1989; 1999). Because Shatsky Rise formed at a spreading-ridge triple junction, some authors believe that parts may have been rifted away by the adjacent plates and accreted at Pacific-rim subduction zones as the Izanagi and Farallon plates were subducted (Sager et al., 1988; Larson, 1991; Kimura et al., 1994; Ichiyama et al., 2014). The magnetic lineations indicate that the triple junction migrated northeast, along the axis of Shatsky Rise (Fig. 3) as younger edifices (Ori and Shishov massifs and Papanin Ridge) were emplaced (Sager et al., 1988; 1999). During this time, the northeastward direction of triple junction migration was not that predicted by plate kinematics (it should have been northwest) and the triple junction jumped northeastward at least 9 times (Sager et al., 1988; Nakanishi et al., 1999). These anomalies imply that something other than plate kinematics dictated the triple junction location. After about M4 time, the triple junction no longer followed Papanin Ridge (Nakanishi et al., 1999). Subsequently, this ridge appears to bend to the SE and may connect with Hess Rise (Sager et al., 1999). Bercovici and Mahoney (1994) hypothesized the two rises are related as being products of a double plume head.

Although Shatsky Rise probably stayed near the equator during its formation (Sager et al., 2015), afterwards it rode the Pacific plate ~35° northward from the equator to its present location (Sager, 2007). Soon after emplacement, it began collecting carbonate pelagic

sediments and accumulated a thick cap during the Mesozoic as it lay beneath the equatorial high productivity zone (Sliter and Brown, 1993). Because of the abundance of siliceous sedimentation within the high productivity zone, the Cretaceous carbonate sediment section later became pervasively infested with chert layers and nodules, frustrating scientific coring of these sediments (e.g., Moberly and Larson, 1975). After the plateau drifted away from the equator, a drape of Cenozoic pelagic sediments topped the sedimentary section (Sliter and Brown, 1993; Bralower et al., 2006).

1.3 Recent Shatsky Rise Research Programs

1.3.1 IODP Expedition 324

IODP Expedition 324 took place during 2009 and had an objective of extensive coring of igneous rock from Shatsky Rise (Expedition 324 Scientists, 2010a). Prior to Expedition 324, igneous basement was cored only once, at Site 1213 (Fig. 2) during ODP Leg 198, where a 47-m basalt section was penetrated (Shipboard Scientific Party, 2002). Although dredged samples had previously been retrieved from Shatsky Rise (Sager et al., 1999), almost all were highly altered and unsuitable for the geochemical and geochronological studies critical to understanding the origin of the plateau. During Expedition 324, five sites were cored (Figs. 2, 4), two on Tamu Massif (Sites U1347 and U1348), two on Ori Massif (Sites U1349 and U1350), and one on Shirshov Massif (Site U1346). Site U1346 penetrated a 52.6-m section of mostly pillow lavas (Fig. 4) from the summit platform of Shirshov Massif (Expedition 324 Scientists, 2010b). Site U1347, on the southeastern upper flank of Tamu Massif, cored a 159.9-m igneous section consisting of alternating massive flows and pillow lavas (Fig. 4; Expedition 324 Scientists, 2010c), whereas Site U1348, on a basement high on the Tamu Massif north flank, recovered ~120 m of volcaniclastics, but no lava flows (Expedition 324 Scientists, 2010d). Site U1349, situated atop a summit ridge on Ori Massif, penetrated 85.3 m

of thin massive flows (Expedition 324 Scientists, 2010e) and Site U1350, on the east flank of the same edifice, cored 172.7 m of igneous basement, consisting mostly of pillow units (Fig. 4; Expedition 324 Scientists, 2010f).

Because the Cretaceous sedimentary cap on Shatsky Rise comprises a relatively well-known succession of pelagic chalk and limestone and recovery is poor owing to the pervasive occurrence of chert, sediment coring in all Expedition 324 holes was not initiated until near basement. Nevertheless, basal sediment layers other than chert and chalk were recovered at all sites except for U1350 (Figs. 4, 5). At Site U1346, a 19.7-m succession of basalt-limestone breccia was found to overlie turbiditic volcaniclastic sediments situated atop limestones and calcareous mudstones (Expedition 324 Scientists, 2010b). Site U1347 produced a 77-m section of limestone and calcareous sandstone with volcaniclastics atop radiolarian-rich siltstones and sandstones with volcaniclastics (Expedition 324 Scientists, 2010c; Hermann and Stroncik, 2013). Site U1348 yielded several layers of bioclastic sandstone between volcaniclastic units (Expedition 324 Scientists, 2010d). A 29.8-m section of claystone and sandstone overlying sandstone, breccia, and conglomerate was cored at Site U1349 (Expedition 324 Scientists, 2010d). Because so few other drill sites have penetrated to igneous basement, Expedition 324 provided the first extensive sampling of supra-basement sediments on Shatsky Rise and showed that most summit sites were in shallow water shortly after volcanic activity concluded (Expedition 324 Scientists, 2010a).

1.3.2 Seismic Exploration

During cruises in 2010 (MGL1002) and 2012 (MGL1206), the R/V *Marcus G. Langseth* collected seismic refraction and reflection data, mainly over Tamu Massif (Fig. 2). Refraction data were collected on a 420-km transect crossing the summit of Tamu Massif and passing

over Site U1347. Data were recorded by 21 ocean bottom seismometers and these data were used to construct a tomographic velocity section (Korenaga and Sager, 2012). A total of ~3350 km of 2D multichannel seismic (MCS) reflection profiles were collected over southern Shatsky Rise using a 36-airgun array as a sound source and a 6-km, 468 channel streamer (hydrophone array) to record the seismic waves (Zhang et al., 2015). The seismic lines were oriented to provide four cross-axis profiles across Tamu Massif, one along the axis of the massif, and another over Ori Massif (Fig. 2). These lines crossed all of the basement drill sites, except for Site U1346, allowing a comparison between seismic and coring data (Zhang et al., 2015).

1.3.3 Magnetic and Bathymetry Data

Bathymetry and magnetic data were collected on transit tracks between sites on Expedition 324 (Kang and Sager, 2010). Multibeam bathymetry data were collected on all track lines run by the R/V *Marcus G. Langseth*. Despite recent multibeam data acquisition, only about 20% of Tamu Massif has been covered by these high-resolution data, so most data occur along isolated tracks, except where surveys have concentrated on the summit. In addition, a cruise by the JAMSTEC (Japan Agency for Marine Technology) vessel R/V *Yokosuka* (cruise YK08-09) during 2008 collected magnetic, gravity, and multibeam bathymetry data on the southern margin of Tamu Massif, in an effort to elucidate the initial formation of the plateau (Nakanishi et al., 2015).

2. The Making of a LIP: New Observations on the Origin and Evolution of Shatsky Rise

2.1 IODP Expedition 324 Coring

2.1.1 Igneous Basement

Prior to IODP Expedition 324, little was known about the volcanic basement of Shatsky Rise. Although it was clear from dredging that the plateau basement was igneous and of

basaltic composition (Kashintsev and Suzymov, 1981; Sager et al., 1999), most recovered samples were highly altered and often unsuitable for geochemical or geochronological studies. ODP Leg 198 cored a 47-m section of basaltic rock at Site 1213 and the three recovered igneous units were interpreted as diabase sills, i. e., intrusives possibly erupted into the earliest Cretaceous sedimentary layers (Shipboard Scientific Party, 2002). Samples from these cores, produced the first reliable radiometric date for Shatsky Rise, 144.6 ±0.8 Ma (Mahoney et al., 2005), proving that the basement of Tamu Massif was of Late Jurassic-Early Cretaceous age, as had been interpreted from the earliest Cretaceous sediments cored on Deep Sea Drilling Project (DSDP) Leg 32 (Shipboard Scientific Party, 1975). Furthermore, geochemical studies of these same samples concluded that their isotopic signatures were very much like mid-ocean ridge basalt (MORB), deepening the mystery of the Shatsky Rise magma source (Mahoney et al., 2005).

Expedition 324 cores provide a wealth of information about the volcanism that created Shatsky Rise. The signal characteristic of cores recovered on the expedition is the dichotomy between Tamu Massif and the smaller edifices, Ori and Shirshov massifs. Coring at Site U1347 recovered pillow lavas and thick, massive flows up to ~23 m in thickness (Expedition 324 Scientists, 2010a; Sager et al., 2011a; 2011b). The pillow lavas are typical of submarine volcanism at modest effusion rates (e.g., Ballard et al., 1979; McClinton et al., 2013), but the massive flows are interpreted as analogous to "massive sheet flows" mapped in continental flood basalt provinces (Self et al., 1997). They indicate highly effusive volcanism and are formed by inflation as copious lava flows into the chilled skin formed by contact with the surrounding environment (Self et al., 1997). Such flows are capable of flowing long distances and the necessary ingredients are highly fluid lava, produced at prodigious rates, shielded from

cooling by a thick, insulating skin (Kesthelyi and Self, 1998). As the Site U1347 section consists of two sequences of massive flows separated by pillow lavas (Fig. 4), two pulses of effusive volcanism with an intervening period of lesser output were interpreted (Expedition 324 Scientists, 2010a, c).

After re-examining the Site 1213 igneous cores, Expedition 324 scientists re-interpreted the three igneous units as massive flows similar to those at Site U1347 (Koppers et al., 2010). With the entire Site 1213 section being made up of massive flows and 66% of the Site U1347 section also consisting of these flows (Sager et al., 2011b), the implication is that Tamu Massif was formed mainly by massive sheet flows that erupted large volumes of lava and probably flowed for long distances. Interestingly, the Site U1347 section is quite similar to that cored at Site 1185 on OJP, which is also characterized by massive flows (Shipboard Scientific Party, 2001). Evidently, the two large plateaus Tamu Massif and OJP shared similar eruption mechanisms.

A surprise finding within the lava flows of Site U1347 are a number of thick sedimentary layers, unexpected because they imply the passage of time, contrary to the picture of rapid, massive volcanism. Four sedimentary beds were recovered within the basement section of the U1347 cores (Sager et al., 2010), two between the uppermost massive flows (at ~187 and ~204 mbsf) and the other two between pillow units (at ~259 and ~278 mbsf). In Figure 4, only the layer at ~204 mbsf appears to be thick because the graphic lithology diagram is based on recovered rock, which was small for three of these units. Analyses of wireline log data indicate that the upper two sedimentary units are ~9-10 m in thickness and the lower two are ~5 m thick (Fig. 4), suggesting long periods of volcanic quiescence (Tominaga et al., 2014). Although recovered sedimentary rocks from the uppermost layer show signs of soft-sediment

deformation, as could occur from mass wasting, the others do not. Moreover, most of these units contain radiolarian-bearing rocks and one (at ~259 mbsf) contains limestone, both implying pelagic sedimentation (Expedition 324 Scientists, 2010c). Unfortunately, it is impossible to constrain the duration of sedimentation, but the implication is that significant time may have elapsed between lava flows, especially the upper massive flows.

Another surprise from Tamu Massif was the coring of a ~120 m volcaniclastic section from Site U1348. This hole is situated atop a large (~30 km across) basement high on the north flank of the massif. The cored section consists of three layers of volcaniclastics, interbedded with bioclastic sandstones (Fig. 4). The volcaniclastic layers probably represent individual volcanic eruptions, with the sedimentary intervals implying quiescence. Although volcaniclastics can be formed in deep water (Gill et al., 1990; Davis and Clague, 2003; Eissen et al., 2003), shallow water formation is indicated for the upper volcaniclastic units (Units IIIa, IIIc) because fossils of shallow water fauna are found within the section, particularly in the bioclastic sandstone overlying and underlying the volcaniclastics (Units II, IV) (Expedition 324 Scientists, 2010d). Moreover, the presence of reddish scoria throughout the interbedded sandstone unit (Unit IIIb) may indicate subaerial eruption. In contrast, the lower volcaniclastics (Units V, VI) are a mixture of in situ and re-deposited hyaloclastite that are deposited in at depths below wave base but less than ~500 m. A shallow water environment is also supported by dissolved volatiles (CO_2 and H_2O) from fresh hyaloclastite samples, which give water-depth estimates of 287 m (Shimizu et al., 2013). Although coring at Site U1348 did not penetrate deeply (~120 m into basement), they suggest that the large cone-like feature at whose summit the site penetrated (Expedition 324 Scientists, 2010d) may thus be a

volcaniclastic feature. If true, this inference suggests that volcaniclastic deposits may be voluminous in some spots

Similar findings come from other LIPs, suggesting that volcaniclastics are common in the late stages of submarine basaltic eruptions and typically occur in shallow water. At OJP, Site 1184 produced shallow water volcaniclastics (Thordarson, 2004) whereas the recovered lava flows from other sites were emplaced in deep water (Neal et al., 1997; Fitton and Godard, 2004). Basal volcaniclastic sediments were cored at Manihiki Plateau and interpreted as phreatomagmatic products of shallow water eruptions (Jackson and Schlanger, 1976). This plateau is part of the Ontong Java Nui LIP (Ontong Java plus Manihiki and Hikurangi plateaus; Taylor, 2006; Chandler et al., 2012; Hochmuth et al., 2015), implying that such deposits were widespread in the formation of this LIP. Similarly, phreatomagmatic volcaniclastics were recovered from several ODP Leg 183 sites at Kerguelen Plateau (Coffin et al., 2000). ODP Leg 183 scientists reported volcaniclastic successions overlying basalt lava flows are minimally reworked pyroclastic flow deposits that erupted under subaerial and shallow marine environments (Shipboard Scientific Party, 2000; Wallace, 2002). Moreover, similar basaltic volcaniclastic intervals have been found on numerous other oceanic plateaus (e.g., Ross et al., 2005).

Igneous rocks recovered on Ori and Shirshov massifs contrast with those from Tamu Massif. Pillow lavas are more common and massive flows are thinner. At Site U1350 on the Ori Massif flank, pillow lavas make up ~86% of the cored section and at Site U1346 on Shirshov Massif, the section is almost entirely pillow lavas (Fig. 4). In the Site U1349 igneous section, from the Ori Massif summit, all recovered lava flows are massive, but they are much thinner than those found on Tamu Massif. The picture provided by Expedition 324 cores is

that Tamu Massif was built by voluminous, effusive eruptions, whereas the smaller edifices Ori and Shirshov, were constructed by less effusive volcanism (Sager et al., 2011a; 2011b). This finding is consistent with the fact that Ori and Shirshov massifs are much smaller in volume (Sager et al., 1999), indicating the waning of the Shatsky Rise melting anomaly (Sager et al., 2011a; 2011b).

2.1.2 Sedimentary Cover

Calcareous sediments are often well preserved when deposited above the carbonate compensation depth on top of oceanic swells or plateaus. As a result, the thick successions of sediments atop Shatsky Rise edifices have been the target of previous drilling expeditions, most notably DSDP Leg 32 (Moberly and Larson, 1975) and ODP Leg 198 (Bralower et al., 2006). As recovering sediments was not a primary objective of Expedition 324, basement drill sites were chosen at locations with thin sediment cover and only hard rock coring techniques were used, which led to lesser core recovery and more disturbance than would have occurred with coring techniques adapted for sediments. Moreover, the chert-infested carbonate sediments of the Cretaceous sediment cap were known to produce exceedingly poor recovery (e.g., Moberly and Larson, 1975), so sediments shallower than ~50-80 m above the igneous basement were not cored on Expedition 324. Nevertheless, a variety of basal sediment types were recovered from the five sites on Shatsky Rise (Expedition 324 Scientists, 2010a). As with previous coring, only indurated chert fragments were recovered from the Cretaceous chalk and limestone sections at each site. A rare exception is a short (~1.4 m) interval of pelagic ooze recovered at Site U1348, recording the rarely-preserved Santonian-Campanian transition (Ando et al., 2013). This section proves that poorly-consolidated ooze and chalk layers are indeed present deep within the pelagic cap, an assertion often made but rarely proved owing to poor core recovery. Prior to Expedition 324, recovery of a significant amount of non-pelagic

sediments had not been accomplished. Basal sediments retrieved during Expedition 324 range from bioclastic limestones and radiolarian-rich siliciclastics to volcaniclastic sequences (Fig. 5), indicating a complex sedimentation and subsidence history.

Although the sediment layers immediately overlying igneous basement did not always contain fossils that provide precise age constraints or ranges, an Early Cretaceous age of the sediments covering the volcanic rocks was confirmed at all drill sites (Expedition 324 Scientists, 2010a). Where ages were constrained in the basal sedimentary units, they fall in the following ranges: 133 to 140 Ma for Tamu Massif Site U1347, 100 to 127 Ma for Ori Massif Site U1349, and 128 to 142 Ma for Shirshov Massif Site U1346 (Expedition 324 Scientists, 2010a), thus providing minimum ages for the magmatic edifices below. At Tamu Massif flank Site U1348, where no basement was reached, the lowermost recovered microfossils indicate an age of >120 Ma for the edifice below (Expedition 324 Scientists, 2010d). In addition, the Sr isotopic composition of secondary calcite carbonate veins formed within fractures in the recovered lavas was used to constrain precipitation ages by correlation with the global seawater Sr isotopic evolution curve. Results from samples recovered at Sites U1347, U1349, and U1346 are consistent with minimum formation ages for the volcanic host rocks of ~143, ~134, and 128 Ma, respectively (Li et al., 2015). Sediment ages thus are consistent with the limited, newly obtained radiometric ages (Heaton and Koppers, 2014; Geldmacher et al., 2014; Tejada et al., in press, see Section 2.3 “Geochronlogy and Pattern of Volcanism”), support the postulated age decrease of the Shatsky Rise edifices from southwest to northeast as indicated by the magnetic lineations (Nakanishi et al., 1999), and confirm that Shatsky Rise edifices were built on young seafloor (Sager et al., 1999).

Volcaniclastic sediments above the igneous basement at Site U1347 contain a neritic (<200 m water depths) assemblage of benthic foraminifera and bedding structures indicative of shallow water conditions (shoreface environment above wave base) (Expedition 324 Scientists, 2010c). Because the nearby top of the volcano (shallowest basement on seismic profiles) is ~800 m shallower than these sediments (Expedition 324 Scientists, 2010a; Sager et al., 2011), the Tamu Massif summit may have been emergent. At Site U1349, a yellow-red clay layer of weathered basalt fragments at the top of the igneous basement is interpreted as paleosol (Expedition 324 Scientists, 2010e), implying subaerial exposure under tropical conditions (Expedition 324 Scientists, 2010a). In contrast, a shallow submarine depositional environment is indicated by oolitic limestone cored between lava flows ~10 m below the paleosol. Thus, the basement surface at Site U1349 must have been close to sea level. Shallow water depths are less precisely constrained for the basal sediments at Site U1346 on the Shirshov Massif summit; however, abundant shell fragments and a neritic benthic foramineferal assemblage indicate a depositional environment of <500m (Expedition 324 Scientists, 2010b). Taken as a whole, Expedition 324 sediments indicate that Shatsky Rise edifice summits were near sea level, but there is also no evidence for significant emergence.

2.2 Summit Depths and Subsidence

Other data pertaining to water depth give similar indications as the basal sediments, implying that Shatsky Rise edifice tops were in shallow water but not highly emergent. Seismic sections over the summit of Tamu Massif show no apparent truncation owing to wave action (Sager et al., 2013; Zhang et al., 2015), implying that the igneous pedestal was never greatly exposed. Seismic profiles over Ori and Shirshov massifs give similar indications (Zhang et al., 2015).

Backtracking of thermal subsidence for Expedition 324 drill sites brings all of the summit and near-summit sites to near sea level (Fig. 6), consistent with the interpretations from basal sediments (Expedition 324 Scientists, 2010a). Because the Stein and Stein (1992) cooling boundary layer (plate) model predicts less subsidence than the Parsons and Sclater (1977) half-space cooling model, the former predicts initial depths that were slightly submerged, whereas the latter indicates slightly emergent depths (Fig. 6). Nevertheless, both models imply that the present depths of Expedition 324 site basement interfaces are consistent with the inferences from sediments indicating depths near or slightly below sea level.

Additional evidence of emplacement depth comes from measurements of volatiles (CO_2, H_2O) in volcanic glasses from Expedition 324 cores measured by Shimizu et al. (2013). These data indicate that all sites were submarine, but emplaced within 1 km of sea level (U1347 - 943 m ±103 m; U1348 - 381 m ±48 m; U1350 - 767 m ±108 m; U1346 - 781 m ±76 m) and that implied subsidence was between 2500-3300 m. These subsidence values are greater by ~1 km than those estimated previously using fossil paleodepth estimates from sediments recovered at DSDP Site 305 on Tamu Massif (Ito and Clift, 1998), but presumably this difference can be attributed to several factors, including coring not reaching basal sediments at Site 305 and inexact fossil paleodepth estimates. Interestingly the volatile-derived subsidence data also show a progressive increase in subsidence from the center of Tamu Massif (Site U1347) to Ori Massif (Sites U1349, U1350), which may indicate that a buoyant mass retarded the subsidence of the Tamu Massif center (Shimizu et al., 2013). The authors also modeled uplift from isostatic compensation and thermal buoyancy of the mantle and concluded that no thermal component is required if Tamu Massif formed at the ridge crest (i.e., zero age crust) but that a model with the edifice formed on 5 Ma crust and with thinner crust than observed (i.e., ~20 km

rather than the ~30 km from refraction measurements (Korenaga and Sager, 2012)) can also fit the observed plateau elevation.

Overall, data on summit elevations of Shatsky Rise edifices place it near sea level but with no clear evidence of significant emergence. This fits Shatsky Rise between Kerguelen and Ontong Java plateaus in its emplacement depth. The former was largely emplaced subaerially (Coffin, 1992; Frey et al., 2003) whereas the latter was mostly emplaced >1 km below sea level (Michael, 1999; Fitton et al., 2004; Roberge et al., 2005). That Shatsky Rise was never highly emergent implies that its evolution was different than Iceland, a ridge-centered hotspot and possible mantle plume, which has an elevation of ~ 2 km (Ito et al., 2003).

2.3 Geochronology and the Pattern of Volcanism

Prior to Expedition 324, only one reliable radiometric date existed for Shatsky Rise, the 144.6 ±0.8 Ma date derived from Site 1213 samples (Mahoney et al., 2005). Ages for the igneous edifices were otherwise extrapolated from the ages of the sediments near the bottom of the sediment cap (Moberly and Larson, 1975) or by inference from magnetic lineations (Nakanishi et al., 1999) and gravity anomalies (Sandwell and MacKenzie, 1989). Research related to Expedition 324 has produced the first radiometric date for Ori Massif, ~134 Ma (Heaton and Koppers, 2014). If this date, from Site U1350 on the east flank, is accurate and does not reflect late-stage volcanism, it indicates a significant gap between the formation of the upper carapace of Ori Massif and the surrounding lithosphere. The current geomagnetic polarity time scale assigns 134 Ma to anomaly M10 (Gradstein et al., 2012; all magnetic anomaly ages herein use this time scale). By this time, magnetic lineations show that the triple junction was ~600 km farther northeast (Figs. 2, 3). Taken at face value, this difference implies off-ridge formation for Ori Massif, but this edifice contains magnetic anomalies that

are parallel to the nearby seafloor anomalies (see Section 2.7, "Magnetic Anomalies and Tectonic Evolution"), indicating formation at the ridge. An alternative explanation is a several-million-year gap between the eruption of last flows and the main shield building flows below, similar to findings at Tamu Massif (see below).

New radiometric dates also give important insights about the construction of Tamu Massif. The lower part of the recovered Site U1347 lava flow section is dated at ~143-145 Ma, nearly equal to that reported by Mahoney et al. (2005) for Site 1213 (Heaton and Koppers, 2014; Geldmacher et al., 2014). A significant age gap (~3 Myr from Heaton and Koppers (2014) and ~10 Myr from Geldmacher et al. (2014)) exists between the upper and lower massive lava flows within the U1347 section. What is more, recalibration of the 144.6 Ma date from Site 1213 shifts it to an age near that of the upper flows from Site U1347 (A. Koppers, personal communication, 2014). This surprising result implies that Tamu Massif was quiescent for at least several million years before another massive sheet flow complex was emplaced, capping the volcano at Sites 1213 and U1347. In a similar vein, the new radiometric date of ~129 Ma for Toronto Ridge (Tejada et al., in press), suggests that this ridge erupted ~15 Myr after the last large eruptions of Tamu Massif.

2.4 Seismic Imaging of Internal Structure

Although illuminating, Expedition 324 results suffer from being a small number of spot samples from a large plateau with uncertain extrapolation to the entire plateau. Seismic imaging carried out by the R/V *Marcus G. Langseth*, provided a crucial data set for integrating these results into the broad-scale structure of the plateau.

A tomographic seismic refraction cross-section across Tamu Massif imaged the Moho for the first time beneath the thickest part of the plateau, revealing a maximum crustal

thickness of ~30 km (Fig. 7; Korenaga and Sager, 2012). The observed thickness is consistent with complete Airy isostasy (Zhang et al., 2016). At the center of Tamu Massif, the ~3 km height (above the surrounding abyssal seafloor) is supported by ~18 km of isostatic root. Multichannel seismic transects also show seismic Moho beneath the distal flanks of the plateau, with the observed crustal thicknesses also consistent with Airy isostasy (Zhang et al. 2016). Complete Airy isostatic compensation explains the small, observed gravity anomaly values over the plateau. These observations indicate that most of the bulk of Tamu Massif lies within the mantle.

The refraction data provide two important clues about Tamu Massif crustal structure. No high-velocity lower layer was revealed at the base of the massif crust (Fig. 7), as is sometimes interpreted as magmatic underplating (e.g., Ito and Clift, 1998). In addition, these results also revealed a negative correlation between lower crustal seismic velocity and crustal thickness (Korenaga and Sager, 2012). Because hotter mantle temperature should cause greater melting (and thus greater crustal thickness), this finding can be taken as evidence that the source mantle was cool instead (Korenaga and Sager, 2012). This interpretation depends on the entire crustal column being formed at the same time (Korenaga et al., 2002), which may not be true if the volcano was built by long-traveled lava flows from the central region (Sager et al., 2013).

Multichannel seismic profiles from the R/V *Marcus G. Langseth* cruises display deep penetration into igneous basement, revealing faint, sub-parallel intrabasement reflectors (Figs. 8, 9) at two-way travel times of up to 2.0-2.5 seconds below the basement horizon (Sager et al., 2013; Zhang et al., 2015). Assuming an average seismic wave velocity of ~4 kms^{-1} in the upper crust (Korenaga and Sager, 2012), such travel-times imply depths of ~4-5 km within the

plateau. Comparison of velocity and density log data from Expedition 324 boreholes (Sites U1347, U1348) with the seismic data shows that the intrabasement reflectors result from acoustic impedance contrasts between groups of lava flows with different characteristics, such as the alternations of massive and pillow flows cored at Site U1347 (Zhang et al., 2015). A similar seismic expression is observed in multichannel seismic profiles collected from Ontong Java Plateau (Inoue et al., 2008) and Manihiki Plateau (Pietsch and Uenzelmann-Neben, 2015). At Site U1347, some reflectors resulted also from the thick sediment layers between lava flows (Zhang et al., 2015). Both findings imply that the intrabasement reflectors trace the surfaces of lava flows, so their geometry can be used to infer the lava-layer-cake structure within the edifice.

The intrabasement reflectors are often weak and discontinuous, a result of the small acoustic contrast between igneous units and the rough nature of the interfaces (Figs. 8, 9). However, these horizons are frequently observed for 10-15 km and can be readily connected into longer, piecewise continuous reflectors (Sager et al., 2013; Zhang et al., 2015; Vuong et al., 2015). The overall pattern of intrabasement reflectors is subparallel and follows the basement interface (Figs. 8, 9), implying lava flows descending from the summit to the flanks (Sager et al., 2013; Zhang et al., 2015). In fact, no matter what direction the seismic line crosses the Tamu summit, the same pattern is seen and no large secondary source of volcanism is observed (Sager et al., 2013; Zhang et al., 2015). This observation can be used to infer that Tamu Massif is an immense, single, shield volcano (the largest known single volcano) built by eruptions mainly from its center (Sager et al., 2013). Only a single deep-penetration multichannel seismic line was collected over the center of Ori Massif. This profile suggests that Ori Massif has a similar structure; although, another profile over the Ori Massif west flank suggests

internal complexity and hints at more than one volcanic center, similar to other large volcanic complexes, such as Hawaii (Zhang et al., 2015).

An interesting observation from the deepest reflections inside Tamu Massif is that the apparent dip of the intrabasement reflectors changes little with depth (Fig. 8; Zhang et al., 2015). If lavas emanated from the center and were preferentially deposited there, the center should have subsided owing to isostatic adjustment, causing reflectors to dip inward towards the center, similar to seaward dipping reflectors (Mutter et al., 1982; Mutter, 1985; Planke et al., 2000) – but this is not observed. This finding implies that the edifice was constructed in complete isostatic balance.

The multichannel seismic profiles also show the depth of Moho beneath the deep parts of the plateau between edifices (Zhang et al., 2016). In the region between Ori and Tamu massifs, the crust is about 60% thicker (~11 km vs. ~7 km outside the plateau). This is an important observation because the crust produces magnetic anomalies that appear to be from seafloor spreading (Fig. 2) (Nakanishi et al., 1999) and there was speculation that the crust between massifs was essentially normal (Sager et al., 1999). Seismic data indicate that this crust is significantly thicker than normal, yet it retains the magnetic anomaly signature and was thus formed by the seafloor spreading process.

2.5 Secondary Volcanism Atop Shatsky Rise Edifices

On almost any profile across Shatsky Rise, apparent secondary volcanic cones are observed (Sager et al., 1999; Sager et al., 2013; Zhang et al., 2015). These cones are generally distinguished by a small footprint, having diameters from a few to few tens of km (Fig. 10), and steeper flank slopes compared with the main plateau (>5 vs. ~1°). Indeed, because of the low slopes of the plateau flanks, these smaller features appear to tower over the main edifice in

vertically-exaggerated profiles (Fig. 8) whereas their smaller size is more evident on wide-area bathymetry plots (Figs. 1, 2, 10). It is also evident from seismic profiles that secondary cones are buried beneath the sediment cap on all three massifs (Zhang et al., 2015), implying that they erupted shortly after the main shield. Some secondary cones are larger, one example being the ~30 km-wide mound on the Tamu Massif north flank where Site U1348 was drilled (Expedition 324 Scientists, 2010a, d). Other large secondary features are summit ridges on both Tamu and Ori massifs. Toronto Ridge, located near the summit of the Tamu Massif shield (Figs. 8, 10), is ~ 1 km in height and ~50 km in length. Similar, buried and poorly mapped ridges are found atop Ori and Shirshov massifs (Klaus and Sager, 2002; Zhang et al, 2015), but their dimensions are ill defined.

The apparent flank slopes of the secondary cones and ridges are steeper (5°-10°) than the shallow flanks of the main Shatsky Rise massifs (Fig. 8), but nonetheless consistent with common seamount slopes (e.g., Smith, 1988). Other secondary cones consist of volcaniclastic deposits. Coring at Site U1348 penetrated ~120 m of volcaniclastic sediments (hyalocloastite, hyaloclastite breccia, and volcaniclastic sandstone), demonstrating that this mound is capped by material formed by explosive volcanism in shallow water (Expedition 324 Scientists, 2010d). Both types of cone (basalt and volcaniclastic) are commonly found on the flanks of large shield volcanoes (e.g., MacDonald and Abbott, 1970; Clague and Dalrymple, 1989). Those from Shatsky Rise seem to follow no particular trend nor do they form obvious groups or lineaments (Fig. 10), suggesting that they occur at more-or-less random locations.

Although some secondary volcanic cones are formed during the shield-building stage of a large volcano, others post-date the main volcano construction, sometimes by as much as ~5-10 Myr (e.g., MacDonald and Abbott, 1970; Clague and Dalrymple, 1989; Lonsdale et al.,

1993). Age constraints on Shatsky Rise secondary eruptions are mostly lacking. Those imaged on seismic lines appear to have bases at or near the bottom of the sediment section, implying that they formed near the time that the volcano was done erupting. This is true for Toronto Ridge, atop Tamu Massif, which has been radiometrically dated at ~129 Ma (see Section 2.3), ~15 Myr younger than the youngest flows from nearby Sites 1213 and U1347 (Heaton and Koppers, 2014; Tejada et al., in press). This age gap fits the inference from subsidence that Toronto Ridge could not have formed until the summit of Tamu Massif subsided ~1 km (Sager et al., 1999). The long hiatus indicates that small-scale eruptions occurred on Tamu Massif long after the primary locus of volcanism moved away. If the date for the rocks from Toronto Ridge is accurate, the primary locus of volcanism was by then located near magnetic anomaly M1, ~1300 km to the northeast.

2.6 Paleomagnetic Evidence for Eruption Timing and Paleolatitude

Paleomagnetic data can provide clues about the timing of volcanic eruptions by comparison with known rates of geomagnetic secular variation as well as about the tectonic evolution from shifting paleolatitudes. It has been known for some time that Shatsky Rise formed near the equator (Larson et al., 1992; Sager et al., 2005; Tominaga et al., 2005) before drifting northward to its current location, but few reliable data have previously been available from the plateau. Expedition 324 paleomagnetic measurements (Pueringer et al., 2013; Carvallo and Camps, 2013; Carvallo et al., 2013; Carvallo, 2014) show that the variation in paleoinclination at most sites is small, implying that a small amount of time elapsed during the emplacement of most of the cored sections. Data from Sites 1213, U1346, and U1349 essentially show no variation in magnetic inclination, consistent with formation over periods of 100-200 yr (Sager et al., 2015). Site U1347 data are similar, with only one significant change in paleoinclination, but this finding is at odds with a likely hiatus of at least several million

years between the upper massive flows and the rest of the section (Geldmacher et al., 2014; Heaton and Koppers, 2014) as well as the finding of thick sedimentary layers in the upper igneous section (Tominaga et al., 2014). This discrepancy likely reflects the fact that the quasi-periodic nature of geomagnetic secular variation means that rocks having a significant time gap do not necessarily display a significant change in paleoinclination.

Another reflection of a possible age gap within the Site U1347 section is the finding that magnetic logs collected within the borehole show a change in the sign of the inferred paleoinclination near the bottom of the section (Tominaga et al., 2012). This was interpreted as having resulted from an eruptive hiatus during which Tamu Massif drifted across the paleoequator (Tominaga et al., 2012). At odds with this conclusion is the finding that paleomagnetic samples from the Site U1347 cores do not show a change the inclination sign, so the log data may affected by complexity of the borehole magnetic field and are thus misleading (Sager et al., 2015).

Site U1350 is the only site that shows significant changes in paleoinclination between inclination groups with these differences ascribed to paleosecular variation (Sager et al., 2015). This section is thought to have formed over a period long enough to permit significant paleosecular variation (~1000 yr) but not enough to completely average the variations (~10,000 yr). The result implies that lava flows at lower flank sites (Site U1350) can build up much more slowly than at summit sites (e.g., Sites 1213, U1346, U1347, U1349).

New Shatsky Rise paleolatitude data are also consistent with prior data indicating that the plateau formed near the equator (Larson et al., 1992; Tominaga et al., 2005; Sager et al., 2005). Paleolatitudes at all sites are low and mostly <5° from the equator (Sager et al., 2015).

It appears that the paleolatitude of Shatsky Rise was equatorial throughout its formation history. Because the locus of volcanism drifted northeast relative to the Pacific plate, Shatsky Rise staying at the equator implies that the Pacific plate drifted southward during this period, supporting prior studies that made the same claim (Larson and Lowrie, 1975; Larson et al., 1992; Sager, 2006).

2.7 Magnetic Anomalies and Tectonic Evolution

Magnetic lineations are found within Shatsky Rise (Sager et al., 1988; 1999; Nakanishi et al., 1999). Because there are large gaps between tracks in many places, it is difficult to trace and identify these lineations through the higher elevations of the plateau; although, it appears that lineations traverse parts of all three massifs (Nakanishi et al., 1999). The lineations within Ori Massif are particularly striking in their linearity and the close correspondence in strike with those in adjacent seafloor (Fig. 10; Nakanishi et al., 1999; Huang and Sager, 2013). Although most of Tamu Massif is characterized by a broad anomaly that can be fit by a model of the volcano shape (Sager and Han, 1993), lineations likely traverse the north flank of the edifice (Fig. 2) (Nakanishi et al., 1999). This difference is an important dichotomy. Magnetic lineations only form where magmatic eruptions are constrained laterally to a narrow zone, as at mid-ocean spreading ridges (e.g., Gee and Kent, 2007). In contrast, the massive flows cored from the center of Tamu Massif imply voluminous, far-traveled flows (Sager et al., 2013). This dichotomy may be further evidence of the change in eruption volume from Tamu Massif to Ori and Shirshov massifs. The possibility that Tamu Massif has different characteristics between its center and north flank may indicate a fundamental change in the style of volcanism during the evolution of the plateau.

Magnetic and bathymetry data from cruise YK09-09, southwest of Tamu Massif, give a better understanding of the evolution of the triple junction and the onset of Shatsky Rise volcanism. These data indicate that the reorganization of the triple junction, formerly thought to have occurred between M21-M20 time (Sager et al., 1988; Nakanishi et al., 1999), actually occurred slightly earlier. As shown by lineations southwest of Tamu Massif, the reorganization began between M23 to M22 time (153-151 Ma) ~2 Myr prior to the earliest possible beginning of Tamu Massif eruptions (Nakanishi et al., 2015). Although the timing of the start of Tamu Massif eruptions is unknown, it must have been later than ~150 Ma, the age of magnetic anomaly M21, because the plateau sits on younger lithosphere. The implication is that the plate boundary and triple junction reorganization were not caused by the eruptions at Tamu Massif (Nakanishi et al., 2015).

2.8 Geochemical Clues About Magma Genesis and Evolution

2.8.1. Magma types

Sano et al. (2012) and Husen et al. (2013) reported chemical compositions of a total of 170 fresh glass samples from four of the Expedition 324 drilling sites (U1346, U1347, U1348, and U1350). Such fresh glass samples are preferred for geochemical studies owing to their lack of alteration. No fresh glass was recovered from Site U1349, so whole rock analyses were done on the freshest basalt samples (loss on ignition, LOI, <3.2 wt %). In plots of elements and oxides versus MgO content, the data from glass and fresh rocks show that Shatsky Rise igneous rocks are abyssal tholeiitic basalts whose compositions are similar to MORB and OJP basalts (Fig. 13). Chemical compositions and Nb/Ti ratios (both alteration resistant elements; Table 1) allow the division of Shatsky Rise basalts into four types: (1) normal, (2) low-Ti, (3) high-Nb, and (4) U1349 types (Sano et al., 2012).

Chemical compositions of the normal type basalts are similar to normal-MORB (N-MORB), with trends that can be explained by fractional crystallization under low-pressure conditions (Fig. 13). These rocks vary from less evolved (MgO ~8.5 wt %) to more evolved (MgO ~5.0 wt %). Most basalt samples from Sites 1213, U1346, U1347 and U1350 are classified as the normal type, the dominant basalt in Shatsky Rise, with 94% of Tamu Massif, 43% of Ori Massif, and 100% of Shirshov Massif rocks being of this class (Table 1).

Low-Ti type rocks are present at Site U1347 on Tamu Massif and Site U1350 on Ori Massif. The total percentage of low-Ti type among cored lavas is estimated to be 6%, the smallest among the four types (Table 1). This rock type has slightly lower TiO_2, FeO*, MnO, V, and Sr, and higher Al_2O_3 contents compared to the normal type basalt. In addition, this class includes only rocks with evolved compositions (MgO <7.0 wt %). Comparison of low-Ti rocks from Site U1347 versus Site U1350 shows that the former are more highly evolved (MgO <5.5 wt %) than those of the latter (MgO >6.0 wt %). This fact suggests that the lavas from these two sites have different magma sources, an interpretation supported by Nd and Hf isotopic data from one of the samples from Site U1350, which has a slightly enriched isotopic composition (slightly lower $^{143}Nd/^{144}Nd$ and $^{176}Hf/^{177}Hf$) compared to those from Site 1347 (Heydolph et al., 2014).

The high-Nb type is characterized by distinctly high contents in K, Nb, Ta, Zr and rare earth elements (REEs). Trace-element signatures for these rocks are similar to enriched-MORB (E-MORB) (Fig. 13) from the East Pacific Rise. The enriched characteristics are also confirmed by isotopic data; higher $^{207}Pb/^{204}Pb$ and lower $^{143}Nd/^{144}Nd$ and $^{176}Hf/^{177}Hf$ (Heydolph et al., 2014), suggesting the presence of an enriched mantle source. Simple fractional crystallization processes cannot explain the differences between the normal-type and

the high-Nb type, implying different mantle source characteristics. The high-Nb type only appears at Site U1350 on Ori Massif, but is identified in several lava flows from this site. The percentage of high-Nb type rocks among the total cored lavas is estimated to be 10% (Table 1). Similar trace-element enriched rocks were recovered from one interval of the ~120 m-thick volcaniclastic section at Site U1348; however, compositions of the Site U1348 rocks are different from the high-Nb type basalts of Site U1350 and because only volcaniclastics were cored at this site, the Site U1348 samples have not been factored into the estimated percentage of magma types (Sano et al., 2012). In addition, similar isotopically-enriched lavas have been identified in dredged seamount samples from the northern sector of Shatsky Rise (Tejada et al., in press).

Despite the effect of alteration on Site U1349 samples, which affected these rocks more than at other sites, the rocks from this site appear to represent significantly less evolved magmas (MgO, 9-12 wt %) than those of other magma types (Fig. 13). Moreover, the Site U1349 lavas are highly depleted in incompatible trace elements compared to the normal type lavas, a difference indicating that the former cannot be parental for the latter. Less evolved compositions are consistent with analyses of melt inclusions contained in fresh olivine phenocrysts from Site U1349 (Almeev et al., 2011). These melt inclusions have less evolved compositions with high MgO (>11 wt %) and are very similar to those of the whole rocks (Almeev et al., 2011; Sano et al., 2012). Since melt inclusions in fresh olivine give information about the magma before alteration, the U1349 lavas can be confirmed as being derived from a fourth magma type (i.e., type U1349). The 85-m-thick basement section at Site U1349, on the summit of Ori Massif, is composed of only the U1349 type basalt. The percentage of this type is estimated to be 19% of the total recovered lavas from Shatsky Rise (Table 1). Compositions

of U1349 samples are the most depleted among MORB samples worldwide. Before the report of U1349 type basalt, the most depleted MORB sample was reported to be depleted basalts from Lamont seamounts and adjacent East Pacific Rise (Allan et al., 1989).

2.8.2 Transition of Magma Types with Time

An advantage for studying Shatsky Rise among various LIPs is that its formation history is relatively well known. The largest volcanic edifice, Tamu Massif, was formed first, and smaller Ori and Shirshov massifs were constructed subsequently (Sager et al., 1999; Nakanishi et al., 1999). This knowledge makes it possible to infer the transition of magma types with time from the observed differences in lava chemistries.

The percentage of cored section composed of the normal type basalts decreases from ~94% at Tamu Massif to only ~43% at Ori Massif. At Shirshov Massif, only normal type lavas were recovered, but the significance of this finding is unclear because the 53-m thick section is only one eruptive unit. This short section may not be as representative of the whole edifice as are the basalts recovered from the considerably deeper (up to ~173 m) basement sections at the other drill sites (Expedition 324 Scientists, 2010a). Nevertheless, the normal type lavas from Shirshov differ from all other drilled Shatsky Rise lavas in their Hf and Nd isotopic characteristics (Heydolph et al., 2014).

In order to identify geochemical evolution with time, we use a discrimination diagram, a logarithmic plot of Nb/Y versus Zr/Y (Fig. 14). The advantage of this diagram is that it can separate enriched basalts (e.g., E-MORB and/or ocean island basalts) and N-MORB (Fitton et al., 2003). The diagram shows that Tamu Massif basalts have nearly homogeneous N-MORB-compositions, but in contrast, Ori Massif basalts have a large compositional variety from highly depleted U1349 type basalts to enriched high-Nb type basalts (Fig. 14). Moreover, most

high-Nb type basalts plot on the Iceland array field (Fitton et al., 1997), suggesting that the magma source was affected by enriched materials such as plume components (e.g., Campbell, 2007) or fusible recycled oceanic crust (e.g., Korenaga, 2005; Foulger, 2011). The compositional differences between Tamu and Ori massifs further suggest that geochemical variation increased with time as the magma volume decreased. This geochemical evolution is also observed in isotopic data (Heydolph et al., 2014), which show $^{143}Nd/^{144}Nd$ and $^{176}Hf/^{177}Hf$ ratios becoming more heterogeneous with time (see Section 2.9 "Isotope Chemistry").

High Zr/Y and Nb/Y tholeiitic basalts were also dredged from Cooperation Seamount (Fig. 14), located in Helios Basin between Tamu and Ori massifs (Tatsumi et al., 1998). The age of this seamount is unknown, but a minimum age of ~122 Ma is implied based on recent attempts of $^{40}Ar/^{39}Ar$ dating (Tejada et al., in press) so it likely formed after Tamu Massif. Thus the Cooperation Seamount geochemical data also suggest that enriched characteristics evolved with time. Further progress on geochemical evolution awaits systematic sampling and age determinations for igneous rocks of potential late stage volcanism, including the Papanin Ridge and Ojin Rise Seamounts (Fig. 1).

2.8.3 Melting conditions

The best sample to estimate melting conditions is an igneous rock with a primary composition that formed in equilibrium with mantle peridotite. Such primary rocks should have olivines with high forsterite content (Fo: 100 x Mg/(Mg+Fe2+) >90). However, no such rocks have been recovered from any of the Pacific LIPs. The next best candidate is a high-Mg primitive rock that experienced partial crystallization of olivine only. The discovery of high-Mg Kroenke type basalts from the OJP has made it possible to estimate the primary composition and has extended our knowledge of their melting conditions considerably (Fitton

and Godard, 2004; Herzberg, 2004). However, a fresh, high-Mg basalt has yet to be recovered from Shatsky Rise. Therefore it is not easy to estimate the melting conditions. Despite this difficulty, melting conditions of the normal type magma on Shatsky Rise have been roughly estimated by two different methods, one using immobile trace element geochemistry (Sano et al., 2012) and another using major element chemistry (Husen et al., 2013).

Using primitive mantle-normalized patterns, Sano et al. (2012) noted that normal type lavas display relative enrichment of highly incompatible elements and slight but systematic depletion of heavy REEs (HREEs), indicating melting in the residual garnet temperature field. Model calculations of immobile trace elements indicate that the normal type basalts can be formed by ~15% melting of a depleted mantle source. One result of the calculations is shown in Figure 14, a model calculation for Nb/Y that estimates 15~20% melting of garnet-lherzolite to produce an average of the normal type basalts. The degree of melting for the normal type magma is similar to N-MORB, but the residual garnet implies a greater depth of melting. This model implies a melting depth >30 km beneath Shatsky Rise, which is considerably deeper than that for N-MORB magmas (<15 km; Langmuir et al., 1992).

Deep melting of the normal type magma was also proposed by Husen et al. (2013), based on a correlation between fractionation-corrected FeO parameter (i.e., Fe_8) with the depth of final melting (Klein and Langmuir, 1987; Niu and O'Hara, 2008). Husen et al. (2013) also reported that Shatsky Rise basalts have lower Na_8 (fractionation-corrected Na_2O contents) and higher Ca_8/Al_8 (fractionation-corrected CaO/Al_2O_3) than East Pacific Rise (EPR) MORBs (Fig. 15). This finding implies higher degrees of partial melting (20~23%) than those of N-MORBs.

When we combine the two results outlined above (Sano et al., 2012; Husen et al., 2013), the estimated degrees of partial melting for Shatsky Rise magmas (15~23%) are equal to or greater than those of MORB magmas, but less than the ~30% inferred from the OJP (Fitton and Godard, 2004). The lower Nb/Y and Zr/Y ratios in the OJP basalts are consistent with the estimated high degree of melting inferred from the garnet-lherzolite melting model (Fig. 13).

Although the abundant normal type basalts yield data that allow us to interpret melting depth, magma genesis for the other three basalt types is still uncertain. The low-Ti type basalts from Site U1347 on Tamu Massif may have formed by partial melting of the same depleted mantle source as the normal type because low-Ti basalts are generally isotopically indistinguishable from the normal type (Heydolph et al., 2014). The lower TiO_2 content of the low-Ti type basalt compared with the normal type basalt (at the same MgO content) could be explained by a higher degree of partial melting of the former. However, as Sano et al. (2012) pointed out, this suggestion fails to explain the observed compositional variety of other incompatible trace elements (e.g., Nb, Ta, and La). A reasonable explanation for the origin of the Site U1347 low-Ti type is magma mixing between less evolved (MgO ~8 wt %) normal type magma and highly evolved (MgO <4 wt %) magma that experienced fractional crystallization of Fe-Ti oxide minerals such as magnetite. Figure 13 illustrates that TiO_2 and V contents decrease with decreasing MgO when MgO content is lower than 4 wt %. This trend is explained by magnetite fractionation from the highly evolved magma. When this highly evolved magma (MgO <4 wt %) is mixed with less evolved magma (MgO ~8 wt %), a low-Ti type magma composition can result (J. H. Natland, personal communication 2014). As for the low-Ti type rock recovered at Site U1350 on Ori Massif, isotopic ratios are slightly enriched compared to the normal type (Heydolph et al., 2014), suggesting contamination by a more

enriched mantle source. Because low-Ti type rocks often appear adjacent to the high-Nb type at Site U1350, the enriched high-Nb type magma could have easily mixed with normal type magma to produce the low-Ti type magma. Therefore assimilation of high-Nb type magma is a likely explanation of low-Ti type chemistry at Site U1350. However, this possibility should be examined by future work because only one sample of the low-Ti type from Site U1350 was analyzed for isotope chemistry (Heydolph et al., 2014).

Melting conditions to produce the high-Nb type basalts cannot be estimated by the methods of Sano et al. (2012) because source mantle compositions have not been constrained for this magma type. Distinctly higher concentrations of the more incompatible trace elements and lower $^{143}Nd/^{144}Nd$ and $^{176}Hd/^{177}Hf$ and higher $^{207}Pb/^{206}Pb$ ratios reflect an enriched source for the high-Nb magmas (Heydolph et al., 2014) (see Section 2.9, "Isotope Geochemistry" below).

The highly depleted U1349 type basalt was proposed to have formed by melting of a very depleted mantle from which a large amount of normal type magma was previously extracted (Sano et al., 2012). This proposal was based solely on elemental concentration data. Isotope compositions, however, indicate that the U1349 type samples are more depleted than those of the normal type and overlap with early Cretaceous (129 Ma) local MORB (Heydolph et al., 2014), recovered ~200 km to the northwest of Shatsky Rise at ODP Site 1179 (Fig. 1). Thus, the U1349 type magma could presumably have formed by high degree partial melting of the local depleted (MORB-source) mantle (Heydolph et al., 2014). Since incompatible trace element data of the U1349 type basalts indicate even more depletion than normal depleted mantle (DM, Fig. 14), previous melt depletion cannot be ruled out.

2.8.4 Source temperature

As the crustal thickness of Shatsky Rise is several times thicker than that of normal oceanic plates, the presence of a thermal anomaly (i.e., a thermal plume head) beneath the plateau was proposed as a mechanism to produce a large amount of magma (Sager and Han, 1993). Whether such an anomaly existed beneath Shatsky Rise is thus an important facet of understanding the formation of the plateau. Because temperature increases with depth, temperature comparison at depth is commonly done with a one-atmosphere reference, termed the mantle potential temperature (T_P: McKenzie and Bickle, 1988). The T_P is the temperature that the solid, adiabatically-convecting mantle would attain if it could reach the surface without melting.

Figure 16 shows a set of melt-fraction-depth profiles for T_P ranging from 1300° to 1600 °C, assuming perfect fractional melting (Iwamori et al., 1995). This model was derived by compilation of results of melting experiments on mantle peridotites and the determination of pressure-temperature-degree of partial melting (P-T-X) relationships (Iwamori et al., 1995). In the P-T-X space, the degree of partial melting was calculated by assuming adiabatic upwelling of mantle peridotite. The calculations were conducted on two melting models, batch and perfect fractional melting models. Since the latter model is thought to be a better approximation of processes of seafloor creation, it is preferred here. These profiles show the extent to which mantle of a given T_P would melt if decompressed instantaneously at the depth shown. Thus, mantle with T_P = 1300 °C would begin to melt a depth of 40 km, and melting would increase with decreasing depth until it reached ~16 % at the surface. The melting model (Fig. 16) depends on the vertical axis only, but melt zones beneath mid-ocean ridges are assumed to be two-dimensional (triangular in cross section). Melting is maximal beneath the ridge axis and decreases to zero with distance from the axis (e.g., Langmuir et al., 1992), so the

modeled melting is applicable to the ridge axis. Integrating the melt fraction across the melt zone gives the volumetric average of the melting, which will be less than the maximum degree shown in Figure 16. Thus, an exact T_P estimation by using this method requires a complex calculation. However, comparative estimations are possible when we assume the same simple melting model (i.e., decompression melting only along a vertical axis). Because Shatsky Rise is thought to have formed at a spreading ridge triple junction (Nakanishi et al., 1999), we may simply compare the Shatsky Rise basalts to present MORB.

It is clear from the model profiles (Fig. 16) that melt fractions required to produce Shatsky Rise and OJP magmas cannot be achieved using decompression melting at a reasonable temperature beneath an oceanic lithosphere of normal thickness (~100 km). The lithosphere must have been thinner than normal but cannot have been thinner than the Shatsky Rise and OJP crust (~30 km) by the time the lava flows were erupted. Assuming that the melting stopped at ~30 km (Sano et al., 2012), the T_P of Shatsky Rise magma is estimated to be 1400-1500°C (Fig. 16) so as to achieve the proposed melt fraction (15~23 %). Figure 16 also indicates that the T_P of Shatsky Rise is ~100°C lower than that estimated for the OJP and ~50°C higher than MORB. Similar to Shatsky Rise, crust and lithosphere beneath the OJP is thick (e.g., Ishikawa et al., 2004). The higher T_P estimation for the OJP magma resulted from the higher melt fraction estimated for the OJP magma (~30 %).

Recently, the T_P of the Shatsky Rise magma was estimated by another approach, a numerical trace element mass balance model considering a pyroxenite-bearing peridotite source mantle (Kimura and Kawabata, 2015). On the basis of this model, the T_P of normal type magma from Shatsky Rise was calculated to be 1360-1403 °C, distinctly higher than that of MORB (<1310°C) but in accord with the estimate from Figure 16.

2.8.5. Magmatic Evolution

Magmatic evolution in magma chambers is deeply related to formation of the crust. For example, solidified shallow magma chambers are thought to form gabbros in the lower oceanic crust and deep magma chambers are presumably located near the Moho. Therefore it is important to estimate the depth of a magma chamber for evaluating the magmatic evolution.

The depth of the magma chamber(s) beneath the Shatsky Rise was first estimated by comparing observed rock compositions with cotectic lines of experimentally-determined liquids that are in equilibrium with three phases: olivine, plagioclase, and augite (Sano et al., 2012). This method depends on saturation of the observed compositions with the three phases and if this is not achieved, the pressure cannot be estimated because the liquid compositions will not plot on cotectic lines. Because less evolved, high MgO (>8 wt %) samples would not be saturated with augite, Sano et al. (2012) selected only relatively evolved (MgO <8 wt %) samples for pressure estimations. The comparison of observed compositions with cotectic lines of previously experimentally determined liquids shows that all the evolved (MgO <8 wt %) Shatsky Rise basalts crystallized at depths <6 km (Sano et al., 2012). Husen et al. (2013) judged that the compositional trend of the less evolved samples (CaO of normal and U1349 type basalts increases with decreasing MgO for samples with MgO >8 wt% in Fig. 13) was not a fractional crystallization trend and proposed that the most Mg-rich glasses from Ori Massif are saturated with the three phases at ~650 MPa (Husen et al., 2013). The estimated high pressure is appropriate for a depth near the base of thick plateau crust (~20 km), suggesting a deep magma chamber. The inference of the deeper magma chamber (~400 MPa) has been confirmed by a study of melting experiments (Husen et al., 2016). Likewise, high-pressure crystallization (~700 MPa) of one spinel sample from Site 1349 was inferred from geobarometer calculations using the pressure dependence between the compositions of melts

and those of spinels (J. Natland and R. Almeev, personal communication, 2014). However, all other spinel crystals from the entire Shatsky Rise show crystallization at low pressure, implying shallower crystallization levels (Natland and Almeev, unpublished manuscript, 2014). The recognition of both shallow and deep pressure regimes implies that magmas within Ori Massif gather at least two levels, one shallow (<6 km) and one deep (~20 km) near the base of the crust. Unfortunately, evidence for the deep magma chamber beneath the Tamu and Shirshov massifs is missing owing to the lack of suitable samples for making this inference.

2.9 Isotope Geochemistry: Fingerprints of Mantle Reservoirs

The isotopic investigation of Shatsky lavas aimed to distinguish the four magma types defined by Sano et al. (2012) by their isotopic signatures and to provide clues on the origin of the magmas (Heydolph et al., 2014). Normal type and low-Ti type lavas are relatively depleted (with respect to the high-Nb type lavas and global OIB) in terms of trace elements (Fig. 17) and also have relatively depleted initial Nd, Pb and Hf isotopic compositions (high Nd and Hf but low Pb isotope ratios) overlapping with Pacific MORB (age corrected to the Early Mesozoic). The close genetic relationship of these two groups (normal and low-Ti), as suggested by Sano et al. (2012), is corroborated by their overlapping isotopic compositions. In contrast, the High-Nb type lavas reflect a more enriched source, based on their lower $^{146}Nd/^{147}Nd$ and $^{176}Hf/^{177}Hf$ ratios (Fig. 17) but higher $^{207}Pb/^{204}Pb$, $^{208}Pb/^{204}Pb$, and $^{87}Sr/^{86}Sr$ (not shown) that trend towards enriched global mantle endmembers such as Enriched Mantle (EM) I or II (Heydolph et al., 2014). In contrast, the U1349 type lavas yield the most depleted Nd and Hf isotopic compositions and the most depleted $^{206}Pb/^{204}Pb$ ratios. Furthermore, this group overlaps with contemporary, local MORB samples from Site 1179, obtained from early Cretaceous oceanic crust just north of Shatsky (Fig. 1). Overall, the Shatsky Rise magma source appears to become isotopically more heterogeneous with time and decreasing eruption

volume (see also Section 2.8.2. "Transition of Magma Types with time"). Whereas all lavas from Tamu Massif have a limited range of isotopic compositions, lavas from the younger Ori and Shirshof Massifs show a larger degree of isotopic variation (Fig. 17b).

Obtaining He isotope data from the Shatsky lavas was particularly desirable because high $^{3}He/^{4}He$ ratios are commonly considered to indicate derivation from mantle sources rich in primordial volatiles ("undegassed") derived from the lower, unprocessed mantle (e.g., Kurz et al., 1982; Hanan and Graham, 1996). Unfortunately, fresh volcanic glass suitable for He isotope analyses could only be recovered from the normal-type samples. Although these lavas possess Nd, Pb and Hf isotope compositions within the MORB range (Fig. 16), their $^{3}He/^{4}He$ ratios are systematically lower than MORB (<6 $^{3}He/^{4}He_{(Ra)}$, Hanyu et al., 2015). Normal and low-Ti lavas also yield $\delta^{51}V$ values heavier than MORB (Prytulak et al., 2013). The interpretation of V isotopes with respect to mantle source provenances is not clear yet, but the combined He and V isotope data indicate that the normal and low-Ti-type lavas are distinct from MORB, despite their otherwise compositional similarity. Interestingly, the single High-Nb type sample analyzed for V isotopes shows a lighter value than MORB, underlining the dissimilarity of the high-Nb type magma source to all other lava types of Shatsky Rise. It seems that the high-Nb type lavas are also distinct in their Li isotopic composition (based, however, only on one analysis from this group), showing combined enriched trace element composition and high $\delta^{7}Li$, consistent with the involvement of recycled slab or subduction modified material in the magma source (Sano and Nishio, 2015).

2.10. Igneous Rock Alteration

2.10.1. Low-temperature Hydrothermal Alteration

The entire sequence of basaltic basement samples recovered from Shatsky Rise has undergone low-temperature water-rock interactions, resulting in complete replacement of olivine and mesostasis (Expedition 324 Scientists, 2010a). Macroscopic observation and mineralogical investigation show that the degree of alteration follows a pattern tied to basement elevation. The three sections from the rise flanks (Sites 1213, U1347, U1350) are only slightly altered, resulting from low-temperature interaction with seawater-derived fluids in anoxic to sub-oxic conditions. In contrast, the three sections cored at high points (Sites U1346, U1348, U1350) are highly altered, and alteration types differ among the three sites. Since the high point basement is made of permeable basalts or volcaniclastic rocks and sediment cover does not greatly inhibit circulation, hydrothermal circulation was significant.

The ~120-m-thick volcaniclastic, typically hyaloclastite, sequences of Site U1348 are highly altered and mostly transformed to secondary palagonite and cemented with zeolite and/or calcite. The two summit sites, U1346 and U1349, are the most altered sites among the Shatsky Rise drill sites and show the greatest variability in alteration type. Therefore the main targets of alteration work for Shatsky Rise were these summit sites (Delacour and Guillaume, 2013). The alteration types are characterized by secondary mineral assemblages including smectites, calcite, celadonite, kaolinite, illite, chlorite, zeolite, sulfides, Fe oxides, and Fe oxyhydroxides.

At Site U1346, three types of alteration were reported: green alteration, dark gray alteration, and brown alteration (Expedition 324 Scientists, 2010b). The green alteration is characterized by celadonite and zeolite of heulandite, suggesting interaction of the basalt with

low-temperature (<100 °C) seawater-derived fluid. The dark gray alteration results from generation of several smectite minerals (saponite, hectorite, stevensite, montmorillonite) and variable amounts of calcite. The brown alteration is caused by presence of smectites, kaolinite, and calcite. Kaolinite was firstly described as an alteration product of oceanic basaltic rocks and may result from alteration of feldspar (Delacour and Guillaume, 2013). The secondary mineral assemblages of the Site U1346 samples indicate that the alterations occurred under low temperature conditions (<100 °C).

Site U1349 basement rocks are divided into three units based on alteration type: from top to bottom, red-brown alteration, transition zone, and green alteration (Expedition 324 Scientists. 2010e). The red-brown alteration is characterized by iddingsite (composed of nontronite and hematite), illite, and calcite. The occurrence of iddingsite implies subaerial alteration of Site U1349 lava flows because this mineral is generated by fluid-rock interaction under low-temperature and highly oxidizing conditions. The transition zone and green alteration zone are composed of smectites, kaolinite, chlorite, calcite and illite. The presence of chlorite suggests interaction of the basalts with relatively high temperature (>100 °C) fluid under more reducing conditions. The occurrence of secondary minerals in Site U1349 cores indicates that alteration temperatures increase and redox conditions become more reducing with increasing depth.

At Site U1348, turbiditic tuffs were recovered from the upper part of the basement section (Expedition 324 Scientists, 2010d). They are almost completely transformed to clays and zeolites, and only thin sections reveal that they first went through formation of palagonite. The characteristic palagonite attribute, the occurrence of secondary “spherulites”, is pronounced in each sample, but the other typical characteristic of palagonite (orange color of

replaced glass) is no longer present. Clay minerals are ubiquitous, and clays and zeolites hold together the formerly glassy beds.

Low-temperature alteration identified by a mineralogical study (Delacour and Guillaume, 2013) is also confirmed by a geochemical study (Miyoshi et al., 2015). Among several elements, boron (B) is the most powerful tracer to identify low-temperature alteration because a significant amount of B is removed from seawater-derived fluid and incorporated into secondary minerals at low temperatures. Altered lavas from Sites U1346 and U1349 are highly enriched in B (i.e., high B/K; Fig. 18), suggesting high degrees of low-temperature hydrothermal alteration. In contrast, altered lavas from Shatsky Rise are not enriched in Cl, a tracer of high-temperature hydrothermal alteration (Fig. 18). This fact suggests that lavas recovered from IODP Expedition 324 have not experienced considerable high-temperature hydrothermal alteration after the emplacement.

Petrographical, mineralogical, and geochemical comparisons between fresh glass and whole rock samples in the same lava flows from the U1347 and U1350 sites have suggested that the onset of seawater alteration is largely dependent on the initial crystallinity and abundance of olivine (Romanova et al., submitted). Highly crystalline, high-Mg basalts undergo olivine decomposition to saponite clays and calcite, resulting in Mg-loss by 2–3 wt %. In contrast, highly-crystalline, low-Mg basalts show no significant change in MgO compositions (±0.2 wt%). A decrease in crystallinity is associated with increase in smectite clay formation and correlates with higher Mg and Ca content.

2.10.2. High-temperature Hydrothermal Alteration

There is no mineralogical observation for fluid-rock interaction at high temperature conditions in basaltic lavas from Shatsky Rise, but indirect evidence in fresh samples imply

magma contamination of hydrothermally influenced crust. Cl-enrichment (i.e., high Cl/K) in fresh glasses from Site U1350 (Fig. 18), suggests that magmas may have assimilated hydrothermally altered host rocks (e.g., high Cl/K gabbro) surrounding the magma chambers. Furthermore, the contamination of hydrothermally influenced crust is also indicated by the presence of high δ^7Li and low Yb/Li samples; Figure 19 shows that relationship between δ^7Li and Yb/Li of fresh glasses from Shatsky Rise suggests binary mixing between basaltic Li and hydrothermally influenced crustal Li (Sano and Nishio, in 2015).

Evidence for magmatic assimilation of previously hydrothermally influenced crust is also seen at fast spreading ridges (Michael and Cornell, 1998) and the Ontong Java Plateau (Michael, 1999; Sano and Nishio, 2015). These observations imply that beneath the Pacific LIPs as well as fast spreading ridges, well-established melt lenses were present and acted as filters through which most extruded magmas passed, and by doing so, may assimilate hydrothermally altered wall rocks.

3. Discussion

3.1 Evolution of an Oceanic Plateau

Recent research on Shatsky Rise has greatly improved our knowledge of the structure and development of oceanic plateaus. Once these LIPs were enigmatic features, but they are now coming into better focus as enormous shield volcanoes with a life cycle similar but not identical to other large basaltic volcanoes. Indeed, the morphologies and eruption style of these volcanoes is sufficiently different from more common seamounts that they should be considered a different class altogether.

3.1.1 Structure and Volcanic Style

Shatsky Rise consists of three individual massifs and two of them (Tamu and Ori) have been shown by deep-penetration seismic data to be large shields with low (0.5°-1.0°) flanks. The interior structure of Tamu Massif shows no indication of any other significant source of lava flows other than its center. It is thus the largest known single volcano (Sager et al., 2013). At less than a third the volume of Tamu Massif, Ori Massif is nonetheless an enormous. Its structure is also that of a large shield; although, it may be somewhat more complex, perhaps having more than one volcanic center (Zhang et al., 2015), but deep-penetration seismic data are sparse over this edifice, so the validity of this conclusion is uncertain. Core data show that Tamu Massif is characterized by massive sheet flows (Expedition 324 Scientists, 2010a), similar to those from OJP (Shipboard Scientific Party, 2001) and continental flood basalt provinces (see articles in MacDougall, 1988; and reviews by Jerram and Widdowson, 2005; Bryan et al, 2010). This correspondence implies the similarity of volcanic processes in oceanic plateaus and continental flood basalt provinces. Although core data imply a waning of magmatic effusion rate as the plateau evolved, even the smaller edifices were likely the result of enormous eruptions, as indicated by their size and structure (Zhang et al., 2015) as well as paleomagnetic evidence that indicates rapid emplacement of cored volcanic sections (Sager et al., 2015).

Having multichannel seismic profiles over the drill sites provided a rare opportunity for ground-truthing of LIP seismic imaging. Intrabasement reflectors have been imaged at a number of oceanic plateaus, including Ontong Java Plateau (Phinney et al., 1999; Inoue et al., 2008), Manihiki Plateau (Pietsch and Uenzelmann-Neben, 2015), Kerguelen Plateau (Schaming and Rotstein, 1990; Rotstein et al., 1992), Hikurangi Plateau (Davy et al., 2008), and Agulhas Plateau (Parsiegla et al., 2008). Aside from Shatsky Rise, only Ontong Java

Plateau has core and log results that allow seismic modeling. Similar results were found in both locations, with individual lava flows being generally too thin to be imaged individually. Instead, the reflections occur from alternations of thick, massive lava flows with pillows at Ontong Java Plateau (Inoue et al., 2008) and the same in addition to thicker sediment layers at Tamu Massif (Zhang et al., 2015). Although prior authors attributed the imaged intrabasement reflectors to lava flows, these two studies offer proof.

Intrabasement reflectors have also been imaged by seismic profiles on volcanic rifted margins, especially on the Vøring and Greenland margins (Hinz, 1981; Mutter et al., 1982; Planke and Eldholm, 1994; Planke and Cambray, 1996; Planke et al., 2000). Here coring demonstrated that the shallower layers are lava flows and volcaniclastic layers (Planke et al., 2000). These margins have generally complex structures owing to changes in tectonic setting across the margin as well as the combination of subaerial, submarine, and shallow-water explosive volcanic products (Eldholm et al., 1989; Larsen et al., 1994). The closest analog to oceanic plateau volcanism occurs in the outer "seaward dipping reflector" (SDR) complexes, which are interpreted as stacks of submarine sheet flows erupted into deep water (Planke et al., 2000). Nevertheless, the SDR are fundamentally different because they form wedge-shaped or arcuate layers because of differential subsidence making greater accommodation space on one side of the basin in which they were emplaced (Mutter et al., 1982).

Tamu Massif seismic profiles display some key differences from those of other oceanic plateaus that may be indicative of tectonic disparities. Whereas the layering over Tamu Massif is generally quite regular and simple, with layers dipping monotonically downslope, other plateaus show greater short wavelength structure (Rotstein et al., 1992; Davy et al., 2008; Parsiegla et al., 2008; Pietsch and Uenzelmann-Neben, 2015), implying more complex

formation. Moreover, the high quality seismic data from Ontong Java and Manihiki plateaus display stronger and more coherent reflectors at certain depths, suggesting different phases of volcanism (Inoue et al., 2008; Pietsch and Uenzelmann-Neben, 2015). In contrast, Shatsky Rise seismic layering appears more uniform (Zhang et al., 2015), possibly indicating more uniform volcanism.

Owing to isostasy, much of the bulk of Shatsky Rise is buried in the mantle. Seismic refraction data show a crust that is about 3-4 times thicker than normal oceanic crust, albeit with similar velocity structure (i.e., sections with both upper and lower crust velocities are thickened by about the same amount) (Fig. 8; Korenaga and Sager, 2012). This thick crust was produced by deeper melting (>30 km), with higher maximum partial melting as compared with normal mid-ocean ridges (Sano et al., 2012; Husen et al., 2013). Geochemical data indicate that both shallow (<3-6 km) and deep (>20 km) magma chambers (Sano et al., 2012; Husen et al., 2013; 2016) probably existed within these volcanoes. The shallow depth estimate is near the base of the upper crust at the center of Tamu Massif, whereas the deeper chamber may have occurred at the base of the thickened crust (Fig. 8).

It is clear from the large volume of Shatsky Rise, including its deep root (Korenaga and Sager, 2012) that an extraordinary volume of magma is required to build the large volcanic edifices. The volume of excess volcanic crust of Tamu Massif was reported at ~3.2 x 10^6 km^3, excluding a 7-km thick crust in case it was emplaced on pre-existing crust (Zhang et al., 2016). Given that Tamu Massif formed near a triple junction of spreading ridges, there may have been no pre-existing crust, in which case the total plateau volume is 6.9 x 10^6 km^3 (Zhang et al., 2016). Assuming 20% partial melting (Sano et al., 2012; Husen et al., 2013), a mantle volume of 3.5 x 10^7 km^3 (1.6 x 10^7 m^3 without pre-existing crust) is required to produce the Tamu

Massif magma. This is a sphere with a diameter of ~400 km (~310 km excluding normal crust). As this estimate assumes a high degree of partial melt over the entire volume, which is unlikely, a more likely scenario is a much larger zone of melting with the highest partial melt near the surface.

The surface morphology of the Shatsky Rise volcanoes is a broad, low shield (Sager et al., 1999; 2013). Seismic profiles (Fig. 9; see Zhang et al., 2015) show that Tamu Massif is ~500 km across, yet only ~3 km in height (excluding the 1-km-tall, late-stage Toronto Ridge). Apparent flank slopes are low, 0.5°-1.5°, especially on the volcano's lower flanks, which blend into the surrounding, flat seafloor without interruption. Common seamounts typically have steeper flank slopes, >~5°, and are not as broad (Smith, 1988), a difference that can be readily grasped by comparing Makarov Guyot, a large seamount south of Tamu Massif (Fig. 1), with its large neighbor. The low flank slopes probably result from lava flow characteristics. Low viscosity and high-effusion-rate should form long, shallow-slope flows owing to their low viscosity (Keszthelyi and Self, 1998). Another factor may be the eruptions occurring on thin, low strength lithosphere near a spreading ridge, where the lithosphere cannot support a large edifice with steep slopes. Deep-penetration seismic data show that lava flows deep within Tamu Massif are remarkably subparallel with the surface (Sager et al., 2013; Zhang et al., 2015). This structure suggests that lava emplacement was isostatically balanced, so that no differential subsidence resulted from the surface load. This scenario could occur if Tamu Massif erupted as an enhanced mid-ocean ridge, so that it formed thick crust with a deep root to balance the surface uplift.

3.1.2 Timing of Volcanism

Although new geochronologic data provide important constraints on the chronology of Shatsky Rise volcano formation, the timing is still poorly known. A big problem is that samples are limited to the near surface and only record the final outpourings, so the beginning of eruptions at any given site is not known. New geochronology data have confirmed the expected northeastward trend of decreasing age, which had previously been inferred only indirectly from magnetic anomaly ages, sediment ages, and gravity anomalies (Sandwell and McKenzie, 1989; Sager et al., 1999). End-of-shield-building ages (~144-142 Ma from Sites 1213 and U1347) provide a minimum age for Tamu Massif eruptions and correlate with magnetic anomalies M17-M18 (143-145 Ma). The beginning of Tamu Massif eruptions is not known, but must have been after M21 (149 Ma), because this magnetic lineation is recorded in the oldest crust bounding the southwest flank of the volcano (Fig. 2; Nakanishi et al., 1999; 2015). Anomalies M18-M20 (145-149 Ma) are mapped northeast of the Tamu Massif summit (Fig. 2; Nakanishi et al., 1999), so it appears that the volcano was emplaced in the interim, perhaps on crust that was part of a microplate accreted to the Pacific plate after triple junction reorganization (Sager et al., 1988; Nakanishi et al., 1999). Taking the magnetic polarity and radiometric dates at face value, the top and bottom of the volcano allow ~5 Ma for Tamu Massif to be formed (M21-M17; 149-144 Ma). It is unlikely that the bulk of the volcano formed over this entire period because the northeastward age progression implied for the north flank suggests that the main edifice existed prior to M19-M20. Assuming that Tamu Massif volcano was constructed between M21 and M19 implies a period of ~2 My for shield-building. Given the large volume of Tamu Massif, this constraint would imply an emplacement rate of ~1 km^3/yr. A significant problem with this analysis, however, is the poor calibration of M-

sequence anomalies (Tominaga and Sager, 2010; Malinverno et al., 2012), which leaves absolute age uncertainties on the order of several million years for these anomalies.

The radiometric ages from the top of the Tamu Massif shield (~144-142 Ma, corresponding to anomalies M16-M17) imply that the last massive flows were emplaced when the spreading ridge was located ~350 km farther north. Similarly, the ages of magnetic lineations identified within Ori Massif (M16-M15; 140-142 Ma) are older than the radiometric age for the top lavas (~134 Ma), which may indicate that the triple junction was already ~500 km distant at the time of emplacement (Heaton and Koppers, 2014).

New radiometric ages and paleomagnetic data do show, however, that formation of Tamu Massif occurred over a longer time period than the brief (~0.5 Myr) span proposed by Sager and Han (1993). A gap in radiometric ages and the occurrence of sediment layers between the two massive flows groups at Site U1347 indicate a significant hiatus at the end of shield formation lasting at least ~2-3 Myr (Heaton and Koppers, 2014; Tominaga et al., 2014; Geldmacher et al., 2014). Paleomagnetic data from Sites 1213 and U1347 have opposite inclination signs, suggesting that the Tamu Massif shield incorporates lava flows with opposite polarities (Sager et al., 2015), which also argues against rapid formation during a single polarity period (Sager and Han, 1993). The age span of Tamu Massif eruptions is further expanded by the radiometric date of ~129 Ma for Toronto Ridge, suggesting a gap of ~15 Myr from the end of shield building (Tejada et al., in press). This ridge represents late stage eruptions, which are common for large volcanoes, such as the Hawaiian and Emperor volcanoes (Clague and Dalrymple, 1989). Nonetheless, this age gap is substantially larger than the 3-5 Myr usually reported for Hawaiian-Emperor volcanoes (Clague and Dalrymple, 1989; Lonsdale et al., 1993).

3.1.3 Post Shield-Building Evolution

Evidence of late eruptions is scattered around the surface of Shatsky Rise in the form of secondary volcanic cones and ridges. These constructs can be built by both basaltic and volcaniclastic eruptions. Dredges from Toronto Ridge and Ori summit ridges define the former (Sager et al., 1999), whereas Site U1348 coring illustrates the latter (Expedition 324 Scientists, 2010d). Other secondary cones are found at scattered locations on the flanks. It is unclear where such scattered, low volume volcanism comes from, but there is no clear link to particular zones of weakness, such as volcanic rift zones, which appear poorly developed for the Shatsky Rise volcanoes.

Most secondary cones and ridges on Shatsky Rise are undated, but on seismic profiles, their bases are indistinguishable from igneous basement, so formation occurred before significant sediment buildup occurred. Nevertheless, the age gap can be significant, as shown by the ~15 Myr difference between Toronto Ridge and the youngest Tamu Massif flows. The young age for Toronto Ridge and the isotopic similarity of its lavas to the drilled Tamu basement rocks (Tejada et al., in press) implies that magma may have resided within the Tamu Massif volcano for an extended period after the main body of the volcano was constructed.

As the Shatsky Rise volcanoes aged, they subsided owing to thermal subsidence at a rate consistent with normal lithosphere. Prior work suggested that Shatsky Rise subsidence was anomalously low, perhaps because of a buoyant center that subsided more slowly than the flanks (Ito and Clift, 1998). Volatile contents nonetheless indicate a gradient from the center of Tamu Massif to Ori Massif (Site U3147 to Site U1348 to Sites U1349 and U1350), with the latter subsiding ~800 m more than the former (Shimizu et al., 2013). This trend may indicate that a buoyant mass, perhaps underplating beneath the center (Ito and Clift, 1998) is the cause.

Differential subsidence should give rise to normal faulting with the flank down-faulted relative to the center. This is indeed observed on some seismic profiles, but curiously, they are only noted on the west side of Shatsky Rise, rather than being symmetric as might be expected (Zhang et al., 2015). Furthermore, the seismic refraction profile (Korenaga and Sager, 2012) shows no high-velocity lower crustal layer beneath the center of Tamu Massif, as expected from underplating and subsidence estimates appear normal (Fig. 7), so conflicting results leave the subsidence picture unclear.

3.2 Shatsky Rise Origin

Recent investigations of Shatsky Rise were driven by the "plume versus plate" debate (Expedition 324 Scientists, 2010a). Based on the plume head hypothesis of the mid-1990s (Richards et al., 1989; Duncan and Richards, 1991; Coffin and Eldholm, 1994; Campbell, 2007) and the subsequent questioning of the plume hypothesis (Anderson et al., 1992; Anderson, 1995; Foulger, 2007), there were two competing end-member models to explain oceanic plateau formation (Fig. 2). On the one hand, anomalous plateau-forming volcanism could occur from a large thermal diapir having ascended from the deep mantle (usually attributed to the core-mantle boundary) or it could arise by fracturing of the plate atop a region of upper mantle with anomalous properties that result in a lower decompression melting temperature (i.e. presence of volatiles) or increased melt production (i.e., fertile mantle). Shatsky Rise seemed a fortuitously good choice for investigating these two models because it has characteristics that fit either model (Sager, 2005).

3.2.1 Geophysical Evidence

In terms of morphology and structure, Shatsky Rise mostly appears to be a good fit with the plume head model. It is composed of enormous volcanoes and begins with a massive eruption that can be ascribed to a plume head (Sager et al., 1999; Nakanishi et al., 1999).

Massive sheet flow lavas recovered from Tamu Massif imply voluminous eruptions (Expedition 324 Scientists, 2010a), supporting the idea that this is the oceanic cousin of continental flood basalts (Richards et al., 1989; Duncan et al., 1991). Seismic data show that the large volcanic edifices are enormous shield volcanoes that formed anomalously thick crust, again consistent with massive magmatic output (Korenaga and Sager, 2012; Sager et al., 2013; Zhang et al., 2015). Furthermore, seismic transects show little evidence of normal faulting, as might be expected of an edifice built on a spreading ridge (Zhang et al., 2015). If such evidence existed, it must have been paved over by volcanism. Paleomagnetic data indicate rapid emplacement of Shatsky Rise lava sections, consistent with high effusion rate (Sager et al., 2015). Subsequent magmatic output waned, both in effusion rate and total emplacement, as the smaller volume edifices (Ori and Shirshov massifs and Papanin Ridge) were constructed, mainly with pillow and thin sheet flows (Expedition 324 Scientists, 2010a). This trend nicely fits the expected head-to-tail transition of the plume head model.

Other aspects of the structure and tectonics are not as clearly supportive of the plume model. It was argued that the coincidence of a plume emerging precisely at triple junction has low probability if the plume is not steered toward the spreading (Sager, 2005). A counter argument was that a plume head could capture a triple junction because of its excess heat and uplift (Sager et al., 1999; Nakanishi et al., 1999). The tectonic story from magnetic lineations located adjacent to the southwest edge of Tamu Massif shows that the reorganization of the triple junction linked to Shatsky Rise occurred several million years prior to the first plateau eruptions at Tamu Massif (Nakanishi et al., 2015). At the beginning, at least, it appears that the plate boundaries were the controlling factor. On the other hand, it is difficult to explain why the triple junction took the path it did along the axis of Shatsky Rise because simple plate

kinematics indicate that it should have headed northwest instead of northeast (Sager et al. 1988). As a source of heat and uplift, the plume could have caused the triple junction to stay nearby.

Linear magnetic anomalies are found through Ori Massif and the north flank of Tamu Massif and perhaps Shirshov Massif as well (Nakanishi et al., 1999; Huang and Sager, 2013), indicating that much of the plateau formed at a spreading ridge. Moreover, the lineation pattern seems unlikely to develop from far-ranging lava flows erupted from a single volcanic center, as is supposed for Tamu Massif (Sager et al., 2013). Likewise, the internal layering of Tamu Massif is hard to explain by localized eruptions because the lava pouring out on top would depress the crust, causing flows to dip toward the center. Instead, the subparallel layering suggests continual isostatic balance as might occur if the thick Tamu Massif crust was built all at once. Taken together, it seems that at least some of the Shatsky Rise volcanic edifices have characteristics similar to ridges. This conclusion also fits the observation that other oceanic plateaus are found along the paths of triple junctions, an unlikely occurrence if the two are not intimately connected (Sager, 2005).

Aspects of the seismic data seem unsupportive of the plume head model. Despite evidence from cored sediments that the summits of the plateau were in shallow water (Expedition 324 Scientists, 2010a), seismic evidence shows no clear evidence of summit erosion, as would be expected from significant emersion (Sager et al., 2013; Zhang et al., 2015). Significant uplift is expected from the buoyancy of a thermal plume head (~1 km for a 100°C anomaly to ~4 km for a 350°C anomaly) (Griffiths and Campbell, 1991; Farnetani and Richards, 1994). If Shatsky Rise formed above a thermal plume, it should have built above sea level, similar to Iceland, which rises 1-2 km above sea level (Ito et al., 2003). Instead, the

evidence says that Shatsky Rise reached sea level, but not much higher. Thus, Shatsky Rise is between OJP and Kerguelen Plateau, with the former formed well below sea level (Michael, 1999; Fitton et al., 2004) and the latter erupted subaerially (Coffin, 1992; Frey et al, 2003). In addition, seismic refraction data from Tamu Massif display a curious negative correlation between seismic velocity and crustal thickness, not the positive correlation expected from a hotter thermal anomaly (Korenaga and Sager, 2012). This interpretation, however, is weakened because it depends on the assumption that the entire vertical crustal column formed simultaneously (Korenaga et al., 2002) and this may not be true for the location of the seismic transect across the center of Tamu Massif if the edifice formed by flows emanating from its center. These observations could argue instead for a thermochemical plume (e.g. containing 10-15% of recycled oceanic crust in form of eclogite), which could rise through the mantle without causing significant surface uplift (Dannberg and Sobolev, 2014).

3.2.2 Geochronology and Eruption Duration

New geochronology data indicate that the formation of Shatsky Rise volcanoes occurs over a longer period than expected. Radiometric dates show that the last stages of the Tamu Massif volcano construction occurred over several million years or more, with an even larger gap (~15 Myr) between the main shield-building stage and late stage eruptions (Heaton and Koppers, 2014; Geldmacher et al., 2014). Paleomagnetic data also indicate multiple magnetic polarities recorded in the Tamu Massif lava flows, an observation consistent with the passage of significant time (Sager et al., 2015). Although it is tempting to conclude that the longer eruption period does not fit the plume head model, which calls for rapid emplacement, if taken at face value, the geochronology data imply that the last eruptions were occurring when the volcano was at distance of hundreds of kilometers from the plate boundaries for both Tamu and Ori massifs. This observation suggests that the magma source was not connected with the

plate boundaries or that the dating of Mesozoic magnetic anomalies is inaccurate. Given a likely uncertainty of several million years in the calibration of the M-series magnetic anomalies (Tominaga and Sager, 2010), the difference may not be significant, especially considering other data implying a close connection between the plateau massifs and the spreading ridges. An alternative explanation is provided by pulsing plume models (e.g. Kumagai, 2002; Lin and van Keken, 2005), which call for multiple episodes of volcanism at the same location. Two (or even multiple) episodes of plateau volcanism also have been observed at other large igneous provinces such as OJP (e.g. Tejada et al., 2002) or Rio Grande Rise/Walvis Ridge (e.g., Rohde et al. 2013).

3.2.3 Geochemical and Isotopic Evidence

Geochemical and isotopic data give tantalizing insights, but can also be aligned with both the plume and fertile mantle models. The plume hypothesis makes no prediction about the specific isotopic composition of mantle plumes. Nevertheless, submarine intraplate volcanic rocks, collectively termed Ocean Island Basalts (OIB), generally possess enriched isotopic compositions (i.e. more radiogenic (higher) Pb and Sr but less radiogenic (lower) Nd and Hf isotope ratios) compared to MORB (e.g. Hofmann and Hart, 1978) reflecting a different magma source. Since rocks from these tectonic settings were proposed to be associated with deep-seated mantle plumes and hotspots according to the initial plume theory (e.g. Morgan, 1971), their isotopic enrichment let to the perception that the source area of mantle plumes is more primitive (less depleted) than the upper mantle MORB source (Schilling et al. 1973; Wasserburg and Depaolo, 1979). In addition, specific isotopic compositions in OIB's are believed to reflect subducted crustal material such as ancient oceanic crust ("HIMU" = high μ= high time-integrated $^{238}U/^{204}Pb$) and associated sediments or subcontinental material ("EM"= Enriched Mantle) (see Hofmann, 2003 for overview). In the framework of the plume theory,

this material is believed to sink to certain depths in the mantle (e.g., the transition zone or core-mantle boundary) where it resides over billions of years (developing enriched isotope ratios due to radiogenic ingrowth) and is eventually entrained into rising mantle plumes (e.g., Jellinek and Manga, 2004). As seen in analog experiments and numerical models, the bulk composition of such plumes is not significantly influenced by entrainment of the upper (depleted) mantle during ascent (e.g., Farnetani and Richards, 1994).

In plume head models, plume tails sample the thermal boundary layer (including available recycled components), whereas plume heads sample a mixture of this material and the lower mantle above the boundary layer source (Griffiths and Campbell, 1990). To further complicate things, internal stirring is thought to be more effective in plume heads than in the more laminar rising plume tails, resulting in homogenization of lavas erupted from plume head melting (Farnetani et al., 2002). These theoretical models seem to be supported by the composition of lavas from oceanic plateaus, such as OJP (e.g. Mahoney et al., 1993), Hikurangi Plateau (Timm et al., 2011), the Caribbean-Columbian plateau (e.g. Hauff et al., 2000) and Shatsky Rise (e.g., Heydolph et al., 2014), which show little geochemical variation, have largely intermediate composition between MORB, HIMU and EM, and are similar to each other and similar to the assumed composition of the lower mantle (e.g. represented by FOZO, Hart et al. 1992).

The transitional composition (between MORB and OIB) of most Shatsky lavas in terms of trace element and isotopic compositions makes it difficult to use geochemistry to conclude that Shatsky Rise originated from a plume source. Because of the large variability in MORB chemistry, lavas with geochemical characteristics similar to the four Shatsky Rise magma types (Sano et al., 2012) can be found at modern spreading ridges (Natland, 2013). This includes

rocks (E-MORB) enriched in incompatible trace-elements and slightly enriched isotopic signatures (Sr, Nd, and Pb). E-MORB chemistries could reflect a mantle plume contribution to the MORB source (e.g. Schilling, 1985), but are also known to erupt at spreading centers far away from known hotspots (Donelly et al., 2004; Waters et al., 2010). Such E-MORB occurrences, however, are volumetrically minor and locally restricted (never form entire plateaus). In addition, the chondritic composition of heavy rare Earth elements (HREE) (i.e., flat Dy/Yb ratios) as observed in most E-MORB's (Donelly et al., 2004) contrasts with the distinct depletion of HREE's displayed by all Shatsky Rise lavas (except for the extremely depleted U1349-type samples that are proposed to originate in the upper mantle) indicating that Shatsky Rise magma predominantly formed in the deep garnet stability field consistent with a magma source deeper than the E- and N-MORB sources (Sano et al., 2012).

The interpretation of the geochemical characteristics of Shatsky Rise lavas is further complicated by its undoubted formation along a mid-ocean ridge (triple junction). If a mantle plume is assumed, this tectonic setting could allow for stronger entrainment of ambient depleted upper (MORB source) mantle and result in higher degrees of melting for any upwelling plume material. As shown for Hawaii, which is commonly ascribed to a deep mantle plume (e.g., Courtillot et al., 2003), the hotspot produced more depleted, MORB-like magmas when it was located close to the Pacific spreading ridge at ~80 Ma (Regolous and Hofmann, 2003). Assuming a heterogeneous plume source, comprised of geochemically enriched (pyroxenitic?) layers with lower melting temperature surrounded by a more voluminous, geochemically depleted (peridotitic?) and more refractory matrix (e.g. Phipps Morgan, 1999; Hirschmann and Stolper, 1996), the longer melting column under thinner lithosphere results in effective dilution of any enriched geochemical signal by melts from the volumetrically larger

depleted plume matrix. Thus such dilution could obscure the enriched (plume?) signature in the predominant normal and low-Ti type Shatsky lavas.

The calculated degree of partial melting is higher than MORB (Sano et al. 2012; Husen et al., 2014), indicating either hotter melting temperatures or more fertile/fusible (more melt-producing) magma source material. So far, however, no direct petrological evidence for abnormally hot melting temperatures has been found in the recovered Shatsky rocks, weakening support for the mantle plume hypothesis in favor of the fertile mantle explanation. An example of anomalous melt production in a similar setting is ridge-centered Iceland, which is proposed to originate from the re-melting of relatively young subducted oceanic crust that was trapped in the shallow upper mantle and eventually tapped by the melt extraction zone of the westward-migrating mid Atlantic ridge (Foulger et al., 2005b, 2005c). Oceanic crust, transformed to eclogite during subduction, can produce several times more melt during adiabatic decompression melting than regular upper mantle peridotite without requiring higher melting temperatures (e.g. Yasuda et al., 1994). Melting of different portions of the subducted crust (gabbroic lower crustal cumulates versus enriched upper crust) could explain geochemically depleted and enriched endmembers detected in the Iceland magma source but result in an overall Iceland lava composition similar to MORB (Foulger et al. 2005c).

The observation that Shatsky volcanism becomes geochemically more heterogeneous with time, decreasing eruption volume, and lower degrees of melting (Sano et al., 2012; Heydolph et al. 2014) may support the involvement of a plume (head). According to numerical plume head models (e.g., Farnetani and Richards, 1994; Farnetani et al., 2002), such geochemical evolution could reflect less effective stirring, mixing and progressively lower

degrees of melting during the transition from a waning plume head (Tamu Massif) to a plume tail (Shirshov Massif and Papanin Ridge).

An alternative solution that marries both plume and fertile mantle models explaining moderate isotopic enrichment and similar compositions of most oceanic plateau lavas without the need of homogenization due to high degrees of melting/plume head mixing (or accidental encounters of migrating ridges with fertile upper mantle source material) was proposed by Jackson and Carlson (2011). In this model, the relatively flat incompatible trace element patterns, Pb isotopic values near the geochron (a Pb isotope isochron resulting from undisturbed U/Pb ratios since shortly after the formation of the Earth), and primitive mantle-like, non-chondritic, Nd and Hf isotope compositions observed in most flood basalts and oceanic plateaus, reflect an early depleted, primitive mantle reservoir that has not been involved in subsequent differentiation processes but can be slightly modified by incorporation of recycled material (Jackson et al., 2010; Jackson and Carlson, 2011). This reservoir could be hosted in the lower mantle "large, low shear-wave velocity provinces" (LLSVP), from whose margins many oceanic plateaus (including Shatsky Rise) are proposed to have ascended (Torsvik et al., 2006; Burke et al., 2008). Shatsky Rise normal, low-Ti, and U1349 type lavas posses Nd, Pb, and Hf isotopic compositions consistent with a derivation from this ancient reservoir, whereas the high Nb type lavas reflect a larger portion of incorporated recycled material consistent with their more enriched isotopic composition, including high δ^7Li values (Heydolph et al., 2014; Sano and Nishio, 2015). The ancient, primitive mantle material, if brought to shallow depths by a mantle plume, would be more fusible than the ambient upper mantle MORB source that is frequently depleted by ridge melting throughout Earth's history

(Jackson and Carlson 2011). In combination with slightly elevated temperatures, as may be the case at Shatsky Rise, and the increased degree of melting beneath the triple junction, such primitive mantle material could produce abnormally large volumes of melt to form an oceanic plateau.

3.2.4 Plume and Plate?

Much of the motivation for studying Shatsky Rise was to determine whether this oceanic plateau could be explained by either of two end-member models: the thermal plume head (e.g., Richards et al., 1989; Duncan and Richards, 1991; Coffin and Eldholm, 1994) or decompression above fertile, shallow mantle (the plate model) (Foulger, 2007; Anderson and Natland, 2014). Such a test seemed feasible because Shatsky Rise was noted to have characteristics that fit both models (Sager, 2005). The evidence presented in prior sections does not give a simple answer as both new and old evidence can be aligned with either model and no one finding has been sufficient to win the argument. This is partly a result of expansion of the "plume" model from Morgan's (1971; 1972) original idea of a narrow thermal jet arising from the lowermost mantle. Current plume models encompass broader upwelling zones (e.g., O'Connor et al., 2012), thermochemical upwelling (Farnetani et al., 2002; Farnetani and Samuel, 2005; Dannberg and Sobolev, 2015), and upwellings from elsewhere than the lowermost mantle (e.g., Cortillout et al., 2003). The trouble is also partly the difficulty in discerning between simple conceptual models about the lower mantle using surface observations with complexities – most observations from surface features are not diagnostic. It was hoped that geochemical and isotopic studies might provide a "silver bullet" observation that would cinch the argument whether or not Shatsky Rise magmatism had its source in the lower mantle. A consensus about the interpretation of geochemical and isotopic anomalies of oceanic rocks remains elusive (e.g., Anderson and Natland, 2014). In the end, it may be that

the posed “plume vs. plate” dichotomy is misleading, at least for Shatsky Rise, which seems to straddle the fence even as more data have accumulated.

One thing that is clear is that Shatsky Rise formed from an anomalously large transfer of magma from the mantle to the surface at a location where the lithosphere was thin and the surface record probably manifests mantle processes. The volume of magmatic emplacement, thickness of the crust, deeper melting, higher degree of partial melting and slightly higher temperature (compared with MORB), and trend of waning volcanism from massive to minor fit the original idea of the plume head hypothesis. Other observations have been interpreted as fitting the plume model as follows. Evidence for incompatible trace-element and isotopic enrichment of the high-Nb lavas (Sano et al., 2012; Heydolph et al., 2014) and (lower than MORB) $^{3}He/^{4}He$ ratios of normal type lavas from Ori Massif (Hanyu et al., 2015) are interpreted as indication of recycled oceanic crust in the magma source. This interpretation favors a plume model if one assumes that recycled crust descended with a subducted plate into the deep mantle and returned to the surface with a plume (Heydolph et al., 2014). The geochemical homogeneity of Tamu Massif lavas followed by increasing geochemical heterogeneity observed at the later edifices is also argued to favor a plume because it follows the idea of greater mixing and homogenitization in the plume head and the idea that intrinsic heterogeneity is a plume attribute (Farnetani et al., 2002). It is unclear, however, that these traits are inherent to the plume model. In contrast, the plate model argues that subduction can strand crustal material in the upper mantle and can later melt to provide heterogeneous magmas (Foulger, 2007; Anderson and Natland, 2014), so that neither recycled crust nor heterogeneity is explained only by the plume model.

It has also been argued that the paleo-position of Shatsky Rise aligns with the edge of the Pacific LLSVP, favoring a plume origin (Torsvik et al., 2006; Burke et al., 2008). Pacific reconstructions for the Jurassic are unreliable because they are done with an absolute plate motion model based on hotspot trails with a tenuous connection to the Late Cretaceous-Cenozoic plate motion model (Wessel et al., 2006; Wessel and Kroenke, 2008), so this observation is weak for Shatsky Rise. Moreover, the manner of correlation between hotspots and LLSVP is debated (Davies et al., 2015; Austermann et al., 2015; Doubrouvine et al., 2016) and it is also claimed that the correlation of hotspots is greater with zones of upper asthenospheric low velocity (Anderson and Natland, 2014).

Other data appear to favor the plate hypothesis: the strong link with the triple junction path (Nakanishi et al., 1999; Sager, 2005), the apparent occurrence of the plate reorganization several million years prior to the emplacement of Shatsky Rise (Nakanishi et al., 2015), the negative correlation between seismic velocity and crustal thickness as well as the lack of underplating beneath the center of the plateau (Korenaga and Sager, 2012), and the longer-than-expected time span of Shatsky Rise eruptions (Tejada et al., in press; Geldmacher et al., 2014). Although these observations appear favorable, they are nonetheless inconclusive. With only a small number of radiometric ages for Shatsky Rise taken only from the top surface of the plateau coupled with uncertainty in the absolute age calibration of the M-sequence magnetic anomalies (Tominaga and Sager, 2010), the timing of emplacement and duration of eruptions is poorly constrained. Moreover, it appears that volcanism was occurring at both Tamu and Ori massifs when the spreading ridges were hundreds of kilometers distant. However, it should be noted that the sources of late eruptions in large shield volcanoes are poorly known, so it is unclear that this lag favors one model over the other. Furthermore,

although the observation of a negative correlation between seismic velocity and crustal thickness for Tamu Massif can be interpreted as evidence for melting of anomalous mantle, this conclusion is dependent on a particular model for crustal formation (Korenaga and Sager, 2012) whose assumptions may not be met.

Data on the temperature anomaly and uplift of Shatsky Rise appear to support the plate hypothesis by not supporting the plume hypothesis. It was expected that the plume head would create a large temperature anomaly in the upper mantle and cause 1-3 km of uplift (Campbell, 2007). Although geochemical analyses indicate a temperature anomaly, it is smaller (~50°C) than expected. Furthermore, the uplift of Shatsky Rise, which appears to have risen only to sea level, is less than expected from classical plume head models (e.g., Griffith and Campbell, 1991; Campbell, 2007).

In sum, both the plume and plate hypotheses find support in new data and interpretations from Shatsky Rise, which continues to have a foot firmly in both camps. Perhaps the division into plume and plate is a false dichotomy. The plateau clearly formed in concert with spreading ridges but the volcanism was not typical of mid-ocean ridges. Abnormal mantle conditions are shown by geochemistry and isotopic signatures, which imply deeper melting with higher degrees of partial melt and traces of recycled crust (Sano et al., 2012; Prytulak et al., 2013; Husen et al., 2013; Heydolph et al., 2014; Hanyu et al., 2015). Shatsky Rise is not unique in its formation at spreading ridges. As more studies have targeted oceanic LIPs, this seems to be more the norm than exception. As noted by Sager (2005), many Pacific plateaus were formed at triple junctions. Plate reconstructions indicate that the largest known oceanic LIP, the Ontong Java-Hikurangi-Manihiki LIP also formed at a triple junction (Taylor, 2006; Chandler et al., 2012; Hochmuth et al., 2015). The same can be said of the next

largest oceanic LIP, the Indian Ocean's Kerguelen Plateau (Royer et al., 1991), and the Azores Plateau (Gente et al., 2003) in the Atlantic. In addition, it has been noted that many oceanic hotspots have erupted at spreading ridges (Whittaker et al., 2015). In the traditional plume hypothesis, plumes and plate boundaries should be independent (Fig. 2) and the probability of alignment should be small (e.g., Sager, 2005). In contrast, this repeated association implies a deeper connection. It may well be that upwelling – whatever the depth of origin – is entrained into sub-spreading ridge upwelling in the asthenosphere (Fig. 20), which can be strong beneath triple junctions because of the surface divergence (Georgen and Lin, 2002; Georgen 2008; Dordevic and Georgen, 2016).

4. Summary

Recent researches on Shatsky Rise have substantially improved knowledge of the geology and structure of this oceanic plateau and give important clues about its origin and evolution. New data come from an IODP drilling expedition (Expedition 324) that recovered sections of igneous rocks and collected downhole logging data, thus seeding numerous lines of research. New geophysical data on and around Shatsky Rise, including profiles of seismic refraction and reflection as well as magnetic anomalies, give a clearer picture of the structure and evolution of this oceanic plateau.

Core data show that Tamu Massif, the oldest and largest volcanic edifice, is made up of massive sheet flows and pillow flows, with the former predominant. The percentage and thickness of massive flows declines from Tamu Massif to the younger edifices, Ori and Shirshov massifs. This transition is interpreted as a change from highly effusive to less effusive volcanism.

Seismic refraction data indicate that Tamu Massif crust is ~30 km thick and has a velocity structure similar to oceanic crust, albeit much thicker. Crustal thickness is consistent with Airy isostasy and demonstrates that much of the mass of the plateau resides below the surface. Refraction data also display a peculiar negative correlation with crustal thickness, which is different than the positive correlation expected from the melting of hotter mantle, possibly indicating that the mantle beneath Shatsky Rise was cooler than normal, not hotter. Seismic reflection profiles display intrabasement reflectors that indicate the geometry of buried lava flows. On the seismic sections, flows are traced from summit to deep flank, indicating that the Shatsky Rise massifs are enormous shield volcanoes with anomalously low slopes. Such low slopes likely result from emplacement of fluid lava flows from effusive eruptions and perhaps owing to the occurrence of the volcanism near a mid-ocean ridge.

Geochronology data support the previous inference that Shatsky Rise edifices become younger northeastward from Tamu Massif and that the edifices have ages near that of the surrounding crust. This finding emphasizes the connection between the evolution of the triple junction and the formation of Shatsky Rise massifs. Massive flows at Site U1347 atop Tamu Massif were emplaced in two pulses at least 3 Myr apart. The age gap in between is confirmed by log and core data which indicate several thick sedimentary layers in between these two groups. After a hiatus of ~15 Myr, late stage eruptions produced a large summit ridge, Toronto Ridge, at ~129 Ma. Ori Massif gives a radiometric age of ~134 Ma at which time the triple junction, as indicated by magnetic lineations, was ~500 km farther to the northeast. Likewise, when the last massive flows were emplaced at the summit of Tamu Massif, the triple junction was ~350 km to the northeast. As the duration of shield building is poorly known and the absolute age calibration of Mesozoic magnetic anomalies is poor, the significance of this result

is unclear, but it seems to indicate a significant time lag between crustal formation at the triple junction and the final plateau eruptions.

Sedimentary core data show that Shatsky Rise summits were in shallow water, but give little evidence of emergence, a result supported by lack of evidence for wave planation in seismic reflection data. Shatsky Rise is thus similar to Ontong Java Plateau, which also formed mostly in a submarine environment; although, Ontong Java Plateau was deeper. Igneous basement depths and volatile contents from glasses both imply plateau subsidence consistent with the normal subsidence of oceanic lithosphere. Volatile-estimated subsidence data indicate submarine emplacement for all sites, but also show a curious trend of increasing subsidence from the center of Tamu Massif to Ori Massif, possibly indicating that the Tamu Massif center was more buoyant than the flanks.

Geochemical data show that basalts have mainly tholeiitic basaltic compositions with chemistries of most rocks being similar to mid-ocean ridge basalts (MORB). Based on geochemistry, the Shatsky Rise basalts can be divided into four different types: normal, low-Ti, high-Nb, and U1349. The normal type is similar to N-MORB (normal-MORB) samples from the mid-ocean ridges, but represents melting at higher pressure and temperature. This type is predominant and makes up most of the samples from Tamu Massif. The low-Ti type displays a lower MgO content, but Nd-Sr-Pb-Hf isotopes similar to normal-type basalts, whereas the high-Nb type has the enriched trace element and isotopic characteristics of ocean island basalt (OIB). The U1349 type, found only at one site, is the least evolved magma cored on Shatsky Rise and has strongly depleted incompatible element and isotope characteristics. Ori Massif samples fit into three of these categories and also display variety in isotopic patterns, indicating increasing heterogeneity with time and the waning of the eruptions.

Estimates of partial melting for Shatsky Rise basalts range from 15-23%, which is similar to slightly higher than for MORB, but not as high as the estimate (~30%) for Ontong Java Plateau. In addition, normal type basalts indicate significant melting in the garnet stability zone at a depth >80 km. Both the deeper average melting and higher degrees of partial melt imply that Shatsky Rise magmas formed at greater depths and higher temperatures than ordinary MORB. Estimates of potential temperatures from melting models, however, imply that the mantle beneath Shatsky Rise was anomalously warm by only ~50°C. Most samples have chemistries consistent with crystallization at low pressure and temperature within the upper crust (depth < 6 km); however, a small number of samples indicate a high pressure regime indicating a magma chamber deeper within the crust (~20 km).

Normal and low-Ti type basalts have isotopic signatures that reflect a depleted mantle source and overlap with Pacific MORB. High-Nb lavas reflect a more enriched source trending toward mantle endmembers EM1 and/or EM2. U1349 basalts are the most depleted in Nd and Hf isotopic compositions and $^{206}Pb/^{204}Pb$ ratio. Overall, the magma source appears to become more isotopically heterogeneous from Tamu Massif to Ori Massif, perhaps reflecting a less vigorous melting with time. The isotopic enrichment of many Ori Massif basalts implies the entrainment of recycled oceanic crust. Similar conclusions are drawn from low $^{4}He/^{3}He$ ratios and high $\delta^{7}Li$ values.

It is difficult to decide whether to credit a mantle plume or melting of fertile upper mantle caused by plate extension because some data and interpretations favor one or the other and often the ramifications from observations are framed with model-dependent interpretations. The great volume of magma emplacement and the transition from massive to more modest eruptions fit predictions of the thermal plume head model, but the lack of

significant uplift and the clear connection with triple junction tectonics does not. Greater partial melting and depth of melting of Shatsky Rise basalts favor a thermal anomaly, but estimates of this anomaly are small and a negative correlation between seismic velocity and crustal thickness can be interpreted as a sign of cooler than normal melting temperatures. Geochemical and isotopic data show that some parental magmas were enriched by recycled subducted crust, but both the plume and plate models can explain this by different geodynamic models. Perhaps Shatsky Rise indicates that the distinction between plume and plate models is artificial and that both mechanisms come into play. Although a definitive answer about the source mechanism of Shatsky Rise formation is elusive, recent research has greatly expanded our knowledge of oceanic plateau structure and evolution.

Acknowledgments

A significant portion of this research is based on samples and data collected by the Integrated Ocean Drilling Program, which was supported by the U.S. National Science Foundation and participating nations through IODP Management International, Inc. We thank the scientists, staff, and crew of the drilling vessel *JOIDES Resolution* for making the drilling on Shatsky Rise possible. W. S. was supported by the US Science Support Program (USSSP) through the Consortium for Ocean Leadership and by NSF grants OCE-0926611 and OCE-0926945. He also thanks the crew and staff of the R/V Marcus G. Langseth for their diligent work collecting seismic data over Shatsky Rise. Funding for T. S. was partly provided by the Japan Society for the Promotion of Science Kahenhi, grant 26302010. The authors are indebted to James Natland and an anonymous reviewer for improvements in the manuscript.

5. **References**

Abouchami, W., Hofmann, A.W., Galer, S.J.G., Frey, F.A., Eisele, J., and Feigensohn, M., 2005. Lead isotopes reveal bilateral asymetry and vertical continuity in the Hawaiian mantle plume. Nature 434: 851-856, doi: 10.1038/nature03402.

Allan, J. F., Batiza, R., Perfit, M. R., Fornari, D. J., and Sack, R. O., 1989, Petrology of lavas from Lamont Seamount chain and adjacent East Pacific Rise. Journal Petrology, 30: 1245–1298.

Almeev, R., Portnyagin, M., Wengorsch, T., Sano, T., Natland, J.H. and D. Garbe-Schoenberg, 2011. Highly depleted melt inclusions in olivine from Shatsky Rise. Abstract 426, 2011 Goldschmidt Conference, 16 August 2011, Prague, Czech Republic.

Anderson, D.L., 1995. Lithosphere, asthenosphere, and perisphere. Reviews of Geophysics, 33: 125-149.

Anderson, D.L., 2001. Top-down tectonics? Science, 293: 2016-2018.

Anderson, D.L. and Natland, J.H., 2014. Mantle updrafts and mechanisms of oceanic volcanism. PNAS, 111: E4298-E4304, doi:10.1073/pnas.1410229111.

Anderson, D.L., Tanimoto, T. and Zhang, Y.-S., 1992. Plate tectonics and hotspots: the third dimension. Science, 256: 1645-1651.

Ando, A., Woodard, S.C., Evans, H.F., Littler, K., Herrmann, S., MacLeod, K.G., Kim, S., Khim, B.-K., Robinson, S.A. and Huber, B.T., 2013. An emerging palaeoceanographic 'missing link': Multidisciplinary study of rarely recovered parts of deep-sea Santonian-Campanian transition from Shatsky Rise. Journal of the Geological Society of London, 170: 381-384, doi: 10.1144/jgs2012-137.

Austermann, J., Kaye, B. T., Mitrovica, J. X., and Huybers, P., 2014. A statistical analysis of the correlation between large igneous provinces and lower mantle seismic structure. Geophysical Journal International, 197, 1-9, doi:10.1093/gji/ggt500.

Ballard, R.D., Holcomb, R.T. and Van Andel, T.H., 1979. The Galapagos Rift at 86°W: 3. Sheet flows, collapse pits, and lava lakes of the rift valley. Journal of Geophysical Research, 84: 5407-5422.

Bercovici, D. and Mahoney, J.J., 1994. Double flood basalts and plume head separation at the 660-kilometer discontinuity. Science, 266: 1367-1369.

Bralower, T. J., Premoli-Silva, I., and Malone, M. J., 2006. Leg 198 synthesis: A remarkable 120-m.y. record of climate and oceanography from Shatsky Rise, northwest Pacific Ocean. In: T. J. Bralower, I. Premoli-Silva, and M. J. Malone (Editors), Proceedings of the ODP, Scientific Results, v. 198, Ocean Drilling Program, doi:10.2973/odp.proc.sr.101.2006.

Bryan, S.E. and Ernst, R.E., 2008. Revised definition of Large Igneous Provinces (LIPs). Earth-Science Reviews, 86: 175-202, doi: 10.1016/j.earscirev.2007.08.008.

Bryan, S. E., Peate, I. U., Peate, D. W., Self, S., Jerram, D. A., Mawby, M. R., Marsh, J. S., and Miller, J. A., 2010. The largest volcanic eruptions on Earth. Earth Science Reviews, 102, 207-229, doi:10.1016/j.earscirev.2010.07.001.

Burke, K., Steinbergere, B., Torsvik, T. H., and Smethurst, M. A., 2008. Plume generation zones at the margins of Large Low Shear Velocity Provinces on the core-mantle boundary. Earth and Planetary Science Letters, 265, 49-60, doi:10.1016/j.epsl.2007.09.042.

Campbell, I.H., 2007. Testing the plume theory. Chemical Geology, 241: 153-176, doi: 10.1016/j.chemgeo.2007.01.024.

Campbell, I.H. and Griffiths, R.W., 1990. Implications of mantle plume structure for the evolution of flood basalts. Earth and Planetary Science Letters, 99: 79-93.

Campbell, I. H., 2005. Large igneous provinces and the mantle plume hypothesis. Elements, 1:265-269.

Campbell, I. H., and Griffiths, R. W., 1992. The changing nature of mantle hotspots through time: Implications for the chemical evolution of the mantle. The Journal of Geology, 100: 497-523.

Carvallo, C., 2014. Data report: hysteresis measurements on basalts from Holes U1346A, U1347A, and U1350A on Shatsky Rise. In W. W. Sager, T. Sano, J. Geldmacher and the Expedition 324 Scientists (Editors), Proceedings of the IODP, 324: Tokyo (Integrated Ocean Drilling Program Management International, Inc.), doi:10.2204/ iodp.proc.324.205.2014.

Carvallo, C., and Camps, P., 2013. Data report: magnetic properties of basalts from Shatsky Rise. In W.W. Sager, T. Sano, J. Geldmacher, and the Expedition 324 Scientists (Editors), Proceedings of the IODP, 324: Tokyo (Integrated Ocean Drilling Program Management International, Inc.), doi:10.2204/iodp.proc.324.201.2013.

Carvallo, C., Camps, P., Ooga, M., Fanjat, G., and Sager, W.W., 2013. Palaeointensity determinations and rock magnetic properties on basalts from Shatsky Rise: new evidence for a Mesozoic dipole low. Geophysical Journal International, 192 :986–999. doi:10.1093/gji/ggs100.

Chandler, M. T., Wessel, P., Taylor, B., Seton, M., Kim, S.-S., and Hyeong, K., 2012. Reconstructing Ontong Java Nui: Implications for Pacific plate motion, hotspot drift, and true polar wander. Earth and Planetary Science Letters, 331-332, 140-151, doi:10.1016/j.epsl.2012.03.017.

Clague, D.A., Dalrymple, G.B., Wright, T.L., Klein, F.W., Koyanagi, R.Y., Decker, R.W. and Thomas, D.M., 1989. The Hawaiian-Emperor Chain. In: E.L. Winterer, D.M. Hussong and R.W. Decker (Editors), The Eastern Pacific and Hawaii. Geological Society of America, Boulder, CO, pp. 187-237.

Coffin, M. F., 1992. Subsidence of the Kerguelen Plateau: The Atlantis concept. In F. A. Frey, M. F. Coffin, and P. J. Wallace (Editors), Proceedings of the Ocean Drilling Program, Scientific Results. V. 183, pp. 945-949, doi: 10.2973/odp.proc.sr.120.186.1992.

Coffin, M.F. and Eldholm, O., 1994. Large igneous provinces: crustal structure, dimensions, and external consequences. Reviews of Geophysics, 32: 1-36.

Coffin, M.F., Pringle, M.S., Duncan, R.A., Gladczenko, T.P., Storey, M., Müller, R.D. and Gahagan, L.A., 2002. Kerguelen hotspot magma output since 130 Ma. Journal of Petrology, 43(7): 1121-1139.

Crough, S. T., 1983. Hotspot swells. Annual Reviews of Earth and Planetary Science, 11, 165-193.

Courtillot, V., Davaille, A., Besse, J. and Stock, J., 2003. Three distinct types of hotspots in the Earth's mantle. Earth and Planetary Science Letters, 205: 295-308.

Dannberg J., and Sobolev S.V., 2015,. Low-buoyancy thermochemical plumes resolve controversy of classical mantle plume concept. Nature Communications 6, doi: 10.10.1038/ncomms7970.

Davaille, A., 1999. Simultaneous generation of hotspots and superswells by convection in a heterogeneous planetary mantle. Nature, 402:756-760.

Davis, A. E., and Clague, D. A., 2003. Hyaloclastite from Miocene seamounts offshore central California: Compositions, eruptions styles, and depositional processes. In J. D. L. White, J. L. Smellie, and D. A. Clague, D. A. (Editors), Explosive Subaqueous Volcanism. American Geophysical Union, Geophysical Monograph Series, 140:111-128.

Davies, D.R., Goes, S., and Sambridge, M., 2015. On the realtionship between volcanic hotspot locations, the reconstructed eruption sites of large igneous provinces and deep mantle seismic structure. Earth and Planetary Science Letters 411, 121-130, doi: 10.1016/j.epsl.2014.11.052.

Davy, B., K. Hoernle, and R. Werner, 2008. Hikurangi Plateau: Crustal structure, rifted formation, and Gondwana subduction history. Geochemistry, Geophysics, Geosystems, 9, Q07004, doi:10.1029/2007GC001855.

Delacour, A., and Guillaume, D., 2013. Data report: Alteration of basalts from Sites U1346 and U1349 at Shatsky Rise oceanic plateau, IODP Expedition 324. In W.W. Sager, T. Sano, and J. Geldmacher (Editors), Proceedings of the IODP, 324, doi: 10.2204/iodp.proc.324.203.2010.

Donnelly, K.E., Goldstein, S.L., Langmuir, C.H., Spiegelman, M., 2004. Origin of enriched ocean ridge basalts and implications for mantle dynamics. Earth and Planetary Science Letters, 226:347-366.

Dordevic, M., and J. Georgen, 2016. Dynamics of plume–triple junction interaction: Results from a series of three-dimensional numerical models and implications for the formation of oceanic plateaus. Journal of Geophysical Research, 121, doi:10.1002/2014JB011869.

Doubrovine, P. V., Steinberger, B., and Torsvik, T. H., 2016. Failure to reject: Testing the correlation beteen large igneous provinces and deep mantle structures with EDF statistics, Geochemistry, Geophysics, Geosystems, 17, doi:10.1002/2015GC006044.

Duncan, R.A. and Richards, M.A., 1991. Hotspots, mantle plumes, flood basalts, and true polar wander. Reviews of Geophysics, 29: 31-50.

Eissen, J.-P., Fouquet, Y., Hardy, D., and Ondreas, H., 2003. Recent MORB volcaniclastic explosive deposits formed between 500 and 1750 m.b.s.l. on the axis of the Mid-Atlantic Ridge, south of the Azores. In J. D. L. White, J. L. Smellie, D. A. Clague (Editors), Explosive Subaqueous Volcanism. American Geophysical Union, Geophysical Monograph Series, 140:143-166.

Eldholm, O., J. Thiede, and E. Taylor, 1989. Evolution of the Vøring volcanic margin. In: O. Eldholm, J. Thiede, and E. Taylor (Editors), Proceedings of the Ocean Drilling Program, Scientific Results, v. 104, Ocean Drilling Program, College Station, TX, pp. 1033-1065, doi:10.2973/odp.proc.sr.104.191.1989.

Ernst, R. E., and Buchan, K. L., 2001. Large mafic magmatic events through time and their links to mantle plume heads. In: R. E. Ernst and K. L. Buchan (Editors), Mantle plumes: Their identification through time. Geological Society of America, Special Paper, 352:483-575.

Expedition 324 Scientists, 2010a. Expedition 324 summary. In W.W. Sager, T. Sano, and J. Geldmacher (Editors), Proceedings of the IODP, 324, doi: 10.2204/iodp.proc.324.101.2010.

Expedition 324 Scientists, 2010b. Site U1346. In W.W. Sager, T. Sano, and J. Geldmacher (Editors), Proceedings of the IODP, 324, doi: 10.2204/iodp.proc.324.103.2010.

Expedition 324 Scientists, 2010c. Site U1347. In W.W. Sager, T. Sano, and J. Geldmacher (Editors), Proceedings of the IODP, 324, doi: 10.2204/iodp.proc.324.104.2010.

Expedition 324 Scientists, 2010d. Site U1348. In W.W. Sager, T. Sano, and J. Geldmacher (Editors), Proceedings of the IODP, 324, doi: 10.2204/iodp.proc.324.105.2010.

Expedition 324 Scientists, 2010e. Site U1349. In W.W. Sager, T. Sano, and J. Geldmacher (Editors), Proceedings of the IODP, 324, doi: 10.2204/iodp.proc.324.106.2010.

Expedition 324 Scientists, 2010f. Site U1350. In W.W. Sager, T. Sano, and J. Geldmacher (Editors), Proceedings of the IODP, 324, doi: 10.2204/iodp.proc.324.107.2010.

Farnetani, C. G., Legras, B. and Tackley, P.J., 2002. Mixing and deformation in mantle plumes.

Earth and Planetary Science Letters, 196: 1-15.

Farnetani, C. G., and Richards, M. A., 1994. Numerical investigations of the mantle plume initiation model for flood basalt events. Journal of Geophysical Research, 99, 13,813-13,833.

Farnetani, C. G. and Samuel, H., 2005. Beyond the thermal plume paradigm. Geophysical Research Letters, 32: doi: 10.1029/2005GL022360.

Fitton, J.G. and Godard, M., 2004. Origin and evolution of magmas on the Ontong Java Plateau. In: J.G. Fitton, J.J. Mahoney, P.J. Wallace and A.D. Saunders (Editors), Origin and evolution of the Ontong Java Plateau. The Geological Society, London, pp. 151-178.

Fitton, J.G., Mahoney, J.J., Wallace, P.J. and Saunders, A.D., 2004. Leg 192 synthesis: Origin and evolution of the Ontong Java Plateau, Proceedings of the Ocean Drilling Program, Scientific Results, v. 192. Ocean Drilling Program, College Station, TX, pp. 1-18, doi: 10.12973/odp.proc.sr.192.101.2004.

Fitton, J. G., Saunders, A. D., Norry, M .J., Hardarson, B. S. and Taylor, R. N., 1997. Thermal and chemical structure of the Iceland plume. Earth and Planetary Science Letters, 153: 197-208.

Fitton, J. G., Saunders, A. D., Kemoton, P. D. and Hardarson, B. S., 2003. Does depleted mantle form an intrinsic part of the Iceland plume? Geochemistry, Geophysics, Geosystems, 4, doi:10.1029/2002GC000424.

Foulger, G. R., 2002. Plumes, or plate tectonic processes? Astronomy & Geophysics, 43: 6.19-6.23.

Foulger, G. R., 2011. Plate vs. plumes: A geological controversy. Wiley-Blackwell, 328 p.

Foulger, G.R., 2005. Mantle plumes: Why the current skepticism? Chinese Science Bulletin, 50: 1555-1560.

Foulger, G.R., 2007. The "plate" model for the genesis of melting anomalies. In: G.R. Foulger and D.M. Jurdy (Editors), Plates, Plumes, and Planetary Processes. Geological Society of America, Boulder, CO, pp. 1-28.

Foulger, G.R. and Anderson, D.L., 2005a. A cool model for the Iceland hotspot. Journal of

Volcanology and Geothermal Research, 141: 1-22.

Foulger, G.R. and Natland, J.H., 2003. Is "hotspot" volcanism a consequence of plate tectonics? Science, 300: 921-922.

Foulger, G.R., Natland, J.H., Anderson, D.L., 2005b. Genesis of the Iceland melt anomaly by plate tectonic processes. In: G. R. Foulger, J. H. Natland, D. C. Presnall, and D. L. Anderson (Editors), Plates, plumes and paradigms. Geological Society of America, Spec. Paper, 388:595-625.

Foulger, G.R., Natland, J.H., Anderson, D.L., 2005c. A source for Icelandic magmas in remelted Iapetus crust. Journal of Volcanology and Geothermal Research, 141:23-44, doi: 10.1016/j.jvolgeores.2004.10.006.

French, S. W., and Romanowicz, B., 2015. Broad plumes rooted at the base of the Earth's mantle beneath major hotspots. Nature, 525, 95-99, doi:10.1038/nature14876.

Frey, F.A., Coffin, M.F., Wallace, P.J. and Weis, D., 2003. Leg 183 Synthesis: Kerguelen Plateau-Broken Ridge- A large igneous province, In F. A. Frey, M. F. Coffin, and P. J. Wallace (Editors), Proceedings of the Ocean Drilling Program, Scientific Results, v. 183, Ocean Drilling Program, College Station, TX, doi: 10.2973/odp.proc.sr.183.015.2003.

Gee, J. S., and Kent, D. V., 2007. Source of oceanic magnetic anomalies and the geomagnetic polarity timescale. In G. Schubert (editor), Treatise on Geomagnetism, v. 5, Academic Press, New York, pp. 455-507.

Geldmacher, J., van den Bogaard, P., Heydolph, K., and Hoernle, K., 2014. The age of the Earth's largest volcano: Tamu Massif on Shatsky Rise (northwest Pacific Ocean). International Journal of Earth Science, doi:10.1007/s00531-014-1078-6.

Gente, P., Dyment, J., Maia, M., and Goslin, J., 2003. Interaction between the Mid-Atlantic Ridge and the Azores hot spot during the last 85 Myr: Emplacement and rifting of the hot spot-derived plateaus. Geochemistry, Geophysics, Geosystems, 4, doi:10.1029/2003GC000527.

Georgen, J. E., 2008. Mantle flow and melting beneath oceanic ridge-ridge-ridge triple junctions. Earth and Planetary Science Letters, 270(3-4): 231, doi: 10.1016/j.epsl.2008.03.040.

Georgen, J. E., and Lin, J., 2002. Three-dimensional passive flow and temperature structure beneath oceanic ridge-ridge-ridge triple junctions. Earth and Planetary Science Letters, 204, 115-132.

Gill, J. P., Torssander, H., LaPierre, P., Taylor, R., Kaiho, K., Koyama, M., Kusakabe, M., Aitchison, J., Cisowski, S., Dadey, K., Fujioka, K., Klaus, A., Lovell, M., Marsaglia, K., Pezard, P., Taylor, B., and Tazaki, K., 1990. Explosive deep water basalt in the Sumisu backarc rift. Science, 248:1214-1217.

Gradstein, F. M., Ogg, J. G., Schmitz, M. D., and Ogg, G. M., 2012. The geologic time scale 2012, vol. 2. Elsevier, Amsterdam. 1144 pp.

Griffiths, R.W. and Campbell, I.H., 1990. Stirring and structure in mantle starting plumes. Earth and Planetary Science Letters, 99: 66-78.

Griffiths, R.W. and Campbell, I.H., 1991. Interaction of mantle plume heads with the Earth's surface and the onset of small-scale convection. Journal of Geophysical Research 96, 18295-18310

Hanan, B., and Graham D., 1996. Lead and helium isotope evidence from oceanic basalts for a common deep source of mantle plumes. Science, 272:991-995

Hanyu, T., Shimizu, K., Sano, T. Noble gas evidence for the presence of recycled material in magma sources of Shatsky Rise. In C. Neal, W. Sager, T. Sano and E. Erba (Editors), The Origin, Evolution, and Environmental Impact of Oceanic Large Igneous Provinces. Geological Society of America, Special Paper 511: 57–67, doi:10.1130/2015.2511(03)

Hart, S.R., Hauri E.H., Oschmann L.A., and Whitehead, J.A., 1992. Mantle plumes and entrainment: isotopic evidence. Science, 256:517-520.

Hauff, F., Hoernle, K., Tilton, G., Graham, D., Kerr, A.C., 2000. Large volume recycling of oceanic lithosphere: Geochemical evidence from the Caribbean Large Igneous Province. Earth and Planetary Science Letters 174: 247-263.

Heaton, D. E., and Koppers, A. A. P., 2014. Constraining the rapid construction of TAMU Massif at an ~145 Myr old triple junction, Shatsky Rise. Abstract 4093, 2014 Goldschmidt Conference, 8-13 June 2014, Sacramento, CA.

Herzberg, C., 2004. Partial melting below the Ontong Java Plateau. In: J. G. Fitton, J. J. Mahoney, P. J. Wallace, and A. D. Saunders (Editors), Origin and Evolution of the Ontong Java Plateau. Geological Society of London, Special Publication, 299:179-183.

Heydolph, K., Murphy, D.T., Geldmacher, J., Romanova, I.V., Greene, A., Hoernle, K., Weis, D. and Mahoney, J., 2014. Plume versus plate origin for the Shatsky Rise oceanic plateau (NW Pacific): Insights from Nd, Pb and Hf isotopes. Lithos, 200-201:49-63, doi:10.1016/j.lithos.2014.03.031.

Hilde, T.W.C., Isezaki, N. and Wageman, J.M., 1976. Mesozoic sea-floor spreading in the north Pacific, In G. H. Sutton, M. H. Manghnani, R. Moberly, and E. McAfee (Editors), The Geophysics of the Pacific Ocean Basin and its Margin, Geophysical Monograph 19, American Geophysical Union, Washington, D. C., pp. 205-228, doi:10.1029/GM19p0205.

Hinz, K., 1981. A hypothesis on terrestrial catastrophes: Wedges of very thick oceanward-dipping layers beneath passive margins – Their origin and paleoenvironmental significance. Geologisches Jahrbuch, E22, 3-28.

Hirschmann M.M., and Stopler E. ,1996. A possible role for garnet pyroxenite in the origin of the "garnet signature" in MORB. Contributions to Mineralogy and Petrology, 124:185-208.

Hochmuth, K., Gohl, K., and Uenzelmann-Neben, G., 2015. Playing jigsaw with large igneous provinces – A plate tectonic reconstruction of Ontong Java Nui, west Pacific. Geochemistry, Geophysics, Geosystems, 16, 10.1002/2015GC006036.

Hoernle, K., Werner, R., Morgan, J.P., Garbe-Schönberg, D., Bryce, J., and Mrazek, J., 2000. Existence of complex spatial zonation in the Galápagos plume for at least 14 m.y. Geology, 28: 435–438, doi: 10.1130/0091-7613(2000)28<435:EOCSZI>2.0.CO;2.

Hoernle K., Hauff, F., van den Bogaard, P., 2004. 70 m.y. history (139-69) for the Caribbean large igneous province. Geology 32, 697-700, doi: 10.1130/G20574.1.

Hoernle K., Rohde J., Hauff F., Garbe-Schönberg D., Homrighausen S., Wernder R., Morgan J. P., 2015. How and when plume zonation appeared during the 132 Myr evolution of the Tristan hotspot. Nature Communications, doi: 10.1038/ncomms8799.

Hofmann, A.W., 2003. Sampling mantle heterogeneity through oceanic basalts: isotopes and trace elements. In H. D. Holland and K. K. Turekian (Editors), Treatise on Geochemistry, v. 2, The Mantle and Core. Elsever, Oxford, UK, pp. 61-101.

Hofmann, A.W., and Hart S.R., 1978. An assessment of local and regional isotopic equilibrium in the mantle. Earth and Planetary Science Letters, 39:44-62.

Huang, Y., and Sager, W. W., 2013. Correction of marine magnetic data to make a magnetic anomaly map for Shatsky Rise. Abstract GP13A-1139, American Geophysical Union Fall Meeting, December 9-13, San Francisco, CA.

Husen, A., Almeev, R.R., Holtz, F., Koepke, J., Sano, T. and Mengel, K., 2013. Geothermobarometry of basaltic glasses from the Tamu Massif, Shatsky Rise oceanic plateau. Geochemistry, Geophysics, and Geosystems, 14: 3908-3928, doi: 10.1002/ggge.20231.

Husen, A., Almeev, RR. and Holtz, F., 2016. The effect of H_2O and pressure on multiple saturation and liquids of decent in basalt from the Shatsky Rise. Journal of Petrology, doi:10.1093/petrology/egw008.

Hwang, Y. K., Ritsema, J., van Keken, P. E., Goes, S., and Styles, E., 2011. Wavefront healing renders deep plumes seismically invisible. Geophysical Journal International, 187, 273-277, doi:10.1111/j.1365-246X.2011.05173.x.

Ichiyama Y., Ishiwatari A., Kimura J.-I., Senda R., Miyamoto T., 2014. Jurassic plume-origin ophiolites in Japan: accreted fragments of oceanic plateaus. Contributions to Mineralogy and Petrology 168:1019

Inoue, H., Coffin, M.F., Nakamura, Y., Mochizuki, K. and Kroenke, L.W., 2008. Intrabasement reflections of the Ontong Java Plateau: Implications for plateau construction. Geochemistry, Geophysics, and Geosystems, 9, doi:10.1029/2007GC001780.

Ishikawa, A., Maruyama, S. and Komiya, T., 2004. Layered lithospheric mantle beneath the Ontong Java Plateau: Implications from xenoliths in alnoite, Malaita, Solomon Islands. Journal of Petrology, 45: 2011–2044, doi:10.1093/petrology/egh046.

Ito, G. and Clift, P.D., 1998. Subsidence and growth of Pacific Cretaceous plateaus. Earth and Planetary Science Letters, 161: 85-100.

Ito, G., Lin, J. and Graham, D., 2003. Observational and theoretical studies of the dynamics of mantle plume-mid-ocean ridge interaction. Reviews of Geophysics, 41: 3-1-3-24, doi:10.1029/2002RG000117.

Ito, G. and Taira, A., 2000. Compensation of the Ontong Java Plateau by surface and subsurface loading. Journal of Geophysical Research, 105(B5): 11,171-11,183.

Iwamori, H., McKenzie, D. and Takahashi, E., 1995. Melt generation by isentropic mantle upselling. Earth and Planetary Science Letters, 134: 253-266.

Jackson, E. D., and S. O. Schlanger, 1976. Regional syntheses, Line Islands Chain, Tuamotu Island Chain, and Manihiki Plateau, Central Pacific Ocean. In: S. O. Schlanger and E. D. Jackson (Editors), Initial Reports of the Deep Sea Drilling Project, v. 33, US Government Printing Office, Washington, DC, pp. 915-927, doi:10.2973/dsdp.proc.33.136.1976.

Jackson, M. G. and Jellinek, A. M., 2013. Major and trace element composition of the high $^{3}He/^{4}He$ mantle: Implications for the composition of a nonchonditic Earth. Geochemistry, Geophysics, and Geosystems, 14: 2954–2976, doi:10.1002/ggge.20188.

Jackson, M.G. and Carlson, R.W., 2011. An ancient recipe for flood-basalt genesis. Nature. 476: 316–319.

Jackson, M.G., Hart, S.R., Konter, J., Koppers, A.A.P., Staudigel, H., Kurz, M.D., Blusztajn, J. and Sinton, J.M., 2010. Samoan hot spot track on a "hot spot highway": Implications for mantle plumes and a deep Samoan mantle source. Geochemistry, Geophysics, and Geosystems, 11, doi: 10.1029/2010GC003232.

Jellinek, A.M. and Manga, M., 2004. Links between long-lived hot spots, mantle plumes, D", and plate tectonics. Reviews of Geophysics, 42, doi:10.1029/2003RG000144.

Jerram, D.A. and Widdowson, M., 2005. The anatomy of continental flood basalt provinces: Geological constraints on the process and products of flood volcanism. Lithos, 79: 385-405, doi: 10.1016/j.lithos.2004.09.009.

Kang, M.-H., Sager, W.W., and the Expedition 324 Scientists, 2010. Data report: underway geophysics. In W. W. Sager, T. Sano, J. Geldmacher, and the Expedition 324 Scientists (Editors), Proceedings of the IODP, 324: Tokyo (Integrated Ocean Drilling Program Management International, Inc.), doi:10.2204/iodp.proc.324.108.2010.

Kashintsev, G.L. and Suzymumov, A.Y., 1981. Basalts of the Shatsky Rise. Doklady Akademii Nauk SSSR, Earth Science Section English Translation, 258: 86-90.

Keszthelyi, L. and Self, S., 1998. Some physical requirements for the emplacement of long basaltic lava flows. Journal of Geophysical Research, 103: 27,447-27,464.

Kimura, G., Sakakibara, M., Okamura, M., 1994. Plumes in central Panthalassa? Deductions from accreted oceanic fragments in Japan. Tectonics 13: 905-916.

Kimura, J.-I. and Kawabata, H., 2015. Ocean Basalt Simulator version 1 (OBS1): Trace element mass balance in adiabatic melting of a pyroxenite-bearing peridotite. Geochemistry, Geophysics, Geosystems, doi: 10.1002/2014GC005606.

Klaus, A. and Sager, W.W., 2002. Data report: High-resolution site survey seismic reflection data for ODP Leg 198 drilling on Shatsky Rise, northwest Pacific. Proceedings of the Ocean Drilling Program, Scientific Results, 198: doi: 10.2973/odp.proc.ir.198.111.2002.

Klein, E. M. and Langmuir, C. H., 1987. Global correlations of ocean ridge basalt chemistry with axial depth and crustal thickness. Journal of Geophysical Research, 92: 8089–8115, doi:10.1029/JB092iB08p08089.

Koppers, A. A. P., Sano, T., Natland, J. H., Widdowson, M., Almeev, R., Greene, A. R., Murphy, D. T., Delacour, A., Miyoshi, M., Shimizu, K., Li, S., Hirano, N., Geldmacher, J., and the Expedition 324 Scientists, 2010. Massive basalt flows on the southern flank of Tamu Massif, Shatsky Rise: A reappraisal of ODP Site 1213 basement units. In W.W. Sager, T. Sano, and J. Geldmacher (Editors), Proceedings of the IODP, 324, doi: 10.2204/iodp.proc.324.109.2010.

Korenaga, J., 2005. Why did not the Ontong Java Plateau form subaerially? Earth and Planetary Science Letters, 234: 385-399, doi: 10.1016/j.epsl.2005.03.011.

Korenaga, J., Kelemen, P.B. and Holbrook, J.M., 2002. Methods for resolving the origin of large igneous provinces from crustal seismology. Journal of Geophysical Research, 107, doi: 10.1029/2001JB0010030.

Korenaga, J. and Sager, W.W., 2012. Seismic tomography of Shatsky Rise by adaptive importance sampling. Journal of Geophysical Research, 117, doi: 10.1029/2012JB009248.

Kumagai, I., 2002. On the anatomy of mantle plumes: effects of the viscosity ratio on entrainment and stirring. Earth and Planetary Science Letters 198: 211-224.

Kumagai, I., Davaille, A., Kurita, K. and Stutzmann, E., 2008. Mantle plumes: Thin, fat, successful, or failing? Constraints to explain hot spot volcanism through time and space. Geophysical Research Letters, 35, doi: 10.1029/2008GK035079.

Kurz, M.D., Jenkins, W.J., and Hart, S.R., 1982. Helium isotopic systematics of oceanic islands and mantle heterogeneity. Nature, 297:43-47.

Langmuir, C. H., Klein, E. M. and Plank, T., 1992. Petrological systematics of mid- ocean ridge basalts: Constraints on melt generation beneath ocean ridges. In Morgan J. P. et al. (editors), Mantle Flow and Melt Generation at Mid- ocean Ridges, Geophysical Monograph Series, 71: 183–280, AGU, Washington, D. C.

Larsen, H. C., Dahl-Jenson, T., and Hopper, J. R., 1998. Crustal structure along the Leg 152 drilling transect. In: A. D. Saunders, H. C. Larsen, S. W. Wise, Jr. (Editors), Proceedings of the Ocean Drilling Program, Scientific Results, v. 152, Ocean Drilling Program, College Station, TX, pp. 463-475, doi:10.2973/odp.proc.sr.152.245.1998.

Larson, R.L., 1991. Geological consequences of superplumes. Geology, 19: 963-966.

Larson, R.L. and Lowrie, W., 1975. Paleomagnetic evidence for motion of the Pacific plate from Leg 32 basalts and magnetic anomalies. In: R.L. Larson and R. Moberly (Editors), Initial Reports of the Deep Sea Drilling Project. v. 32, US Government Printing Office, Washington, DC, pp. 571-577, doi:10.2973/dsdp.proc.32.122.1975.

Larson, R.L., Steiner, M.B., Erba, E. and Lancelot, Y., 1992. Paleolatitudes and tectonic reconstructions of the oldest portion of the Pacific plate: A comparative study. In: R.L. Larson and Y. Lancelot (Editors), Proceedings of the Ocean Drilling Program, Scientific Results. Ocean Drilling Program, College Station, TX, pp. 615-631.

Li, S., Geldmacher, J., Hauff, F., Garbe-Schönberg, D., Yu, S., Zhao, S. and Rausch, S., 2014. Composition and timing of carbonate vein precipitation within the igneous basement of the Early Cretaceous Shatsky Rise, NW Pacific. *Marine Geology 357: 321-333, doi: 10.1016/j.margeo.2014.09.046.*

Lin, S.-C., and van Keken, P.E., 2005. Multile volcanic episodes of flood basalts caused by thermochemical mantle plumes. Nature 436: 250-252.

Lonsdale, P., Dieu, J. and Natland, J., 1993. Posterosional volcanism in the Cretaceous part of the Hawaiian hotspot trail. Journal of Geophysical Research, 98: 4081-4098.

MacDonald, G. A., and Abbott, A. T., 1970. Volcanoes in the Sea. University of Hawaii Press, Honolulu, 441 pp.

Macdougall, J. D. (Editor) 1988. Continental flood basalts. Kluwer Academic Publishers, Dordrecht, Netherlands, 341 p.

Mahoney, J.J., Duncan, R.A., Tejada, M.L.G., Sager, W.W. and Bralower, T.J., 2005. Jurrassic-Cretaceous boundary age and mid-ocean-ridge-type mantle source for Shatsky Rise. Geology, 33: 185-188, doi: 10.1130/G21378.1.

Mahoney, J.J., Storey, M., Duncan, R.A., Spencer, K.J. and Pringle, M.,1993. Geochemistry and geochronology of Leg 130 basement lavas: nature and origin of the Ontong Java Plateau. In: W.H. Berger, L.W. Kroenke, L.A. Mayer and et al. (Editors), Proceedings of the Ocean Drilling Program, Scientific Results, 130, doi:10.2973/odp.proc.sr.130.040.1993.

Malinverno, A., Hildebrandt, J., Tominaga, J., and Channell, J. E. T., 2012. M-sequence geomagnetic polarity time scale (MHTC12) that steadies global spreading rates and incorporates astrochronology. Journal of Geophysical Research, 117, doi:10.1029/2012JB009260.

McClinton, T., White, S.M., Colman, A. and Sinton, J.M., 2013. Reconstructing lava flow emplacement processes at the hot spot-affected Galapagos Spreading Center, 95°W and 92°W. Geochemistry, Geophysics, and Geosystems, 15(8): 2731-2756.

McKenzie, D. P. and Bickle, M. J., 1988. The volume and composition of melt generated by extension of the lithosphere. Journal of Petrology, 29: 625–679.

Michael, P.J., 1999. Implications for magmatic processes at Ontong Java Plateau from volatile and major elements contents of Cretaceous basalt glasses. Geochemistry, Geophysics, Geosystems, 1, doi:10.1029/1999GC000025.

Michael, P. J. and Cornell, W. C., 1998. Influence of spreading rate and magma supply on crystallization and assimilation beneath mid−ocean ridges: Evidence from chlorine and major element chemistry of mid−ocean ridge basalts. Journal of Geophysical Research, 103: 18,325–18,356, doi:10.1029/98JB00791.

Miyoshi, M., Sano, T., Shimizu, K., Delacour, A., Hasenaka, T. and Fukuoka, T., 2015, Boron and chlorine contents of basalts from the Shatsky Rise, IODP Expedition 324: Implications for the alteration of oceanic plateaus. In C. R. Neal, W. W. Sager, T. Sano, and E. Erba (Editors), The Origin, Evolution, and Environmental Impact of Oceanic Large Igneous Provinces, Geological Society of America, Special Paper 511, 69-84, doi:10.1130/2015.2511(04).

Moberly, R. and Larson, R.L., 1975. Mesozoic magnetic anomalies, oceanic plateaus, and seamount chains in the northwestern Pacific Ocean. In: R.L. Larson and R. Moberly (Editors), Initial Reports of the Deep Sea Drilling Project, v. 32, U.S. Government Printing Office, Washington, D. C., pp. 945-957, doi: 10.2973/dsdp.proc.32.140.1975.

Montelli, R., Nolet, G., Dahlen, F. A., Masters, G., Engdahl, E. R., Hung, S.-H., 2004. Finite-frequency tomography reveals a variety of plumes in the mantle. Science, 303, 338-343.

Montelli, R., Nolet, G., Dahlen, F. A., and Masters, G., 2006. A catalogue of deep mantle plumes: New results from finite-frequency tomography. Geochemistry, Geophysics, Geosystems, 7, doi:10.1029/2006GC001248.

Morgan, W. J., 1971. Convective plumes in the lower mantle. Nature, 230:42-43.

Morgan, W.J., 1972. Deep mantle convection plumes and plate motions. American Association of Petroleum Geologists Bulletin, 56: 203-213.

Mutter, J. C., M. Talwani, and P. L. Stoffa, 1982. Origin of seaward-dipping reflectors in oceanic crust off the Norwegian margin by “subaerial seafloor spreading”. Geology, 10, 353-357.

Mutter, J. C., 1985. Seaward dipping reflectors and the continent-ocean boundary at passive continental margins. Tectonophysics, 114, 117-131.

Nakanishi, M., Sager, W.W. and Klaus, A., 1999. Magnetic lineations within Shatsky Rise,

northwest Pacific Ocean: implications for hot spot-triple junction interaction and oceanic plateau formation. Journal of Geophysical Research, 104: 7539-7556.

Nakanishi, M., Sager, W. W., and Korenaga, J., 2015. Reorganization of the Pacific-Izanagi-Farallon triple junction in the Late Jurassic: Tectonic events before the formation of Shatsky Rise. In C. Neal, W. Sager, T. Sano and E. Erba (Editors), The Origin, Evolution, and Environmental Impact of Oceanic Large Igneous Provinces. Geological Society of America, Special Paper 511, 85-101, doi:10.1130/2015.2511(05).

Nakanishi, M., Tamaki, K., and Kobayashi, K., 1989. Mesozoic magnetic anomaly lineations and seafloor spreading history of the northwestern Pacific. Journal of Geophysical Research, 94, 15,437-14,462.

Natland, J.H., 2013. Nothing but MORB at Shatsky Rise, Abstract OS43A-1874, American Geophysical Union Fall Meeting, 9-13 December 2013, San Francisco, CA.

Natland, J. H., and Winterer, E. L., 2005. Fissure control on volcanic action in the Pacific. In G. R. Foulger, J. H. Natland, D. C. Presnell, and D. L. Anderson (Editors), Geological Society of America, Special Paper 388: 687-710, doi: 10/1130/2005.2388(39).

Neal. C. R., Mahoney, J. J., and Chazey, W. J. III, 2002. Mantle sources and the highly variable role of continental lithosphere in basalt petrogenesis of the Kerguelen Plateau and Broken Ridge LIP: Results from ODP Leg 183. Journal of Petrolology, 43:1177-1205.

Neal, C. R., Mahoney, J. J., Kroenke, L. W., Duncan, R. A., and Petterson, M. G., 1997. The Ontong Java Plateau. In: J. J. Mahoney, and M. F. Coffin (Editors), Large Igneous Provinces: Continental, Oceanic, and Planetary Flood Volcanism. American Geophysical Union, Geophysical Monograph Series, 100:183-216.

Niu, Y. and Batiza R. 1991. An empirical method for calculating melt compositions produced beneath mid-ocean ridges: Application for axis and off-axis (seamounts) melting. Journal of Geophysical Research, 96, 2156–2202, doi:10.1029/91JB01933.

Niu, Y. and O'Hara, M. J., 2008. Global corrections of ocean ridge basalt chemistry with axial depth: A new perspective. Journal of Petrology, 49: 633–664, doi:10.1093/petrology/egm051.

Nolet, G., Allen, R., and Zhao, D., 2007. Mantle plume tomography. Chemical Geology, 241,

248-263, doi:10.1016/j.chemgeo.2007.01.022.

O'Connor, J. M., Jokat, W., le Roex, A. P., Class, C., Wijbrans, J. R., Keßling, S., Kuiper, K. F., and Nebel, O., 2012. Hotspot trails in the South Atlantic controlled by plume and plate tectonic processes. Nature Geoscience, 5, 735-738, doi:10.1038/NGEO1583.

Parsiegla, N., Gohl, K., and Uenzelmann-Neben, G., 2008. The Agulhas Plateau: Structure and evolution of a large igneous province. Geophysical Journal International, 174, 336-350, doi:10.1111/j.1365-246X.2008.

Parsons, B. and Sclater, J.G., 1977. An analysis of the variation of ocean floor bathymetry and heat flow with age. Journal of Geophysical Research, 82: 803-827.

Phinney, E. J., Mann, P. Coffin, M. F., and Shipley, T. H., 1999. Sequence stratigraphy, structure, and tectonic history of the southwest Ontong Java Plateau adjacent to the North Solomon Trench and Solomon Islands Arc, Journal of Geophysical Research, 104, 20,449-20,466.

Phipps Morgan J., 1999. Isotope topology of individual hotspot basalt arrays: mixing curves of melt extraction trajectories?. Geochemisty, Geophysics, Geosystems, 1, doi:10.1029/1999GC000004.03808.x.

Pietsch, R., and Uenzelmann-Neben, G., 2015. The Manihiki Plateau – A multistage volcanic emplacement history. Geochemistry, Geophysics, Geosystems, 16, doi:10.1002/2015GC005852.

Planke, S., and Cambray, H., 1998. Seismic properties of flood basalts on rifted volcanic margins based on Ocean Drilling Program (ODP) Hole 917A downhole data. In: A. D. Saunders, H. C. Larsen, S. W. Wise, Jr. (Editors), Proceedings of the Ocean Drilling Program, Scientific Results, v. 152, Ocean Drilling Program, College Station, TX, pp. 453-462, doi:10.2973/proc.odp.sr.152.247.1998.

Planke, S., and Eldholm, O., 1994. Seismic response and construction of seaward dipping wedges of flood basalts: Vøring volcanic margin. Journal of Geophysical Research, 99, 9263-9278.

Planke, S., Symonds, P. A., Alvestad, E., and Skogseid, J., 2000. Seismic volcanostratigraphy of large-volume basaltic extrusive complexes on rifted margins. Journal of Geophysical Research, 105, 19,335-19351.

Prytulak, J., Nielson, S. G., Ionov, D. A., Halliday, A. N., Harvey, J., Kelley, K. A., Niu, Y. L., Peate, D. W., Shimizu, K., and Sims, K. W. W., 2013. The stable vanadium isotope composition of the mantle and mafic lavas. Earth and Planetary Science Letters, 365: 177-189, doi: 10.1016/j.epsl.2013.01.010.

Pueringer, M., Sager, W., and Housen, B., 2013. Data report: paleomagnetic measurements of igneous rocks from Shatsky Rise Expedition 324. In W.W. Sager, T. Sano, J. Geldmacher, and the Expedition 324 Scientists, Proceedings of the IODP, 324: Tokyo (Integrated Ocean Drilling Program Management International, Inc.), doi:10.2204/iodp.proc.324.202.2013.

Regelous, M., Hofmann, A.W., Abouchami, W., Galer J. S. G., 2003. Geochemistry of lavas from the Emperor seamounts and the geochemical evolution of Hawaiian magmatism 85-42 Ma. Journal of Petrology, 44:113-140.

Richards, M.A., Duncan, R.A. and Courtillot, V.E., 1989. Flood basalts and hot-spot tracks: plume heads and tails. Science, 246: 103-107.

Roberge, J., White, R. and Wallace P., 2004. Volatiles in basaltic magmas from the Ontong Java Plateau: Implications for mantle source regions, shallow level magmatic processes, and plateau subsidence. In: J.G. Fitton, J.J. Mahoney, P.J. Wallace and A.D. Saunders (Editors), Origin and evolution of the Ontong Java Plateau. Geological Society of London, Special Publication 229, 239-257.

Roberge, J., Wallace, P.J., White, R.V. and Coffin, M.F., 2005. Anomalous uplift and subsidence of the Ontong Java Plateau inferred from CO_2 contents of submarine basaltic glasses. Geology, 33: 501-505.

Rohde, J. K., van den Bogaard, P., Hoernle, K., Hauff, F. and Werner, R., 2013. Evidence for an age progression along the Tristan-Gough volcanic track from new $^{40}Ar/^{39}Ar$ ages on phenocryst phases. Tectonophysics 604: 60-71.

Romanova, I. V., Murphy, D. T., Bryan, S. E., Owen, D. D. R., and Sano, T., Quantitative evaluation of element mobility during seawater alteration of basalts: an example from the Shatsky Rise oceanic plateau, NW Pacific, Geochemica et Cosmochimica Acta, submitted.

Ross, P. -S., Ukstins Peate, I., McClintock, M. K., Xy, Y. G., Skilling, I. P. White, J. D. L. and Houghton, B. F., 2005. Mafic volcaniclastic deposits in flood basalt provinces: a review. Journal of Volcanology and Geothermal Research, 145: 281–314.

Rotstein, Y., Schlich, R., Munschy, M., and Coffin, M. F., 1992. Structure and tectonic history of the southern Kerguelen Plateau (Indian Ocean) deduced from seismic reflection data. Tectonics, 11, 1332-1347.

Royer, J.-Y., Peirce, J. W., and Weissel, J. K., 1991. Tectonic constraints on the hot-spot formation of Ninetyeast Ridge. In J. K. Weissel, J. W. Peirce, and J. Alt (Editors), Proceedings of the Ocean Drilling Program, Scientific Results, v. 121, Ocean Drilling Program (College Station, TX), pp. 763-776, doi:10.2973/odp.proc.sr.121.122.1991.

Sager, W. W., Sano, T., and Geldmacher, J. (Editors), 2010. Proceedings of the IODP, 324, doi:10.2204/iodp.proc.324.101.2010.

Sager, W. W., 2005. What built Shatsky Rise, a mantle plume or ridge tectonics? In G. R. Foulger, J. H. Natland, D. C. Presnell, and D. L. Anderson (Editors), Geological Society of America, Special Paper 388: 687-710, doi: 10/1130/2005.2388(41).

Sager, W. W., 2006. Cretaceous paleomagnetic apparent polar wander path for the Pacific plate calculated from Deep Sea Drilling Project and Ocean Drilling Program basalt cores. Physics of the Earth and Planetary Interiors, 156: 329-349, doi: 10.1016/j.pepi.2005.09.014.

Sager, W. W., 2007. Divergence between paleomagnetic and hotspot-model-predicted polar wander for the Pacific plate with implications for hotspot fixity. In: G.R. Foulger and D.M. Jurdy (Editors), Plates, plumes, and planetary processes. Geological Society of America, Special Paper 430: 335-357, doi:10.1130/2007.2430(17).

Sager, W. W., and Escutia, C., 2005. Leg 191 synthesis: Summary of scientific results. In W. W. Sager, T. Kanazawa, and C. Escutia (Editors), Proceedings of the ODP, Scientific Results, 191, doi: 10.2973/odp.proc.sr.191.001.2005.

Sager, W.W., Evans, H.F. and Channell, J.E.T., 2005. Paleomagnetism of Early Cretaceous

(Berriasian) sedimentary rocks, Hole 1213B, Shatsky Rise. In T. J. Bralower, I. Premoli-Silva, and M. J. Malone (Editors), Proceedings of the Ocean Drilling Program, Scientific Results, 198, doi: 10.2973/odp.proc.sr.198.117.2005.

Sager, W.W. and Han, H.-C., 1993. Rapid formation of the Shatsky Rise oceanic plateau inferred from its magnetic anomaly. Nature, 364: 610-613.

Sager, W.W., Handschumacher, D.W., Hilde, T.W.C. and Bracey, D.R., 1988. Tectonic evolution of the northern Pacific plate and Pacific-Farallon-Izanagi triple junction in the Late Jurassic and Early Cretaceous (M21-M10). Tectonophysics, 155: 345-364.

Sager, W.W., Kim, J., Klaus, A., Nakanishi, M. and Khankishieva, L.M., 1999. Bathymetry of Shatsky Rise, northwest Pacific Ocean: implications for ocean plateau development at a triple junction. Journal of Geophysical Research, 104(B4): 7557-7576.

Sager, W. W., Pueringer, M., Carvallo, C., Ooga, M., Housen, B., and Tominaga, M., Paleomagnetism of igneous rocks from the Shatsky Rise: Implications for paleolatitude and oceanic plateau volcanism. In C. Neal, W. Sager, T. Sano and E. Erba (Editors), The Origin, Evolution, and Environmental Impact of Oceanic Large Igneous Provinces. Geological Society of America, Special Paper 511, doi:10.1130/2015.2511(08).

Sager, W.W., Sano, T. and Geldmacher, J., 2011a. How do oceanic plateaus form? Clues from drilling Shatsky Rise. EOS, Transactions, American Geophysical Union, 92(5): 37-44.

Sager, W.W., Sano, T., Geldmacher, J. and Scientists, I.E., 2011b. IODP Expedition 324: Ocean drilling at Shatsky Rise gives clues about oceanic plateau formation. Scientific Drilling, 12: 24-31.

Sager, W.W., Zhang, J., Korenaga, J., Sano, T., Koppers, A.A.P., Widdowson, M. and Mahoney, J.J., 2013. An immense shield volcano within the Shatsky Rise oceanic plateau, northwest Pacific Ocean. Nature Geoscience, 6: 976-981.

Sandwell, D. T., and MacKenzie, K. R., 1989. Geoid height versus topography for oceanic plateaus and swells. Journal of Geophysical Research, 94: 7403-7418.

Sano, T., Shimizu, K., Ishikawa, A., Senda, R., Chang, Q., Kimura, J.-I., Widdowson, M. and Sager, W.W., 2012. Variety and origin of magmas on Shatsky Rise, northwest Pacfic Ocean. Geochemistry, Geophysics, Geosystems, 13, doi:10.1029/2012GC004235..

Sano, T., Miyoshi, M., Ingle, S., Banerjee, N. R., Ishimoto, M. and T. Fukuoka, 2008. Boron and chlorine contents of upper oceanic crust: Basement samples from IODP Hole 1256D. Geochemistry, Geophysics, Geosystems, 9, doi:10.1029/2008GC002182.

Sano, T. and Nishio, Y., 2015. Lithium isotopic evidence for magmatic assimilation of hydrothermally influenced crust beneath oceanic large igneous provinces. In C. Neal, W. Sager, T. Sano and E. Erba (Editors), The Origin, Evolution, and Environmental Impact of Oceanic Large Igneous Provinces. Geological Society of America, Special Paper 511, pp. 173-183, doi:10.1130/2015.2511(09).

Sano, T. and Yamashita, S., 2004. Experimental petrology of basement lavas from Ocean Drilling Program Leg192: Implications for differentiation processes in Ontong Java Plateau magmas. In J. G. Fitton, J. J. Mahoney, P. J. Wallace, and A. D. Saunders (Editors), Origin and Evolution of the Ontong Java Plateau, Geological Society of London, Special Publication 229: 185–218, doi:10.1144/GSL.SP.2004.229.01.12.

Schaming, M., and Rotstein, Y., 1990. Basement reflectors in the Kerguelen Plateau, south Indian Ocean – Indications for the structure and early history of the Plateau. Geological Society of American Bulletin, 102, 580-592.

Schilling, J.-G., 1973. Iceland mantle plume: Geochemical evidence along Reykjanes Ridge. Nature, 242: 565-571.

Schilling, J.-G., 1985. Upper mantle heterogeneities and dynamics. Nature, 314: 62-67.

Self., S., Thordarson, T., and Keszthelyi, L., 1997. Emplacement of continental flood basalt lava flows. In J. J. Mahoney and M. F. Coffin (Editors), Large igneous provinces: Continental, oceanic, and planetary flood volcanism. American Geophysical Union, Geophysical Monograph Series, 100: 381-410, doi: 10.1029/GM100p0381.

Shimizu, K., Shimizu, N., Sano, T., Matsubara, N. and Sager, W., 2013. Paleo-elevation and subsidence of ~145 Ma Shatsky Rise inferred from CO2 and H2O in fresh volcanic glass. Earth and Planetary Science Letters, 383: 37-44, doi: 10.1016/j.epsl.2013.09.023.

Shipboard Scientific Party, 1975. Site 306: Shatsky Rise. In R. L. Larson and R. Moberly (Editors), Initial Reports of the DSDP, 32: 159-191, doi:10.2973/dsdp.proc.32.105.1975.

Shipboard Scientific Party, 2000. Leg 183 summary: Kerguelen Plateau-Broken Ridge – A large igneous province, In M. F. Coffin, F. A Frey, P. J. Wallace (Editors), Proceedings of the Ocean Drilling Program, Initial Reports, v. 183, Ocean Drilling Program, College Station, TX, doi:10.2973/odp.proc.ir.183.101.2000.

Shipboard Scientific Party, 2001. Leg 192 Summary. In J. J. Mahoney, J. G. Fitton, and P. J. Wallace (Editors), Proceedings of the ODP, Initial Reports, 192, doi:10.2973.odp.proc.ir.192.101.2001.

Shipboard Scientific Party, 2002. Site 1213. In T. J. Bralower, I. Premoli-Silva, and M. J. Malone (Editors), Proceedings of the ODP, Initial Reports, 198, doi:10.2973/odp.proc.ir.198.109.2002.

Sliter, W.V. and Brown, G.R., 1993. Shatsky Rise: seismic stratigraphy and sedimentary record of Pacific paleoceanography since Early Cretaceous. In: J.H. Natland, F. R. Rack, and L. B. Stokking (Editors), Proceedings of the Ocean Drilling Program, Scientific Results, 132: 3-13, doi: 10.2973/odp.proc.sr.132.302.1993.

Smith, D.K., 1988. Shape analysis of Pacific seamounts. Earth and Planetary Science Letters, 90: 457-466.

Smith, W.H.F. and Sandwell, D.T., 1997. Global sea floor topography from satellite altimetry and ship depth soundings. Science, 277: 1956-1962.

Stein, C.A. and Stein, S., 1992. A model for the global variation in oceanic depth and heat flow with lithospheric age. Nature, 359: 123-129.

Tackley, P. J., 1998. Three-dimensional simulations of mantle convection with a thermo-chemical boundary layer: D''? In: M. Gurnis, M. E. Wysession, E. Knittle, and B. A. Buffett (Editors), The Core-Mantle Boundary Region. American Geophysical Union, Geodynamics Series, 28: 231-253.

Tarduno, J.A., Sliter, W.V., Kroenke, L., Leckie, M., Mayer, H., Mahoney, J.J., Musgrave, R., Storey, M. and Winterer, E.L., 1991. Rapid formation of Ontong Java Plateau by Aptian mantle plume volcanism. Science, 254: 399-403.

Tatsumi, Y., Shinjoe, H., Ishizuka, H., Sager, W.W. and Klaus, A., 1998. Geochemical evidence for a mid-Cretaceous superplume. Geology, 26: 151-154. doi:10.1130/0091-

7613.1998.

Taylor, B., 2006. The single largest oceanic plateau: Ontong Java-Manihiki-Hikurangi. Earth and Planetary Science Letters, 241, 372-380.

Tejada, M.L.G., Mahoney, J.J., Castillo, P.R., Ingle, S.P., Sheth, H.C. and Weis, D., 2004. Pin-pricking the elephant: Evidence on the origin of the Ontong Java Plateau from Pb-Sr-Hf-Nd isotopic characteristics of ODP Leg 192 basalts. In: J.G. Fitton, J.J. Mahoney, P.J. Wallace and A.D. Saunders (Editors), Origin and evolution of the Ontong Java Plateau. Geological Society of London, Special Publication 229: 133-150, doi:10.1144/GSL.SP.2004.229.01.09.

Tejada, M.L.G., Mahoney, J.J., Duncan, R.A. and Hawkins, M.P., 1996. Age and geochemistry of basement and alkalic rocks of Malaita and Santa Isabel, Solomon Islands, southern margin of Ontong Java Plateau. Journal of Petrology, 37: 361-394, doi:10.1093/petrology/37.2.361.

Tejada, M.L.G., Mahoney, J.J., Neal, C.R., Duncan, R.A. and Petterson, M.G., 2002. Basement geochemistry and geochronology of central Malaita, Solomon Islands, with implications for the origin and evolution of the Ontong Java Plateau. Journal of Petrology, 43: 449-484.

Tejada M.L.G., Geldmacher J., Hauff F., Heaton D., Koppers A., Garbe-Schönberg D., Hoernle K., Heydolph K., Sager W. W. Geochemistry and Age of Shatsky, Hess, and Ojin Rise seamounts: Implications for a connection between the Shatsky and Hess Rises. Geochemica et Cosmochimica Acta, in press.

Thordarson, T., 2004. Accretionary-lapilli-bearing volcaniclastic rocks at ODP Site 1184: A record of subaerial phreatomagmatic eruptions on the Ontong Java Plateau. In: J. G. Fitton, J. J. Mahoney, P. J. Wallace, and A. D. Saunders (Editors), Origin and Evolution of the Ontong Java Plateau. Geological Society of London, Special Publication, 229: 275-306.

Timm, C., Hoernle, K., Werner, R., Hauff, F., van den Bogaard, P., Michael, P., Coffin, M. F. and Koppers, A., 2011. Age and geochemistry of the oceanic Manihiki Plateau, SW Pacific: New evidence for a plume origin. Earth and Planetary Science Letters. 304: 135-146.

Tominaga, M., Evans, H. F. and Iturrino, G., 2012. "Equator Crossing" of Shatsky Rise?: New insights on Shatsky Rise tectonic motion from the downhole magnetic architecture of the

uppermost lava sequences at Tamu Massif. Geophysical Research Letters, 39: doi:10.1029/2012GL052967.

Tominaga, M., Iturrino, G. and Evans, H.F., 2014. Volcanic evolution of the submarine super volcano, Tamu Massif of Shatsky Rise: New insights from Formation Microscanner logging imagery. Geophysical Research Letters, 42: 8, doi:10.1002/2014GL061630.

Tominaga, M., and Sager, W. W., 2010. Revised Pacific M-anomaly geomagnetic polarity timescale. Geophysical Journal International, 182, 203-232, doi:10.1111/j.1365-246X.2010.04610.x.

Tominaga, M., Sager, W.W. and Channell, J.E.T., 2005. Paleomagnetism of the igneous section, Hole 1213B, Shatsky Rise. In: T.J. Bralower, I. Premoli-Silva and M.J. Malone (Editors), Proceedings of the Ocean Drilling Program, Scientific Results, 198, doi:10.2973/odp.proc.sr.198.113.2005.

Torsvik, T.H., Smethurst, M.A., Burke, K. and Steinberger, B., 2006. Large Igneous provinces generated from the margins of the large low-velocity provinces in the deep mantle. Geophysical Journal International, 167: 1447-1460, doi: 10.1111/j.1365-246X.2006.03158.x.

Vuong, A. K., Zhang, J., Gibson, R. L., Jr., and Sager, W. W., 2015. Appliation of the 2-D continuous wavelet transforms to imaging of Shatsky Rise plateau using marine seismic data. In C. Neal, W. Sager, T. Sano and E. Erba (Editors), The Origin, Evolution, and Environmental Impact of Oceanic Large Igneous Provinces. Special Paper 511, Geological Society of America, Tulsa, OK, pp. 127-146, doi:10.1130/2015.2511(07).

Wallace, P. J., 2002. Volatile in submarine basaltic glasses from the Northern Kerguelen Plateau (ODP Site 1140): implications for surce region compsositions, magmatic processes, and plateau subsidence. Journal of Petrology, 43: 1311–1326.

Wasserburg, G. J., and Depaolo, D. J., 1979. Models of Earth structure inferred from neodymium and strontium isotopic abundances. Proceedings of the National Academy of Science,, 76: 3594-3598.

Waters, C. L., Sims, K. W. W., Perfit, M. R., Blichert-Toft, J., Blusztajn, J., 2011. Perspective on the Genesis of E-MORB from Chemical and Isotopic Heterogeneity at 9–10°N East Pacific Rise. Journal of Petrolology, 52: 565-602.

Wessel, P., Harada, Y., and Kroenke, L. W., 2006. Toward a self-consistent, high-resolution absolute plate motion model for the Pacific. Geochemistry, Geophysics, Geosystems, 7, doi:10.1029/2005GC001000.

Wessel, P., and Kroenke, L. W., 2008. Pacific absolute plate motion since 145 Ma: An assessment of the fixed hotspot hypothesis. Journal of Geophysical Research, 113, doi:10.1029/2007JB005499.

Whittaker, J. M., Afonso, J. C., Masterton, S., Müller, R. D., Wessel, P., Williams, S. E., and Seton, M., 2015. Long-term interaction between mid-ocean ridges and mantle plumes. Nature Geoscience, 479-483, doi:10.1038/NGEO02437.

Wilson, J.T., 1963. A possible origin of the Hawaiian Islands. Canadian Journal of Physics, 41: 863-870.

Woods, M. T. and Davies, G. F., 1982. Late Cretaceous genesis of the Kula plate. Earth and Planetary Science Letters, 58: 161-166.

Yasuda, A., Fujii, T., and Kurita, K., 1994. Melting phase relations of an anhydrous mid-ocean ridge basalt from 3 to 20 Gpa: Implications for the behavior of subducted oceanic crust in the mantle. Journal of Geophysical Research, 99, 9401-9414.

Zhang, J., Sager, W. W., and Korenaga, J., 2015. Shatsky Rise oceanic plateau structure from 2D multichannel seismic reflection profiles and implications for oceanic plateau formation. In C. Neal, W. Sager, T. Sano and E. Erba (Editors), The Origin, Evolution, and Environmental Impact of Oceanic Large Igneous Provinces. Special Paper 511, Geological Society of America, Tulsa, OK, pp. 103-126, doi:10.1130/2015.2511(06).

Zhang, J., Sager, W. W., and Korenaga, J., 2016. The seismic Moho structure of Shatsky Rise oceanic plateau, northwest Pacific Ocean. Earth and Planetary Science Letters, 441, 143-154, doi:10.1016/j.epsl.2016.02.042.

Zhang, J., Durkin, W., and Sager, W. W., in press. Morphology of Shatsky Rise oceanic plateau from high resolution bathymetry. Marine Geophysical Researches.

Figure Captions

Figure 1. Shatsky Rise bathymetry and feature names. Red circle shows the location of Ocean Drilling Program Site 1179, where seafloor basalts coeval to Shatsky Rise were cored (Sager and Escutia, 2005). Depths are shown from satellite-altimetry-derived bathymetry estimates (Smith and Sandwell, 1997). Contours drawn at 500-m intervals.

Figure 2. Cartoon depicting two models invoked to explain oceanic plateau LIP eruptions. (A) The plume head model (Richards et al., 1989; Duncan et al., 1991; Coffin and Eldholm, 1994). A large bulbous mass of hot material is generated at the core-mantle boundary, rises buoyantly through the mantle (A1), and causes a massive eruption when it arrives at the lithosphere (A2). In the oceans, this would form an oceanic plateau. Double lines on the lithosphere surface represent spreading ridges with arrows indicating relative motion. "TJ" denotes the triple junction. Arrows in the upper mantle indicate upwelling beneath the spreading ridges. The dotted line represents the past position of the triple junction before jumping to the location where the plume head arrived at the base of the lithosphere. (B) Fertile mantle model (Foulger, 2007; Anderson and Natland, 2014). A divergent plate boundary moves atop a portion of the upper mantle in which the melting temperature is depressed. The divergence leads to massive decompression melting. Sketches are not to scale.

Figure 3. Southern Shatsky Rise, magnetic lineations, and ocean drilling coring sites discussed in the text. Heavy red lines are magnetic lineations and fracture zones (Nakanishi et al., 1999). Filled red circles denote sites cored during IODP Expedition 324 (Expedition 324 Scientists, 2010a) and filled blue circle shows the location of Ocean Drilling Program Site 1213 (Shipboard Scientific Party, 2002). Color-graded satellite-altimetry-derived bathymetry (Smith and Sandwell, 1997) is depicted with contours at 500-m intervals. Heavy lines indicate

ship tracks with multichannel seismic data. White line shows the seismic profile of Figure 9. Heavier section of the white line shows the seismic refraction profile portrayed in Figure 8. (Sources: Expedition 324 Scientists, 2010a; Korenaga et al., 2012; Sager et al., 2013)

Figure 4. Tectonic evolution of Shatsky Rise during the Late Jurassic and Early Cretaceous. Numbers at upper left of each panel give the magnetic anomaly being formed at the time of the panel and its age in Ma (from Gradstein et al., 2012). Black lines show the magnetic lineations and fracture zones extant at the time. Purple lines show magnetic lineations that will be formed later on the Pacific plate. Heavy red lines show the active spreading ridges. Pink areas show the parts of Shatsky Rise that likely existed at the panel time and gray areas show parts not yet formed. Heavy blue lines and arrows show the path of the triple junction. Yellow zones in the upper right panel denote possible microplates. (sources: Sager et al., 1988; Nakanishi et al., 1989; 1999; Sager, 2005)

Figure 5. Graphic lithology columns for sites on Shatsky Rise where volcanic basement was cored. Sites U1346-U1350 were drilled on IODP Expedition 324 (Expedition 324 Scientists, 2010a) whereas Site 1213 was drilled on ODP Leg 198 (Shipboard Scientific Party, 2002). Sediment log data show estimated thickness of sediment layers at Site U1347 from Formation Microscanner image logs (Tominaga et al., 2014). (modified from Expedition 324 Scientists, 2010a; Sager et al., 2011b).

Figure 6. Overview of basal sediments, Expedition 324. Sites arranged from left to right in geographical order. Age deduced from biostratigraphy indicated to the right of each column. Sites are arranged vertically to suggest general relative distribution of ages at all sites. Early Cretaceous = Berriasian to Albian, Late Cretaceous = Cenomanian to Campanian, Cen = middle Cenozoic. Note long hiatus or lack of recovery between Campanian and middle

Cenozoic at Site U1348. Gray shaded area is the gap between last datable sediment and top of igneous basement (or top of the volcaniclastic sequence, Unit III, at Site U1348). (modified from Expedition 324 Scientists, 2010a)

Figure 7. Subsidence curves, Expedition 324 massif summit sites. (top) Site U1347 upper flank; (middle) Site U1349 Ori Massif summit; (bottom) Site U1346 Shirshov Massif summit. Colored curves show predicted site depth at the time of eruption, calculated from the present depth (corrected for sediment loading; Crough, 1983) using lithospheric subsidence models as follows: PS = Parsons and Sclater (1977); SS = Stein and Stein (1992). Calculated paleodepth estimates are compared with paleodepth indicators from Expedition 324 cores. Black curves = normal mid-ocean ridges, red arrow = difference between normal ridge and observed paleodepth, taken as the amount of uplift caused by volcano construction. Magnetic lineation ages are from Nakanishi et al. (1999) and Gradstein et al. (2012). (modified from Expedition 324 Scientists, 2010a)

Figure 8. Crustal cross section of Tamu Massif with seismic velocity from adaptive-importance refraction tomography. Data were acquired with ocean bottom seismometers (OBS) on a profile across the center of Tamu Massif. OBS locations are shown by open circles. Section location is shown in Figure 2. Base of colored section indicates the Moho discontinuity. Velocity contours in the crust are shown at 0.5 kms^{-1} intervals. (modified from Korenaga and Sager, 2012)

Figure 9. Multichannel seismic profile across the axis of Tamu Massif. Top panel shows original data and bottom panel shows interpretation. Lines within the volcano denote intrabasement reflectors. Location is shown in Figure 3. Dashed box indicates area of detail

shown in Figure 10. Data were collected with a 108.2-liter airgun array and 6 km, 480-channel streamer (Sager et al., 2013; Zhang et al., 2015). Data were processed at a fold of 59 with band-pass filtering, deconvolution, normal-moveout correction, stacking, and time migration. Vertical exaggeration is 37:1. (modified from Sager et al., 2013)

Figure 10. Detail of multichannel seismic profile illustrating intrabasement reflectors. Raw data plot is on the left and interpreted plot is on the right. Dark lines highlight intrabasement reflectors. Location is shown in Figure 9. Vertical exaggeration is 25:1. (modified from Sager et al., 2013)

Figure 11. Bathymetry of Tamu Massif. High resolution bathymetry in swaths is from multibeam echosounder data, mainly from R/V *Marcus G. Langseth* cruises MGL1002 and MGL1206 and R/V *Thomas G. Thompson* cruise TN037, but with contributions from other cruises crossing the massif (Zhang et al., in press). Depths in areas between multibeam echosounder swaths are satellite-altimetry-estimated depths (Smith and Sandwell, 1997). Depths are colored by depth with shallower depths shown in warm colors. Contours are plotted at 500-m intervals and labeled in thousands of meters. Prominent features of the Tamu Massif bathymetry are the Toronto Ridge, at the summit, and scattered secondary cones on the flanks.

Figure 12. Magnetic anomalies over Ori Massif. Red lines show magnetic anomalies identified by Nakanishi et al. (1999). Linear magnetic anomalies are observed over Ori Massif with an orientation parallel to those of the Pacific-Izanagi ridge in surrounding seafloor. Dashed line denotes a prominent linear negative anomaly crossing Ori Massif. (Huang and Sager, 2013)

Figure 13. Plots of TiO_2, CaO, V and Nb versus wt % MgO for fresh glasses from IODP Sites U1346, U1347, and U1350; and less altered (LOI <3.2 wt %) basalts from Site U1349 (Sano et al., 2012; Husen et al., 2013). To compare the measured data with experimental results, liquid compositions obtained in experiments on an OJP basalt at 1 atm under dry and FMQ-buffered conditions (Sano and Yamashita, 2004) are shown. Also shown are fields of fresh glass compositions from the OJP (Roberge et al., 2004; Sano and Yamashita, 2004) and from the EPR (Pet DB). Here we define N-MORB as having low K/Ti (<0.15) and E-MORB high K/Ti (>0.15). TiO_2 and CaO contents of E-MORB are the same as those of N-MORB and the field of E-MORB is not shown for these elements. A possible liquid line of descent (LLD) from one of the least evolved magmas (MgO ~8.5 wt %; V ~280 ppm; Nb ~4.5 ppm) is also shown (purple lines).

Figure 14. Nb/Yb and Zr/Y variation for Shatsky Rise basalts compared with OJP basalts (Kwainbaita- and Kroenke-types) and EPR N-MORB. Melting model results are shown for garnet lherzolite and spinel lherzolite with curved lines with tick marks (percent melting is indicated). The melting models use an accumulated fractional melting of depleted mantle (DM) reported by Sano et al. (2012). Diagram originated from Fitton et al. (1997). Data are from Tatsumi et al. (1998), Fitton and Godard (2004), Mahoney et al. (2005), Sano et al. (2012) and PetDB.

Figure 15. Fractionation corrected average value of Ca_8/Al_8 versus Na_8 for the Tamu, Ori, and Shirshov massifs and OJP, in comparison to EPR MORBs with 7.5-8.5 wt % MgO (after Husen et al., 2013). Dashed lines and open circles represent estimates of partial melt percentage from the model of Niu and Batiza (1991).

Figure 16. Variation of degree of fractional melting (%) with depth for a MORB-source mantle (KLB-1) with potential temperatures ranging from 1300 to 1600 °C (after Iwamori et al., 1995). Heavy vertical line ("melting stops") shows the depth to the base of the Shatsky Rise crust (30 km). Horizontal lines show estimated ranges for melting for Shatsky Rise (15-22 %), OJP (20-30 %) and MORB (12-15 %) primary magmas (Langmuir et al., 1992; Neal et al., 1997; Niu and O'Hara, 2008; Fitton and Godard, 2004; Sano et al., 2012; Husen et al., 2013).

Figure 17. Isotope ratio plots. (a) Pb versus Nd and (b) Nd versus Hf isotopic composition of Shatsky lavas age corrected to 140 Ma (modified after Heydolph et al. 2014). Site 1179 MORB data are interpreted to represent local upper mantle composition at times of Shatsky Rise formation. As shown in (b), isotopic heterogeneity increases with time during Shatsky Rise formation as the eruptive volume decreases. Range of non-chondritic, primitive mantle from Jackson and Jellinek (2013). See Heydolph et al. (2014) for additional data sources.

Figure 18. B/K versus Cl/K for Shatsky Rise basalts (after Miyoshi et al., 2015), in comparison to normal oceanic crust that was formed by fast spreading at the East Pacific Rise (EPR) (ODP Hole 1256D). Note that B/K and Cl/K are powerful tracers to detect low- and high-temperature hydrothermal alteration, respectively (Sano et al., 2008).

Figure 19. Plots of δ^7Li versus Yb/Li for basalts from the Shatsky Rise and OJP, in comparison to MORB, ocean island basalt (OIB), altered oceanic crust (AOC), and the field for hydrothermal fluids sampled from black smokers (after Sano and Nishio, 2015). Note that a linear relationships between δ^7Li and Y/Li for the Shatsky Rise and OJP basalts suggest that

Li in the two oceanic LIPs can be explained as a result of binary mixing between basaltic Li and hydrothermally influenced crustal Li.

Figure 20. Conceptual sketch illustrating the connection between mantle anomalies and oceanic LIPs. Data from Shatsky Rise studies indicate that the mantle melting anomaly was distinct from MORB, but probably did not have a large temperature anomaly nor did it cause a large amount of uplift as expected from a thermal plume head. Because of these discrepancies, if Shatsky Rise formed from a plume, it may have been a thermochemical plume. It is possible that the source was the lower mantle because of isotopic enrichment from recycled crustal material, but only if making the assumption that such material must descend to the core-mantle boundary prior to upwelling. Alternatively, this material may never have left the upper mantle. The sketch shows lithosphere descending into the lower mantle by subduction and returning to the upper mantle via a plume. It also suggest an alternate path in which the heterogeneity descended no further than the upper mantle. Upwelling beneath the triple junction is shown as being strong and entraining nearby mantle anomalies. The toothed line shows a trench. Otherwise, the symbols are the same as in Figure 2.

Table 1. Chemical characteristics of each magma type and percentage of cored lavas (data are from Sano et al., 2012; Heydolph et al., 2014).

	Chemical characteristics		Percentage of cored lavas			
Magma Type	Nb/Ti	143Nd/144Nd(t)	Tamu M.	Ori M.	Shirshov M.	Total
U1349	<0.00017	0.51293-0.51301	0	33	0	19
Normal	0.00038-0.00057	0.51284-0.51297	94	43	100	65
Low-Ti	0.00057-0.00080	0.51284-0.51298	6	5	0	6
High-Nb	>0.00080	<0.51282	0	19	0	10

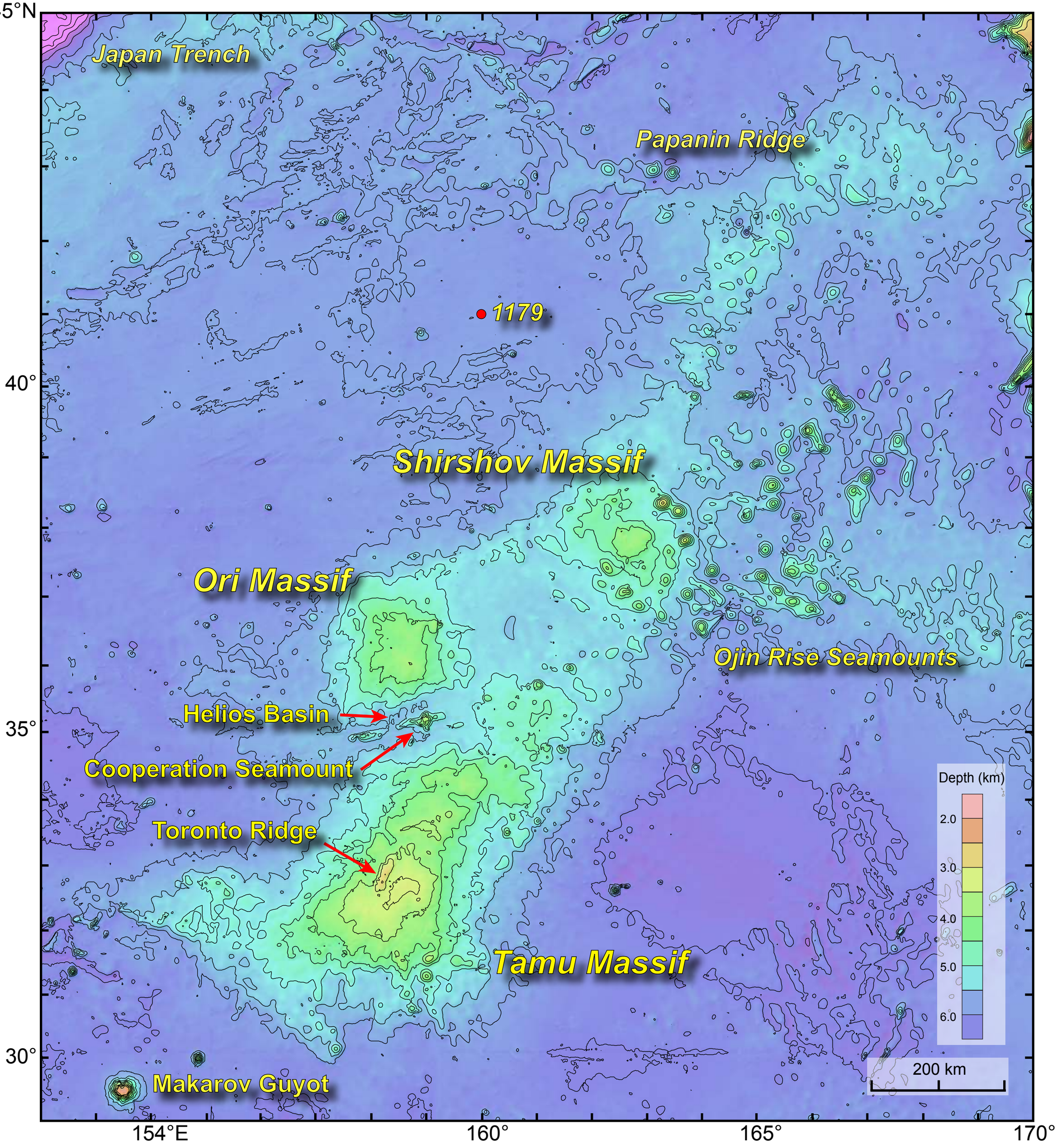

Fig. 1 (Sager et al.)

Figure 2

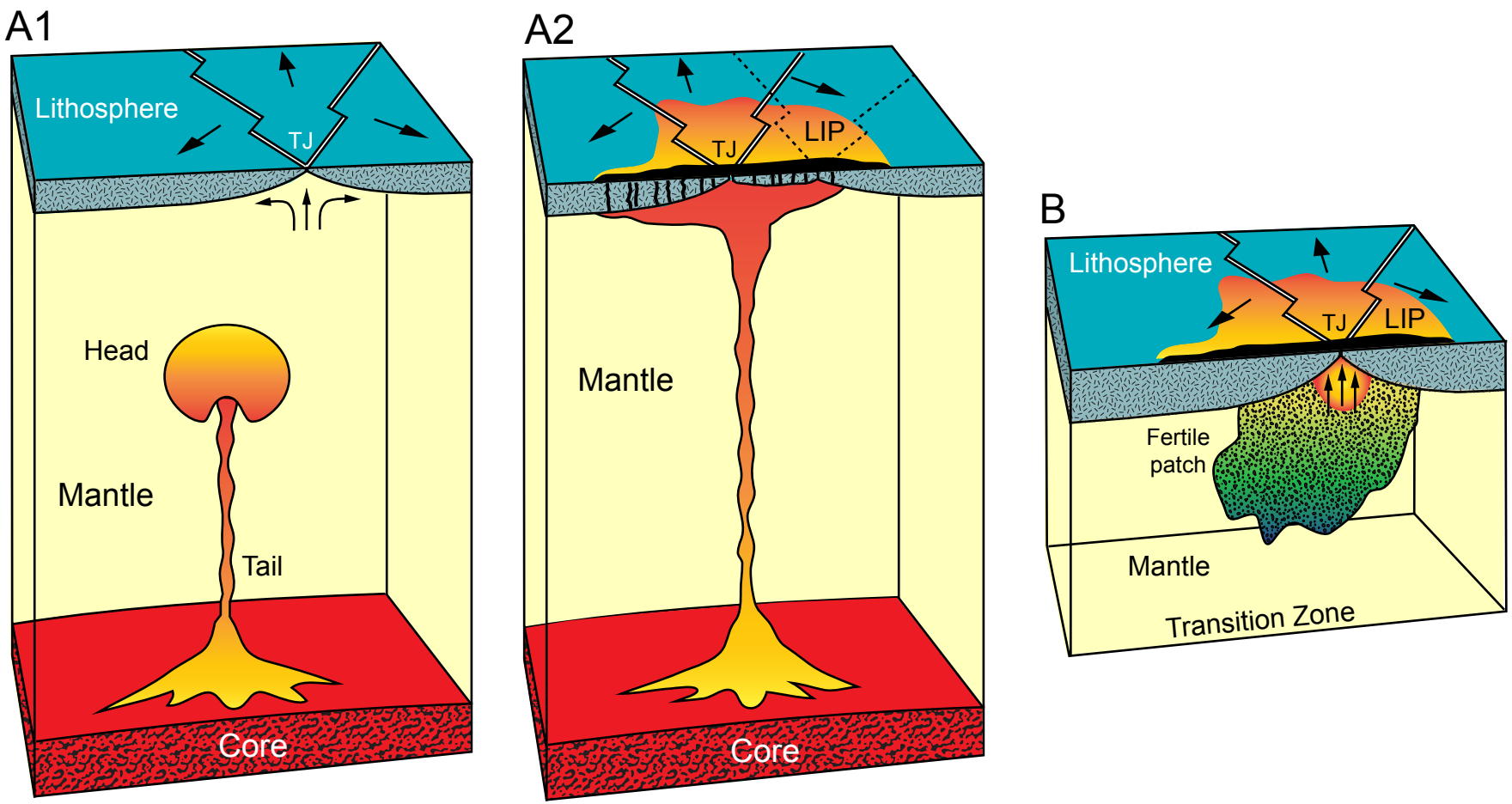
A1
Lithosphere
TJ
Head
Mantle
Tail
Core
A2
TJ
LIP
Mantle
Core
B
Lithosphere
TJ
LIP
Fertile
patch
Mantle
Transition Zone

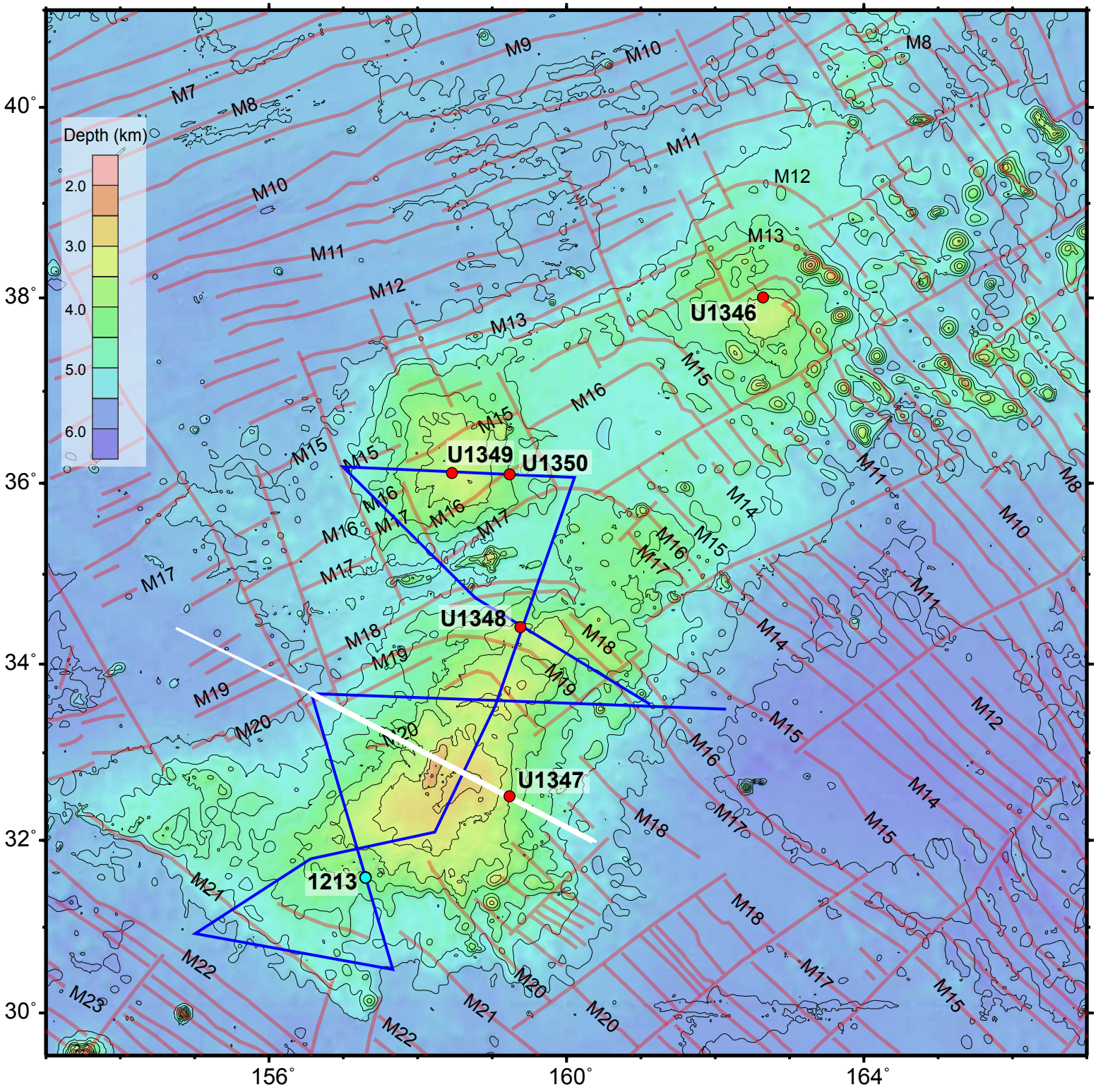

Fig. 3 (Sager et al.)

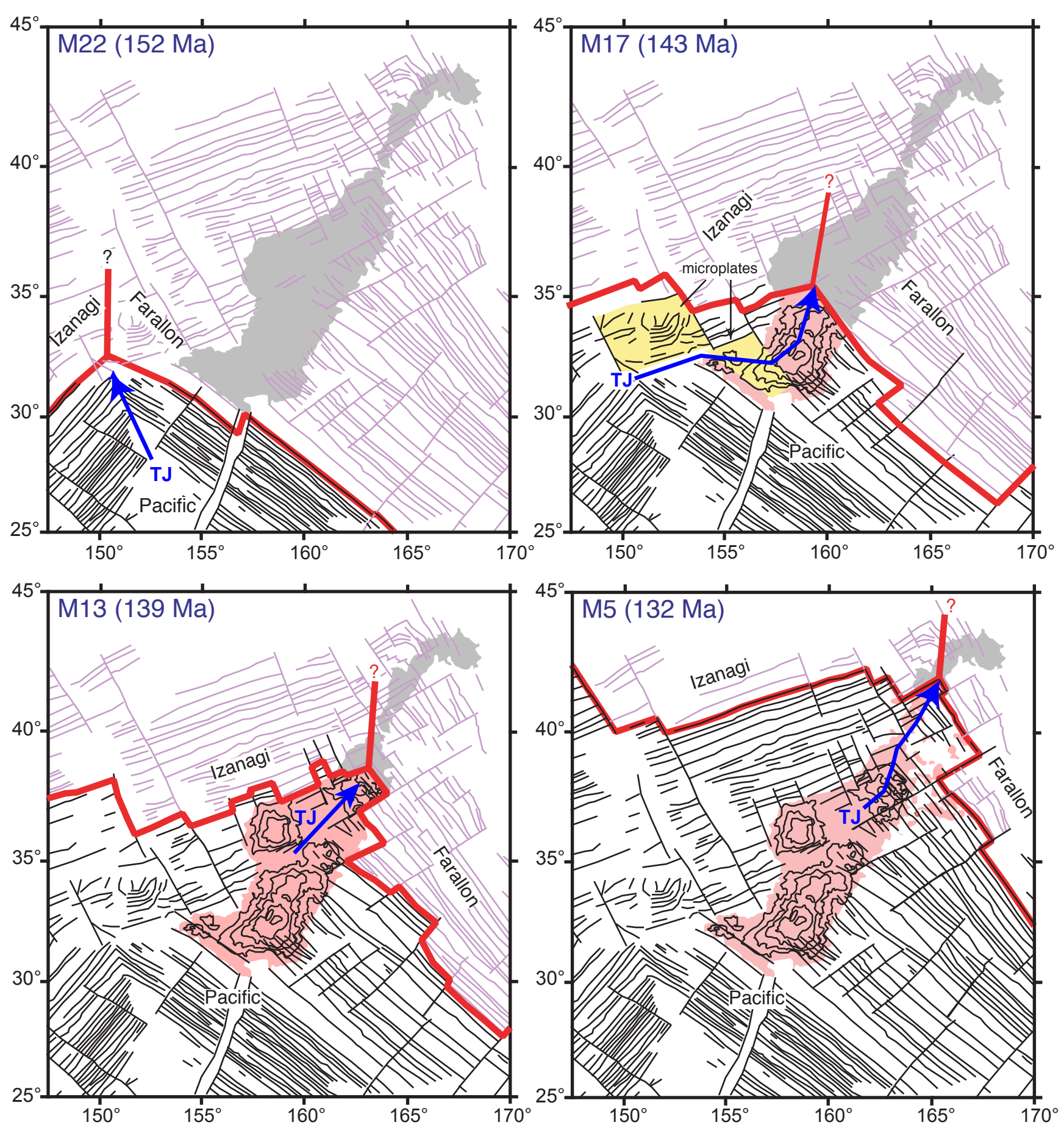

Fig. 4 (Sager et al.)

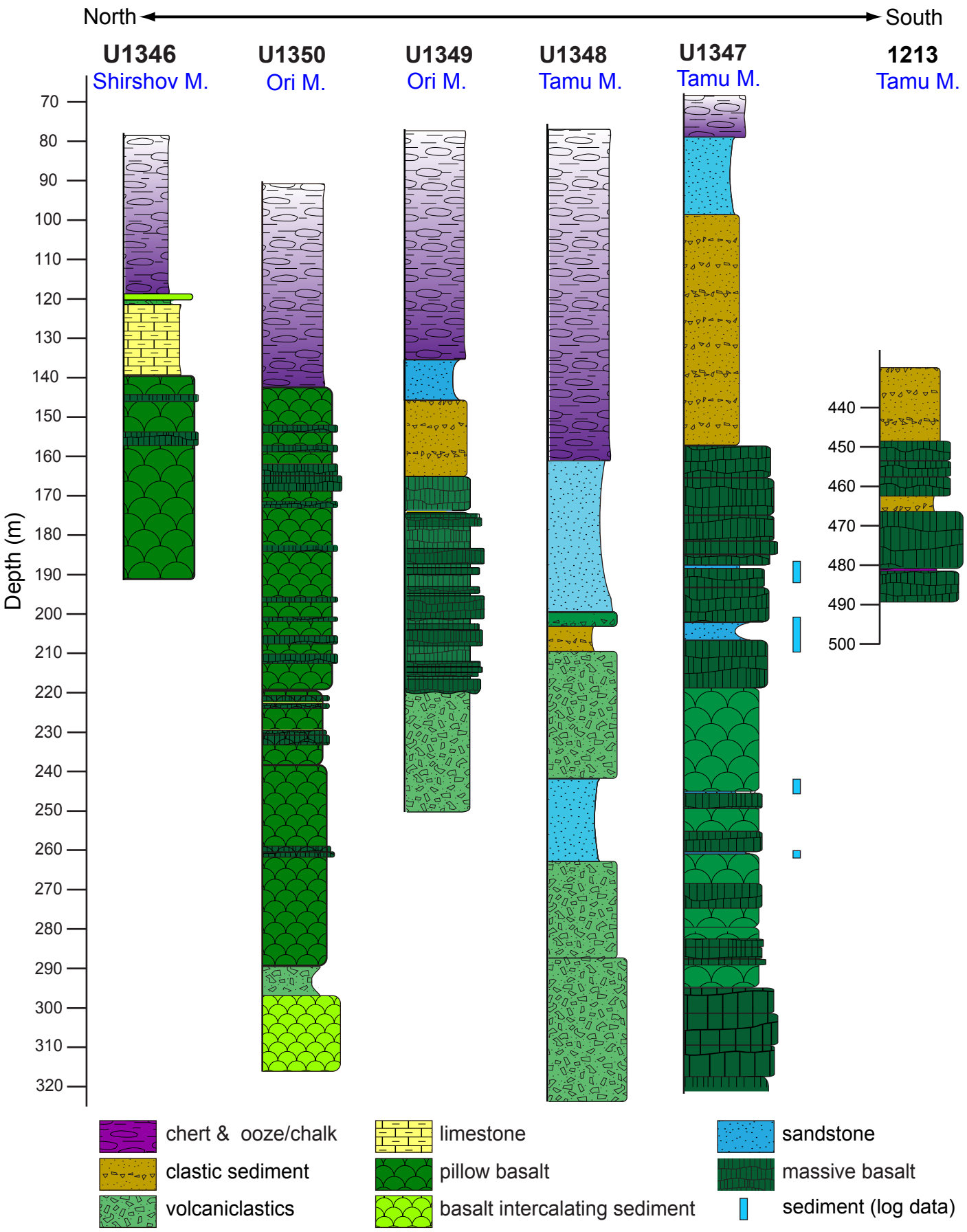

Fig. 5 (Sager et al.)

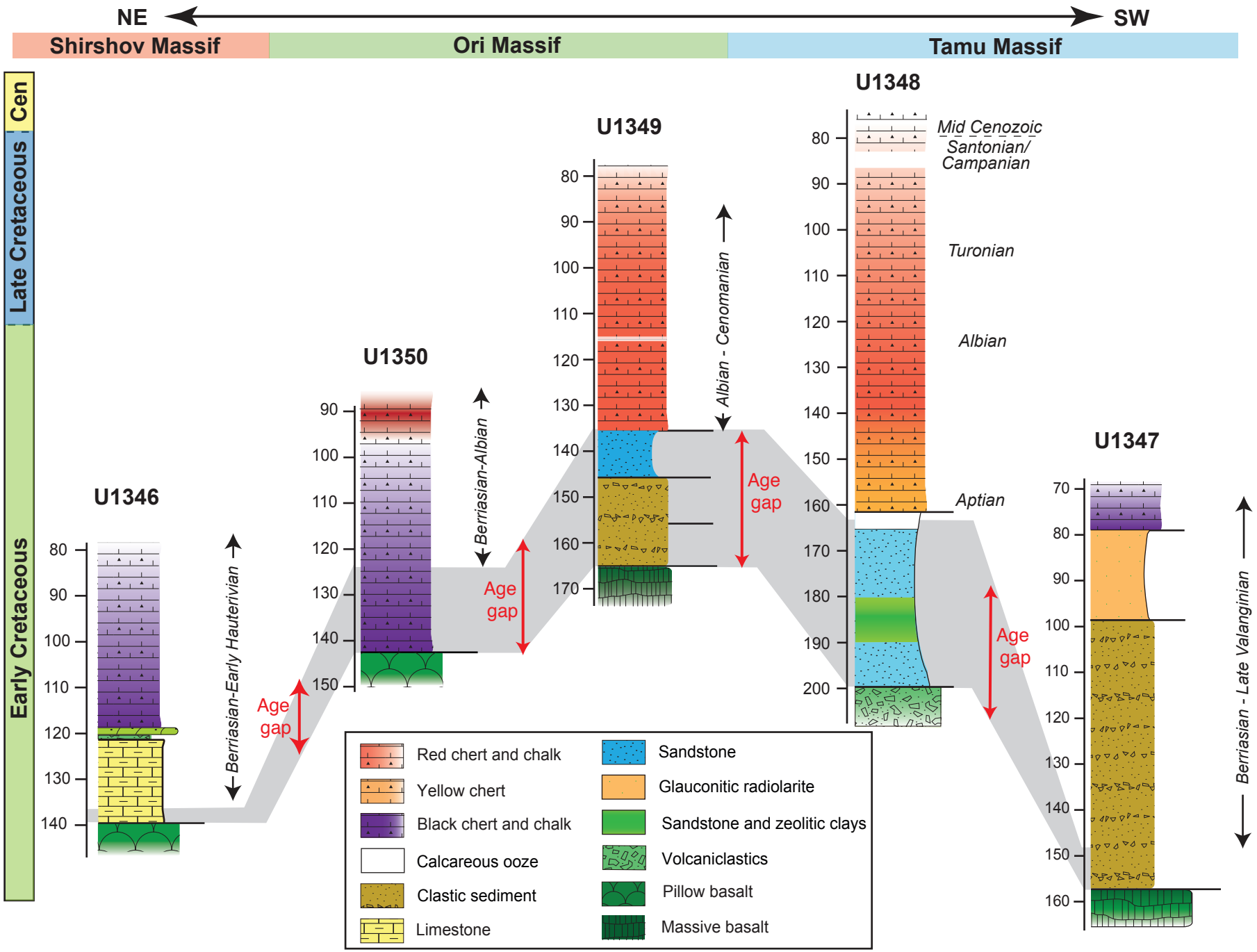

Fig. 6 (Sager et al.)

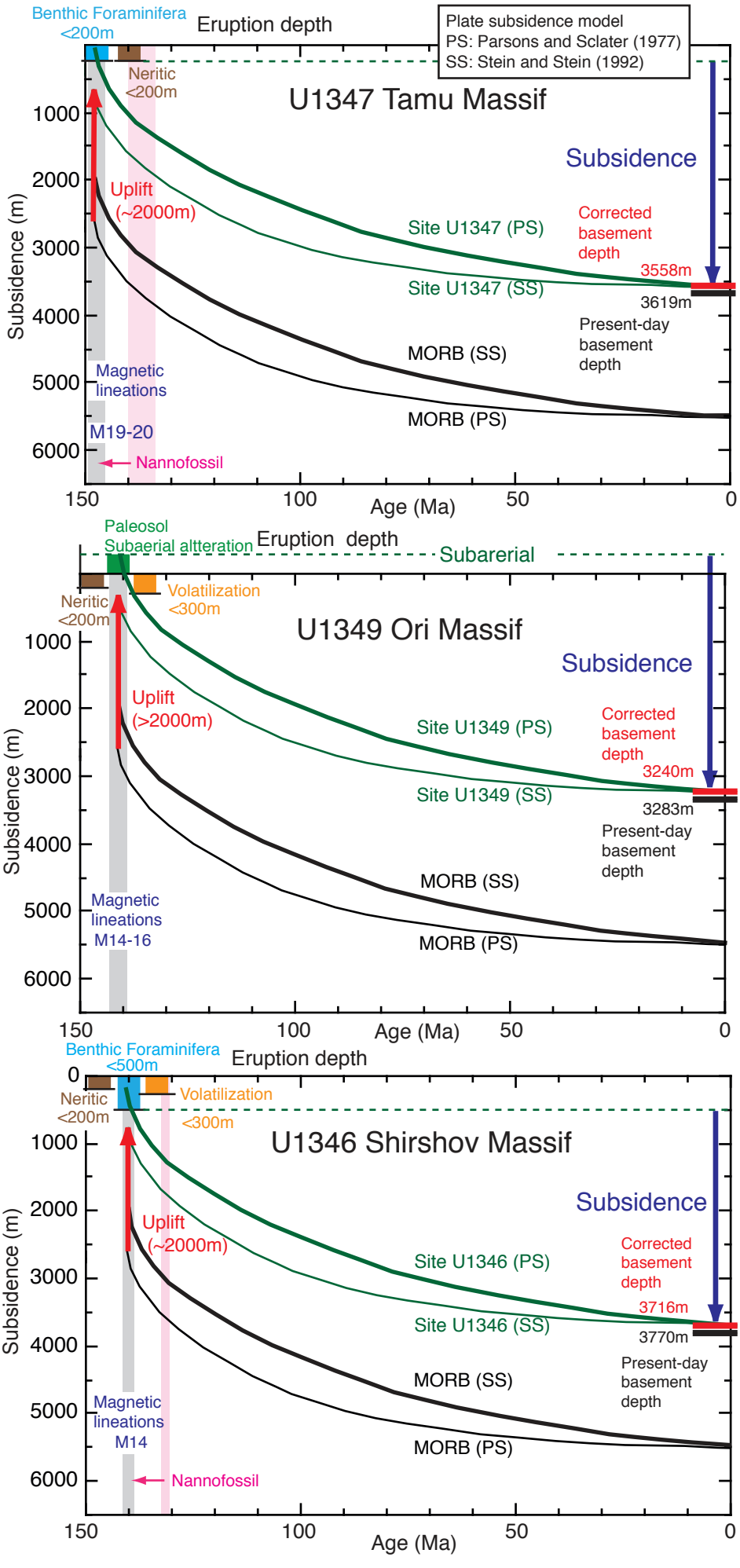

Fig. 7 (Sager et al.)

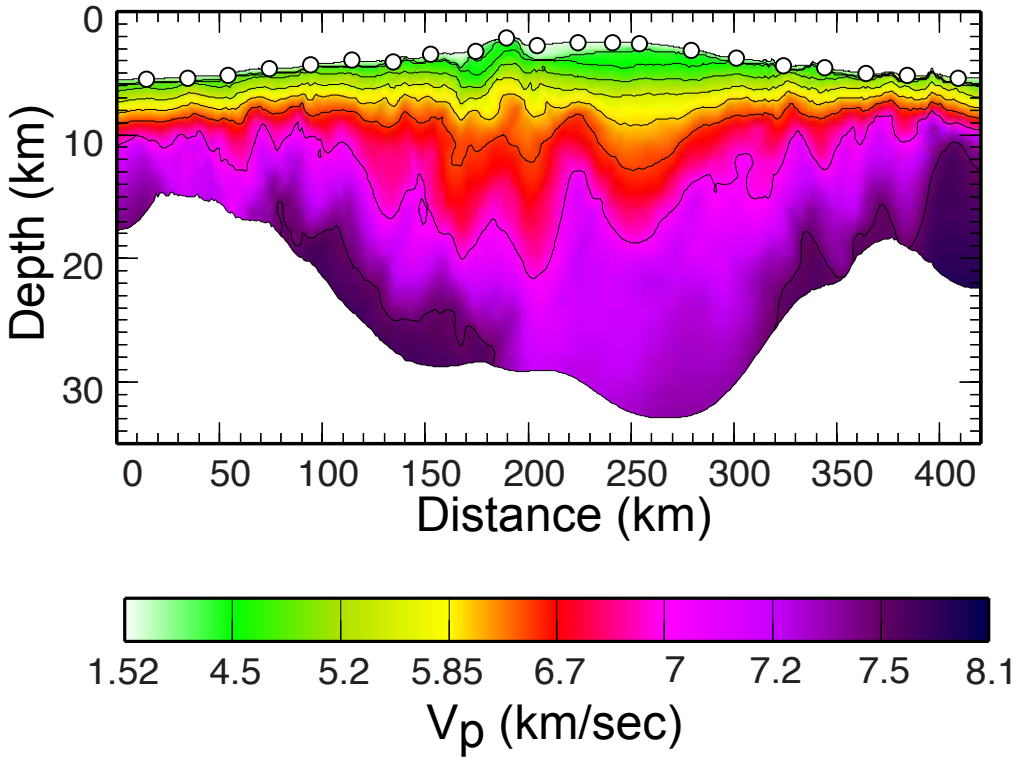

Figure 8 (Sager et al)

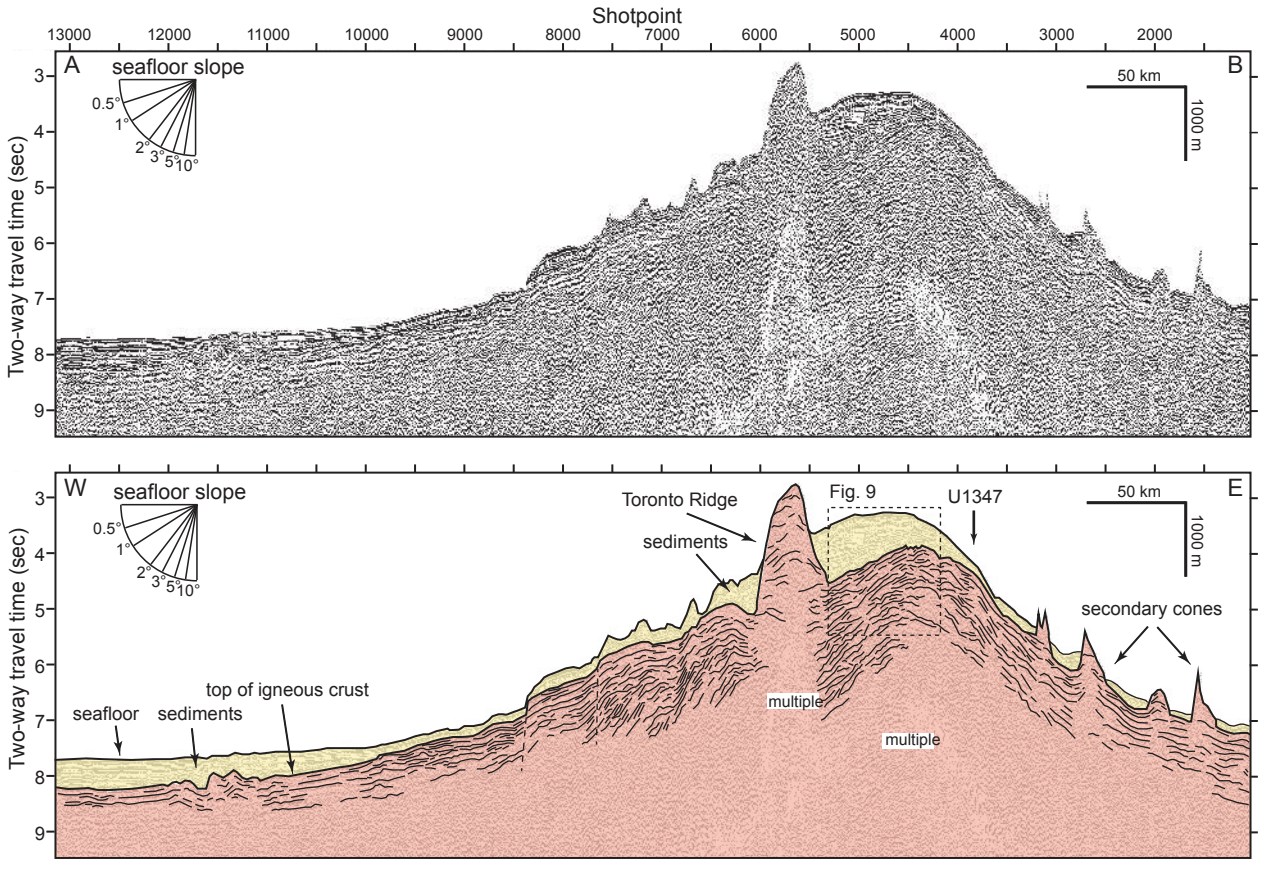

Figure 9 (Sager et al)

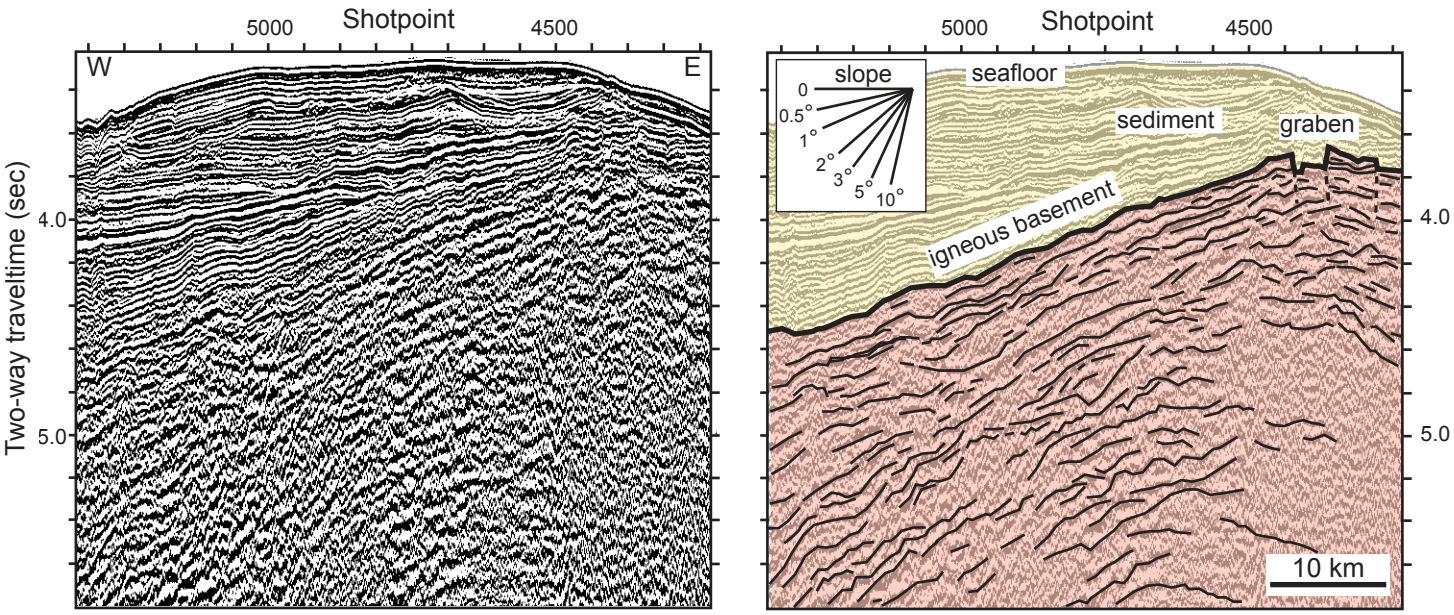

Figure 10 (Sager et al.)

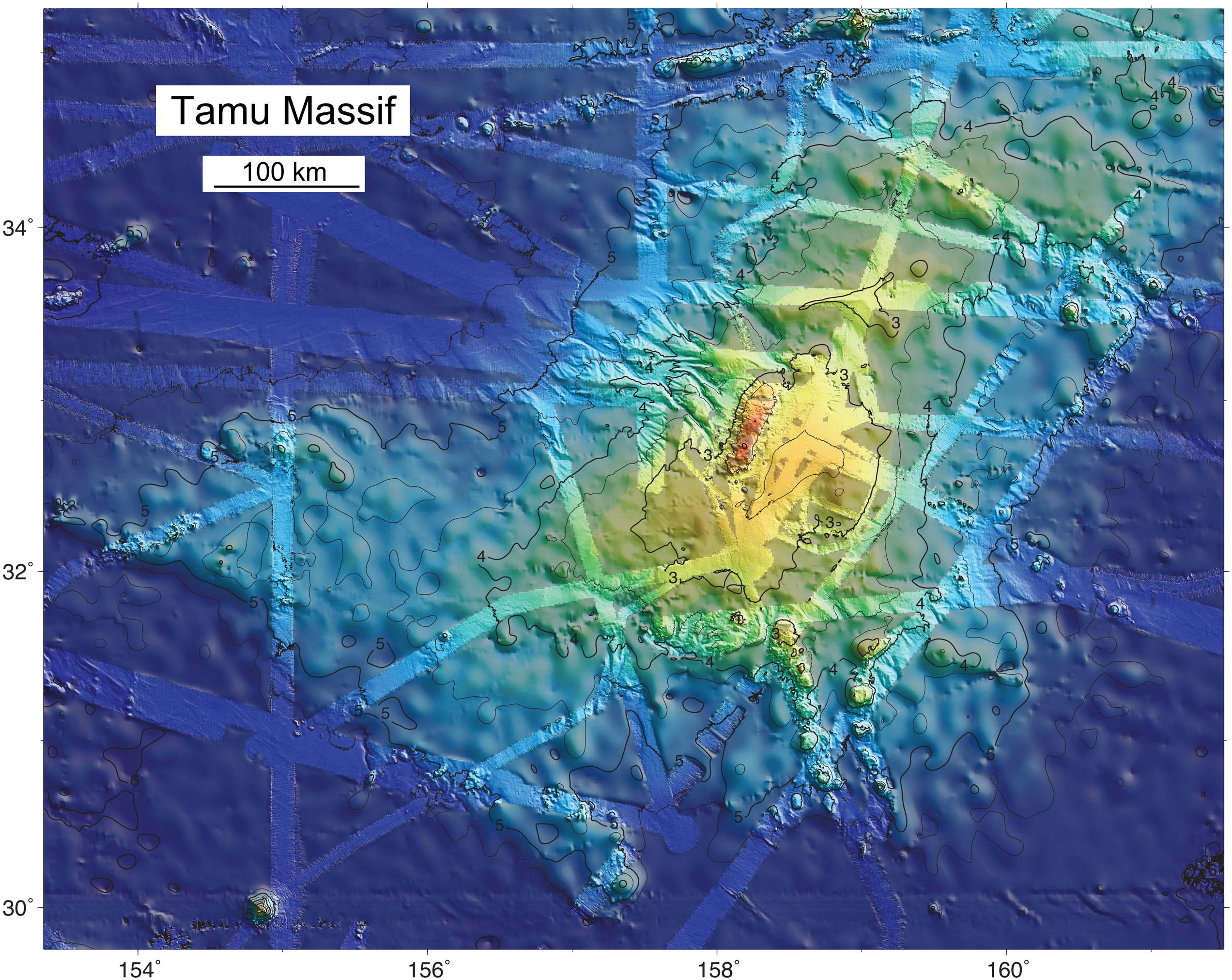

Figure 11 (Sager et al)

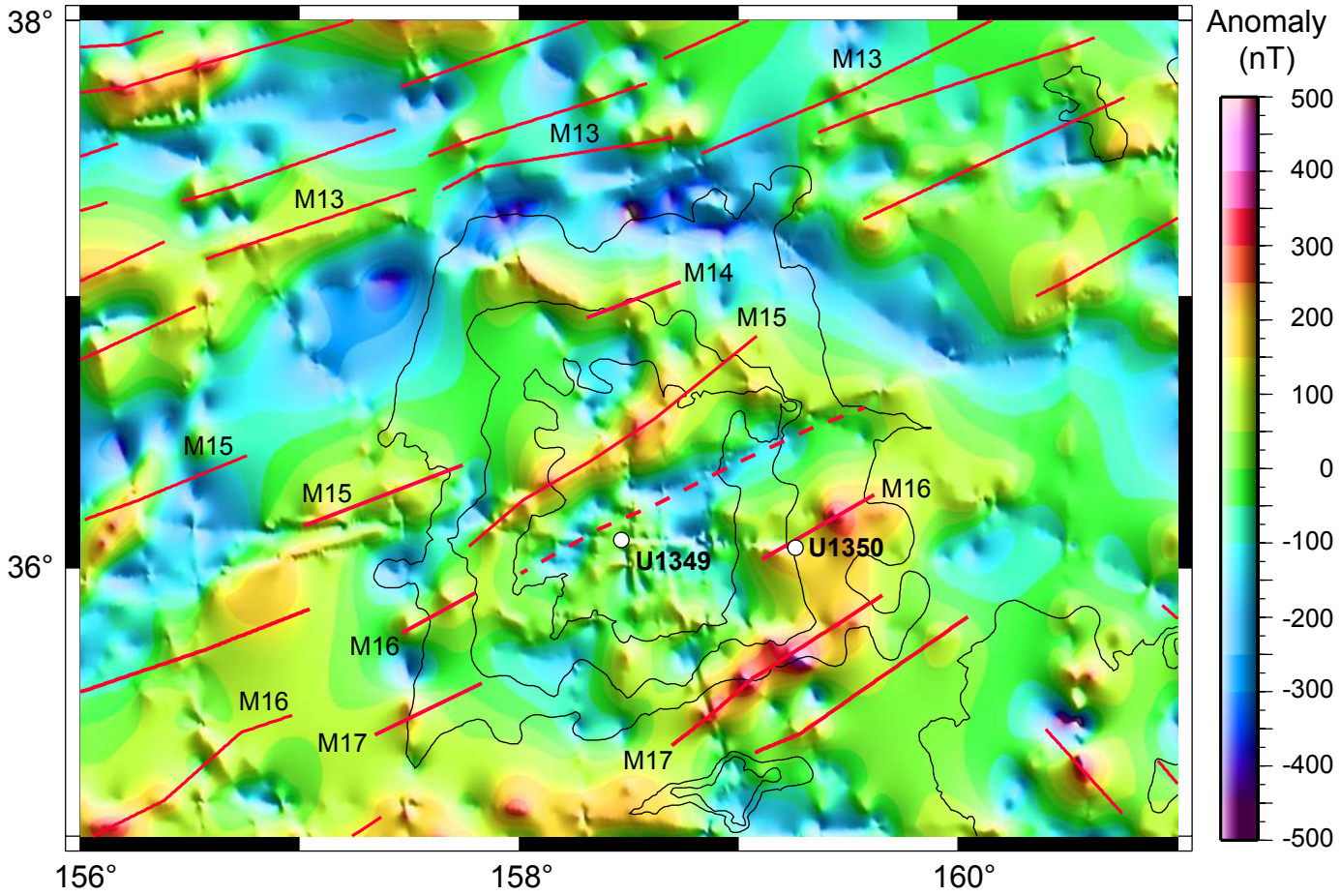

Figure 12 (Sager et al.)

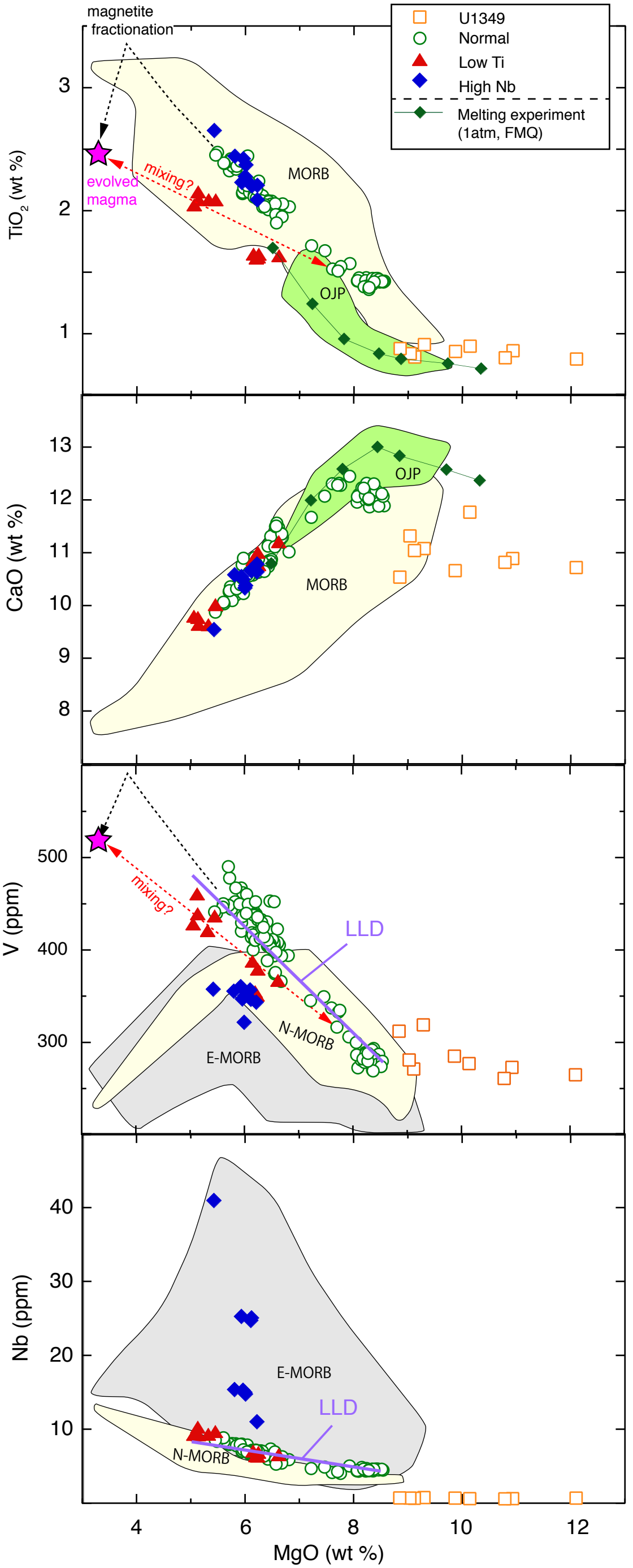

Figure 13 (Sager et al.)

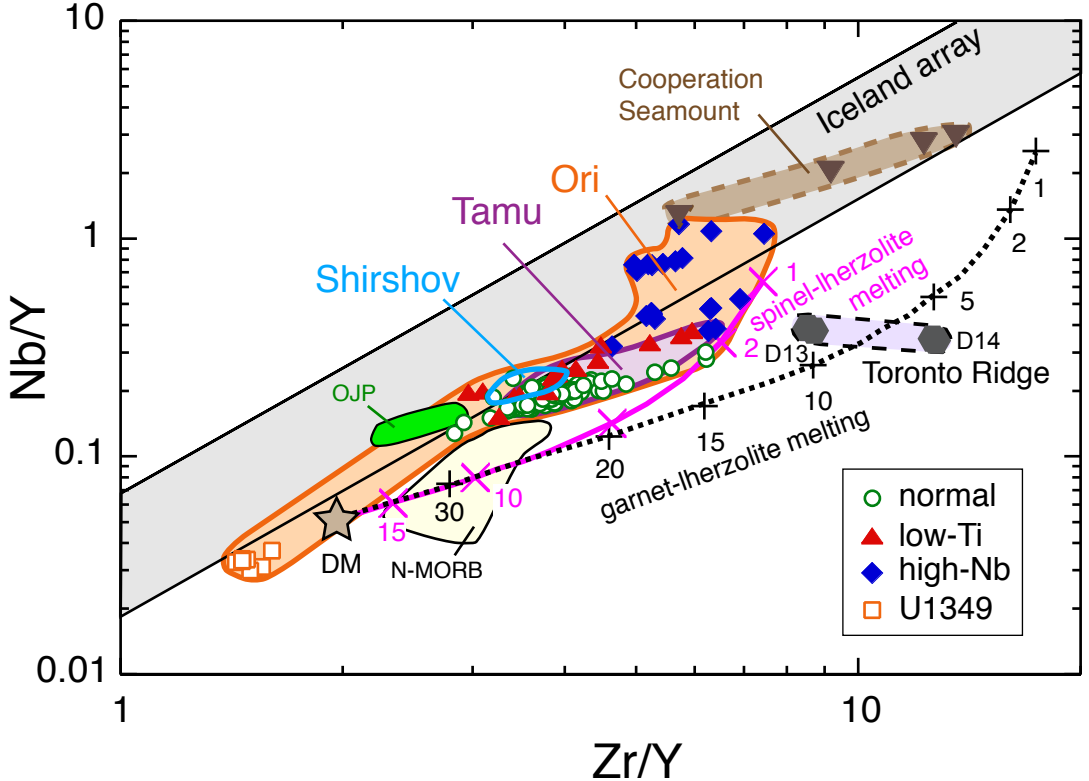

Figure 14 (Sager et al.)

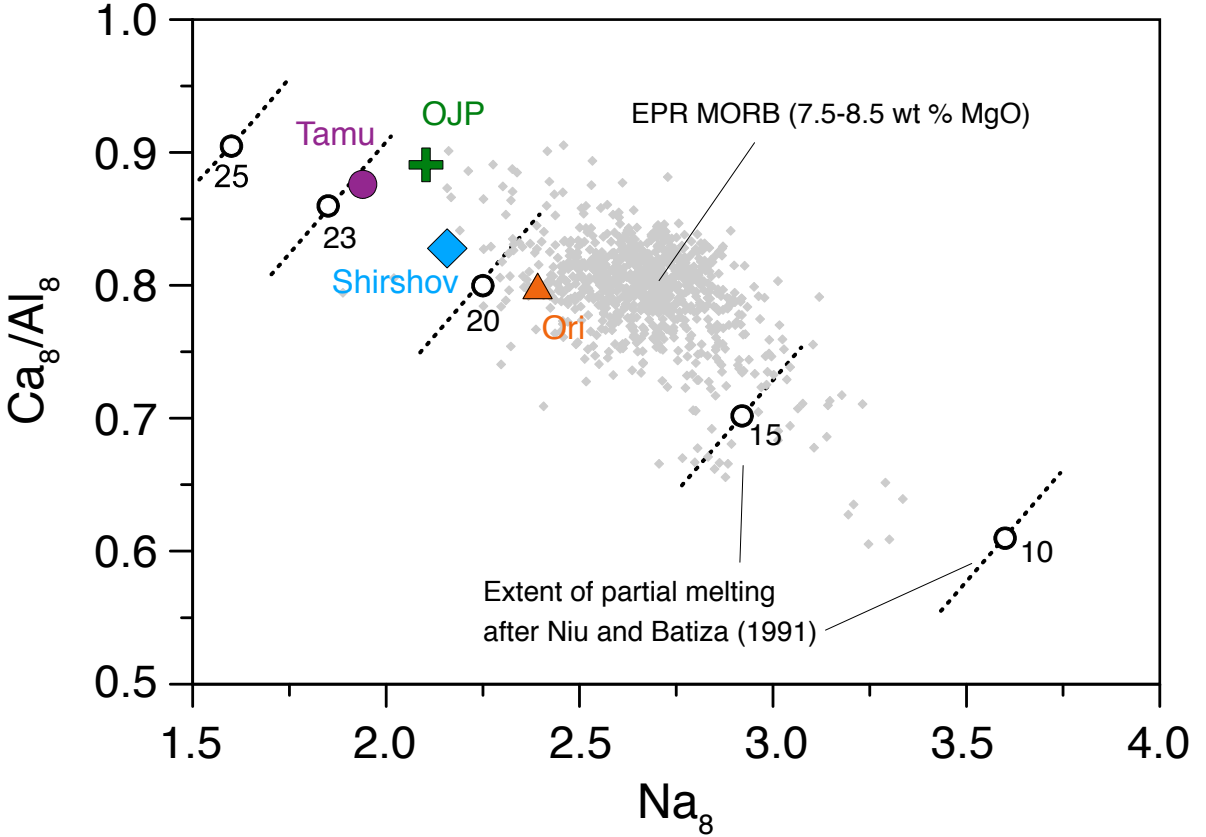

Figure 15 (Sager et al.)

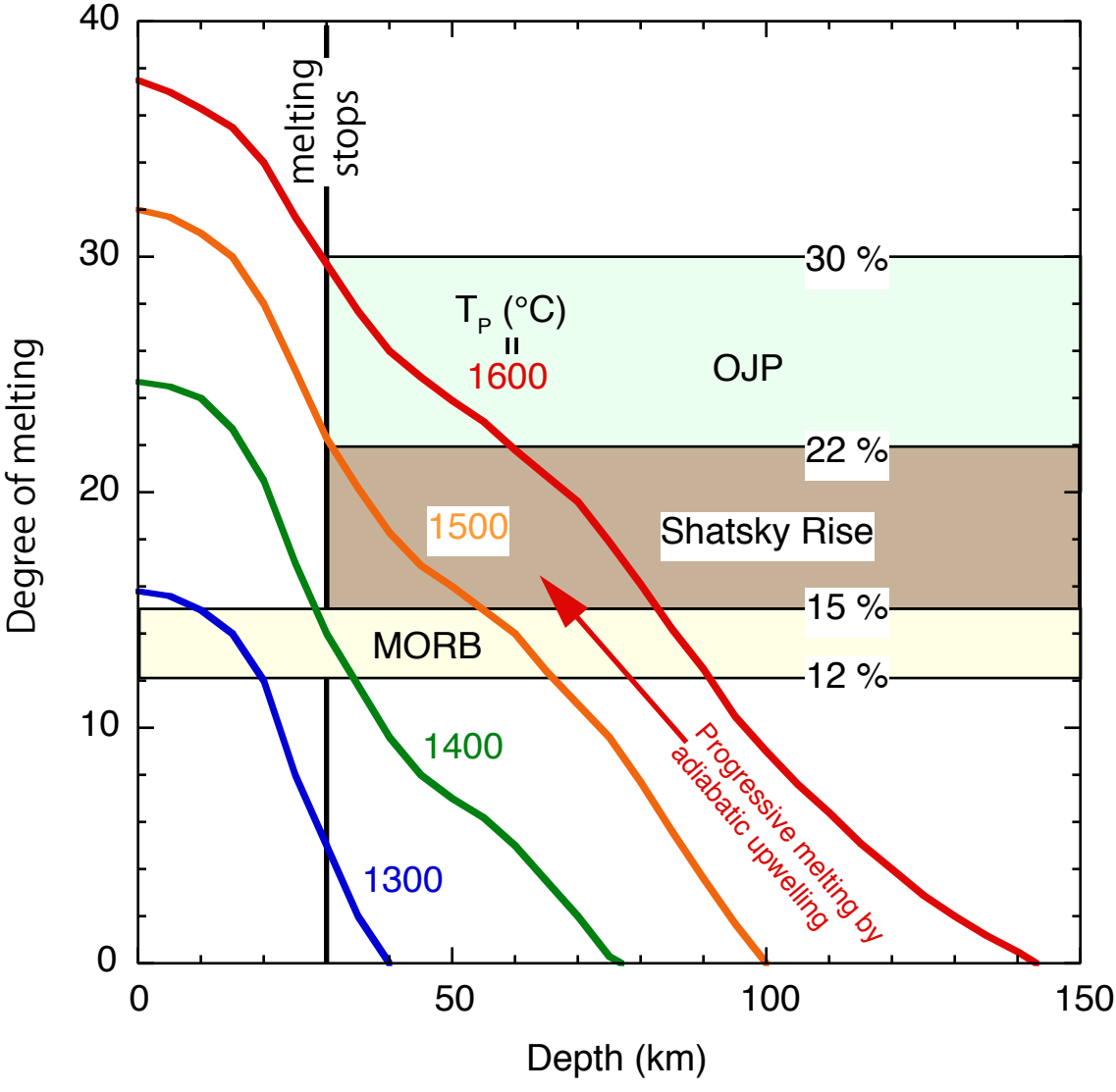

Figure 16 (Sager et al.)

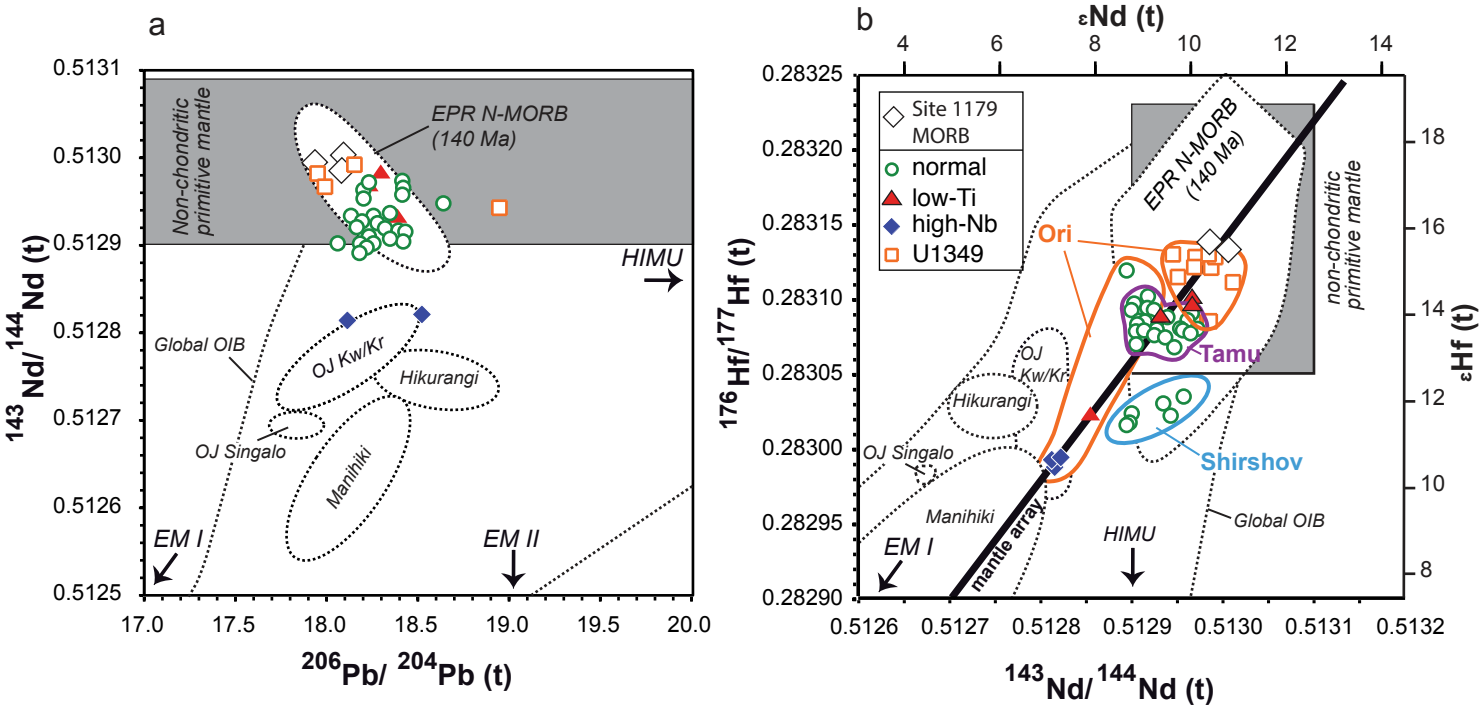

Figure 17 (Sager et al.)

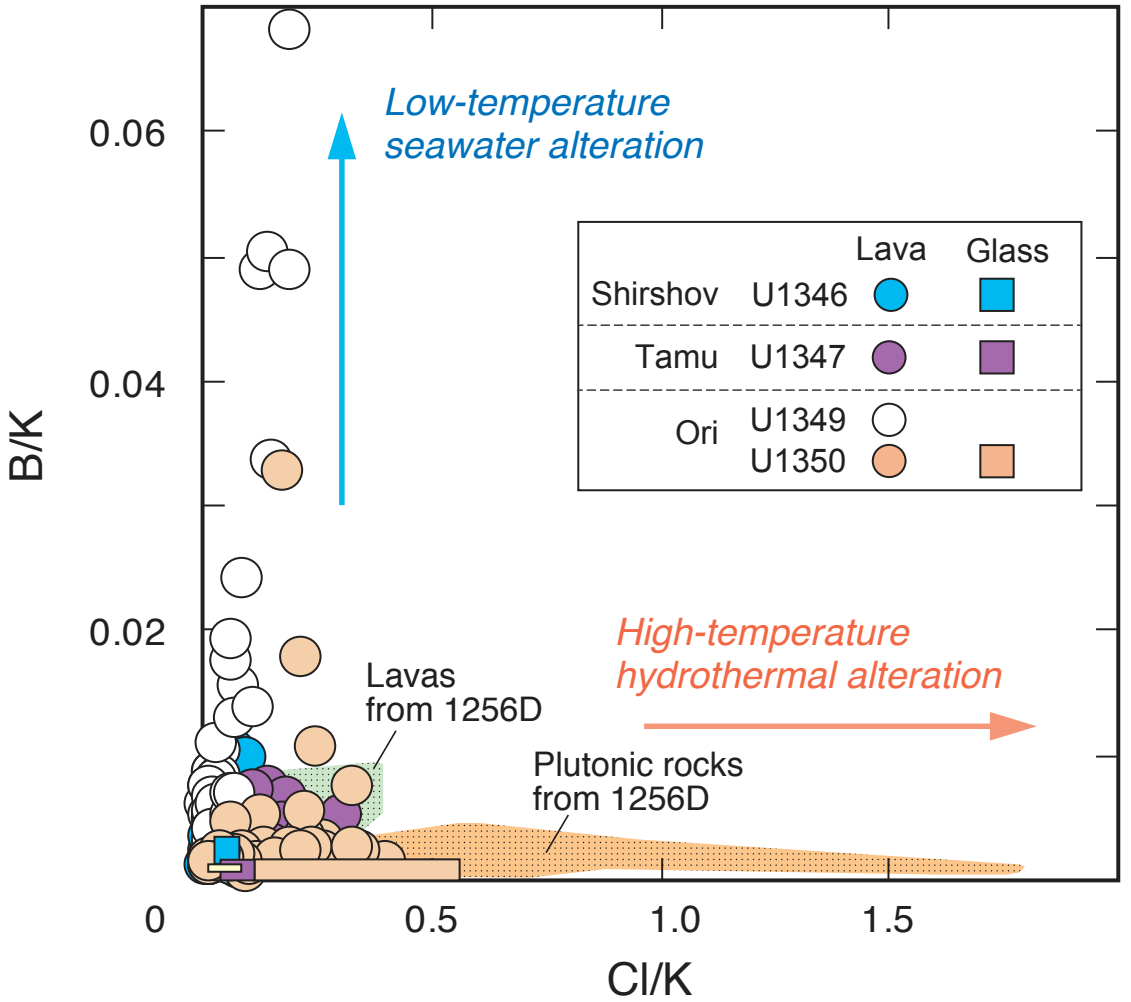

Figure 18 (Sager et al.)

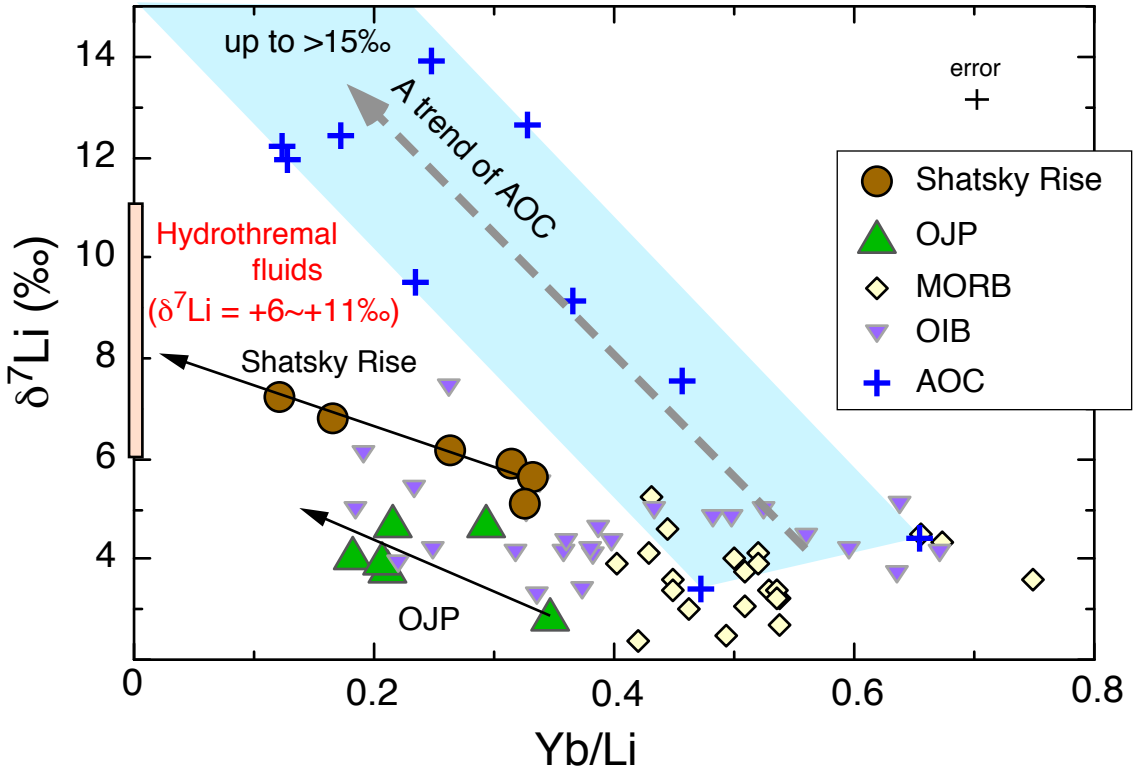

Figure 19 (Sager et al.)

Figure 20